RECURSIVE MULTI-MODEL UPDATING OF BUILDING STRUCTURE: A NEW SENSITIVITY BASED FINITE ELEMENT APPROACH

Shichao Zhu

RECURSIVE MULTI-MODEL UPDATING OF BUILDING STRUCTURE: A NEW SENSITIVITY BASED FINITE ELEMENT APPROACH

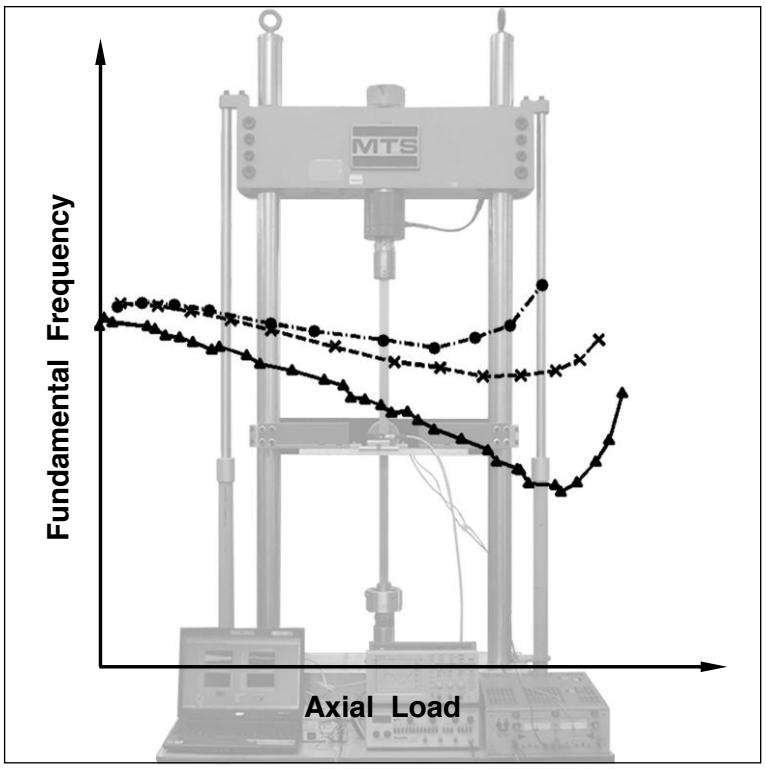

Dottorato di Ricerca in Ingegneria delle Strutture
Politecnico di Torino

Shichao Zhu

RECURSIVE MULTI-MODEL UPDATING OF BUILDING STRUCTURE: A NEW SENSITIVITY BASED FINITE ELEMENT APPROACH

Tesi per il conseguimento del titolo di Dottore di Ricerca
XXVII Ciclo (2012 - 2013 - 2014)

Dottorato di Ricerca in Ingegneria delle Strutture
Politecnico di Torino

Marzo 2016

Dottorato di Ricerca in Ingegneria delle Strutture
Politecnico di Torino, Corso Duca degli Abruzzi 24, 10129 Torino, Italy

Tutore: Prof. Alessandro De Stefano

Coordinatore: Prof. Vincenzo Ilario Carbone

To my parents, my brother and all my dear friends

Acknowledgements

I appreciate Prof. Alessandro De Stefano for his support during the period of my PhD study, at the meantime, I'd like to thank all the members in the seismic laboratory of Politecnico di Torino.

Summary

An invaluable tool for structural health monitoring and damage detection, parametric system identification through model-updating is an inverse problem, affected by several kinds of modelling assumptions and measurement errors. By minimizing the discrepancy between the measured data and the simulated response, traditional model-updating techniques identify one single optimal model that behaves similarly to the real structure. Due to several sources of errors, this mathematical optimum may be far from the true solution and lead to misleading conclusions about the structural state. Instead of the mere location of the global minimum, it should be therefore preferred the generation of several alternatives, capable to express near-optimal solutions while being as different as possible from each other in physical terms.

The present paper accomplishes this goal through a new recursive, direct-search, multi-model updating technique, where multiple models are first created and separately solved for the respective minimum, and then a selection of quasi-optimal alternatives is retained and classified through data mining and clustering algorithm. The main novelty of the approach consists in the recursive strategy adopted for minimizing the objective function, where convergence towards optimality is sped up by sequentially changing only selected subsets of parameters, depending on their respective influence on the error function. Namely, this approach consists of two steps. First, a sensitivity analysis is performed. The input parameters are allowed to vary within a small interval of fractional variation around a nominal value to compute the partial derivatives numerically. After that, for each parameter the sensitivities to all the responses are summed up, and used as an indicator of sensitivity of the parameter. According to the sensitivity indicators the parameters are divided into an indicated number of subsets given by the user. Then every subset is updated recursively with a specified order according to the sensitivity indicator.

Sommario

Uno strumento prezioso per lo Structural Health Monitoring e il rilevamento dei danni, il modal-updating è un problema inverso che consiste nell'individuazione di un sistema parametrico, influenzato da diverse ipotesi di modellazione ed errori di misura. Riducendo al minimo la discrepanza tra i dati misurati e la risposta simulata, le tecniche tradizionali di model-updating permettono di identificare un modello unico ottimale che si comporta in modo simile alla struttura reale. A causa di diverse fonti di errori, questo optimum matematico può essere lontano dalla soluzione reale e portare a conclusioni fuorvianti sullo stato di fatto della struttura. Invece della sola posizione del minimo globale, è da preferire la generazione di diverse alternative, in grado di esprimere soluzioni quasi ottimali il più possibile diverse tra loro in termini fisici.In questo lavoro si raggiunge l'obiettivo prefissato attraverso una nuova procedura ricorsiva, una ricerca diretta e una tecnica di multi-model updating, dove più modelli vengono prima creati e separatamente risolti per il rispettivo minimo. Una selezione di alternative quasi ottimali vengono mantenute e classificate attraverso i dati estratti e un algoritmo di clustering. La novità principale in questo tipo di approccio consiste nella strategia ricorsiva adottata per minimizzare la funzione obiettivo, dove la convergenza verso l'ottimizzazione è accelerata in modo sequenziale variando solamente sottoinsiemi selezionati di parametri, a seconda della loro rispettiva influenza sulla funzione di errore. Questo approccio può essere suddiviso in due fasi. Innanzitutto, viene eseguita un'analisi di sensitività. I parametri di input possono variare in un piccolo intervallo di variazione differenziale attorno ad un valore nominale per calcolare numericamente le derivate parziali. Successivamente, per ogni parametro le sensitività di tutte le risposte vengono sommate e utilizzate come indicatore della sensitività del parametro. Secondo gli indicatori di sensitività i parametri sono suddivisi in un numero prefissato di sottoinsiemi forniti dall'utente stesso. Poi ogni sottoinsieme viene aggiornato in modo ricorsivo con un ordine specificato secondo l'indicatore di sensitività.

Contents

Chapter 1

Introduction

Modern and highly sophisticated finite element procedures are available for structural analysis, although yet practical application often reveals considerable discrepancy between analytical prediction and test results. The way to reduce this discrepancy is through modification of the modelling assumptions and parameters until the correlation of analytical predictions and experimental results satisfies accuracy requirements. (Friswell and Mottershead et al., 1995) Classically, this is achieved by a trial and error approach, which is generally time consuming and may not be feasible in some cases. Thus computational procedures have been developed to update the parameters of analytical models using test data. In particular, modal data, such as natural frequencies and mode shapes, extracted from measured frequency response data have found broad application as a target for model parameter adjustment. This procedure was described in detail by Natke and Friswell and Mottershead (Friswell and Mottershead et al., 1995) and in recent years has developed into a mature technology applied successfully for the correction of industrial-scale FE models.

The parametric system identification through model-updating is an inverse

problem, affected by several kinds of modelling assumptions and measurement errors. The finite element model updating has emerged in the 1990s as a subject of the immense importance to the design, construction and maintenance of mechanical and civil structures. The modern world is one in which the demand for improved performance of the products of engineering design must be achieved in the front of ever increasing energy and material costs. As designs become more refined, it is necessary that the search for improvement is involved with aspects of increasingly intricate detail. Computer based analysis techniques have had a huge impact on engineering design and product development since 1960s. The approach to the numerical predictions of the behaviour of physical system is limited by the assumptions in the development of the mathematical model. Model updating, at its most ambitious, tries to correct assumptions by processing vibration test results. Updating is a process full of numerical difficulties.

The sensitivity-based method is probably the most successful of the many approaches to finite element model-updating of engineering structures based on vibration test data. It has been applied successfully to large-scale industrial problems. By minimizing the discrepancy between the measured data and the simulated response, traditional model-updating techniques identify one single optimal model that behaves similarly to the real structure. Due to several sources of errors, this mathematical optimum may be far from the true solution and cause misleading conclusions about the structural state. Instead of the mere location of the global minimum, it should be therefore preferred the generation of several alternatives, capable to express near-optimal solutions while being as different as possible from each other in physical terms.

The present work accomplishes this goal through a recursive, direct-search, multi-model updating technique, where multiple models are first created and separately solved for the respective minimum, and then a selection of quasi-optimal alternatives is retained and classified through data mining and clustering algorithms. The main novelty of the approach consists in the recursive strategy adopted for minimizing the objective function, where convergence towards optimality is sped up by sequentially changing only selected subsets of parameters, depending on their respective influence on the error function. Namely, this approach consists of two steps. First, a sensitivity analysis is performed. The input parameters are allowed to vary within a small interval of fractional variation around a nominal value to compute the partial derivatives numerically. After that, for each parameter the sensitivities to all the responses are summed up, and used as an indicator of sensitivity of the parameter. According to sensitivity indicators the parameters are divided into a preselected number of subsets. Finally all subsets are updated recursively with a specified order according to the sensitivity indicator. In addition, to get rid of local minimum, the Tikhonov technique is applied.

The methodology is firstly validated with a shear type system and then applied to the finite-element model updating of a large-scaled frame prototype, built in the

Structural Engineering Lab at the University of Basilicata, and recently used as a benchmark for the experimental assessment of the seismic effectiveness of different control strategies, in the framework of the inter-university Italian DPC-ReLUIS 2005-08 Project. And then a case study on an masonry arch bridge is performed, and the interface between Ansys and MatLab is created. During the case study an critical analysis is also performed comparing the new method with generic method and classic sensitivity based method.

The results show that the new recursive approach achieves equally good results with significant time savings. The new recursive approach is proven a useful alternative to traditional sensitivity-based approaches. Furthermore, the comparison with results obtained using genetic algorithm techniques shows a significant robustness in escaping local minima and an improved computational efficiency of the proposed method.

I Glossary

- Degrees of freedom: are the coordinates in the space that are not fixed by any restraints, in this point it is possible to observe a translations or rotation.
- Natural frequencies are the frequencies that characterize a structure. Their reciprocal express the period of the structure.
- Mode shapes: are the displacements associated to every degree of freedom for each natural frequency. The shapes of the structure in resonant conditions
- Parameters are the coefficients that define a model. they might be the mechanical properties of the structure and the geometry.
- Real System is the structure which parameters are unknown and have to be determined by a characterization process.
- Analytical model is the finite element model of the examined structure. While the real system is a continuous structure and with infinite degrees of freedom, the finite element model is a discrete approximation with N degrees of freedom
- Data sets are the measures obtained from the experimental test. These data allow to extract natural frequencies and mode shapes. The objective of the model updating is to minimize the differences between experimental outcomes and numerical simulations through the changes of the parameters.
- Updating is the procedure to calibrate the model to make it fit as much as possible into the experimental evidence.

Chapter 2

Structural health monitoring and system identification techniques

2.1 Structural Health Monitoring

The process of implementing a damage identification strategy for aerospace, civil and mechanical engineering infrastructure is referred to as structural health monitoring (SHM). (John E. Mottershead, Michael Link, Michael I. Friswell et al., 2011) This process involves the observation of a structure or mechanical system over time using periodically spaced measurements, the extraction of damage-sensitive features from these measurements and the statistical analysis of these features to determine the current state of system health. For long-term SHM, the output of this process is periodically updated information regarding the ability of

the structure to continue to perform its intended function in light of the inevitable aging and damage accumulation resulting from the operational environments. Under an extreme event, such as an earthquake or unanticipated blast loading, SHM is used for rapid condition screening. This screening is intended to provide, in near real-time, reliable information about system performance during such extreme events and the subsequent integrity of the system. (Friswell and Mottershead et al., 1995)

SHM is a broad multidisciplinary field both in terms of the diverse science and technology involved as well as in its varied applications. The technological developments necessary to enable practical structural health monitoring are originating from scientists and engineers in many fields including physics, chemistry, materials science, biology, and mechanical, aerospace, civil and electrical engineering. SHM is being implemented on diverse systems and structures such as aircraft, spacecraft, ships, helicopters, automobiles, bridges, buildings, civil infrastructure, power generating plants, pipelines, electronic systems, manufacturing and processing facilities, biological systems, and for the protection of the environment, and for defense.

The SHM in Civil Engineering Structures are divided in three levels:

- Level One: Damage Detection, which gives a qualitative indication that damage might be present in the structure.
- Level Two: Damage Classification, which gives information about the type of damage.
- Level Three: Damage Prognosis, which gives information about the safety of the structure, for example the residual life of the structure.

There are many different types of structural damage phenomena, such as: Corrosion, Cracks, Delamination and de-bonding, Fiber pullout, fiber breakage and matrix cracking, Fretting in crevices: slips, loose joints, and fasteners, Creep, Buckling, Penetration and plastic deformation, Welds, weld defects and Residual stresses.

For SHM, destructive techniques and non-destructive techniques are usually adopted. There are many different non-destructive techniques: Radiography , Ultrasonic testing , Acoustic emission, vibration-based methods, Optical methods, Thermography , Electromagnetic testing, Magnetic particle inspection. In the current work, we focus on the vibration-based methods.

The vibration based SHM studies the damage detection using the Eigen properties of the structure under dynamic tests. (Friswell and Mottershead et al., 1995)

There are two main approaches dealing with the problem of damage identification:

Model-driven approach and Data-driven approaches. In the Model-Driven Approaches, high-fidelity physical model of structure is established. It can potentially work without validated damage model, never the less, the drawback of this method is noise and environmental effects are difficult to incorporate. In contrast, in the Data-Driven Approaches statistical model of system is established. Date is required from all classes of damage, but the advantage is that noise levels and environmental variation are established naturally. The Data-Driven approaches contain the following steps: Sensor, Pre-Processing, Feature Extraction, Post-Processing, Pattern Recognition and Decision.

Series of sensors are installed on the structure, which provide a quantitative electrical signal proportional to structural or environmental variable of interest. Sample rate will depend om data being measured, and issues such as sensor placement and sensor validation should be taken in due account.

Pre-processing consists of two tasks to prepare data for feature extraction: Cleansing of raw data and Dimension reduction. Data cleansing involves noise removal, spike removal, outlier removal and treatment of missing data values. At the same time, dimension reduction means to eliminate redundancy in data. These two tasks are carried out based on the experience and engineering judgment.

Feature Extraction stands for distinguishing feature from pattern recognition

literature, aiming to magnify the characteristics of various damage classes and suppress normal background behavior, based on statistics or engineering judgement.

Post-Processing is the last step of preparation for pattern recognition, which is often subsumed into feature extraction. It could be normalization of feature vectors as required by the pattern recognition algorithm, or more advanced such as nonlinearly transforming the data to produce some probability distribution.

As the most critical stage of the process, Pattern Recognition means feature vectors passed to an algorithm which can classify the data. Depending on desired diagnosis, it can be distinguished into three types of algorithm: Novelty detection, Classification, Regression.

Decision and action are based upon pattern diagnosis. May be automated or may require human intervention.

The stages of Model-Driven Approaches are illustrated as following:

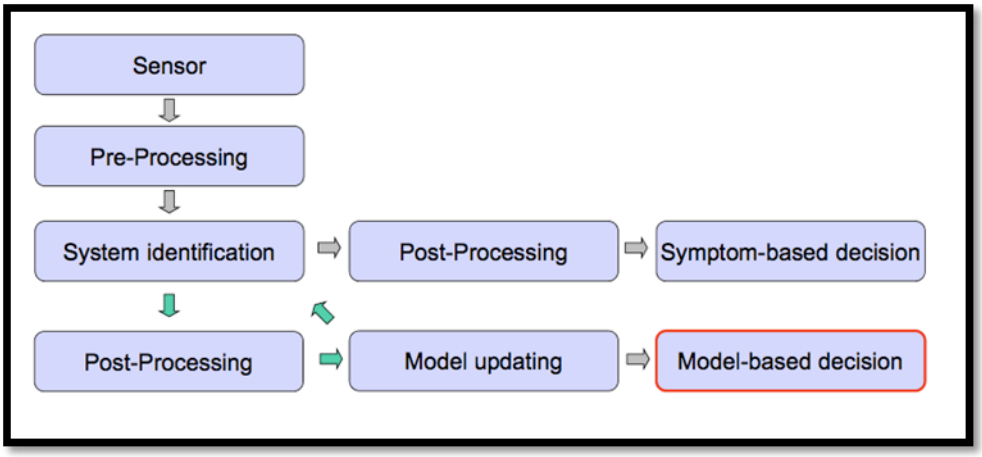

System identification aims at extracting information about the system's model. It is the core of any dynamic characterization process. Identified parameters are expressed in a more convenient form. (Friswell and Mottershead et al., 1995)

Varied or anomalous parameters are associated to damage, and reliability can be defined as a function of identified quantities that reflects the damage, referred to as symptoms.

A numerical model is updated on the grounds of the identified parameters. Model updating may be direct (single step correction) or indirect(recursive minimization of a penalty function).

2.2 System Identification

Few more steps are requested for updating purpose. In the following are summarized the fundamentals:

- The structure is a continuous system. it means that it has infinite degrees of freedom;
- The real frequencies and mode shape are not gotten anymore from a simple eigenvalue decomposition since the masses and stiffness are usually unknown. What people usually extract from experimental test are time series. These time series are plots of how much a quantity such as acceleration, velocity, displacement changes during the time due to an exciting force. The nature of exciting force is hard to determine when it is not applied artificially, it depends by the external environment affected by the uncertainties and noise, especially for real.

In this chapter we explain how to get modal frequencies and mode shapes from a simulated time series data. So, what we are basically doing is:

1. Define a numerical model (one of those proposed in the numerical examples), whose properties such as stiffness and masses are known;
2. From the eigenvalue decomposition we get natural frequencies and mode shapes;
3. Simulate a time series –accelerograms- from the frequencies and mode shapes;
4. Apply the system identification input-output algorithm (Betti & al. 2003) on these accelerograms to get estimated frequencies and mode shapes.
5. Try to update the model using the sensitivity analysis through the natural frequencies and mode shapes detected.

2.2.1 System identification techniques

In order to obtain a dynamically realistic numerical model of a structure, it is necessary to identify the dynamic characteristics such as the natural frequencies and the mode shapes -if a dynamic identification is requested- and also to develop a numerical model that can simulate the real behavior. Modal or system identification can be performed based on different types of test, including free vibration, force vibration and ambient vibration tests. It is simpler for identification purpose the identification of dynamical characteristics when the input forces are known. Using input/output system identification algorithms. For laboratory structure or small-scale structure the forced vibration tests are easy to manage and the exciting forces are manageable, but in a full-scale structure it is seldom possible due to the amplitude and lack of controllability of external forces like traffic, wind and sea waves, earthquake. So, for this structure we know only the output of the sensors record. They require much easier experimental processes, although they are not so reliable as the ones obtained by the input-output techniques. Those methods are called output only stochastic system identification methods. (Juang, Phan, Horta, Richard Longman Nasa Center et al., 2011).

2.2.2 OKID/ERA Method

The choice of a model is strongly affected by the engineer's experience and his/her ability in recognition. After the assumption that a model could represent the dynamical behavior, it is possible to analyze the measurements using a procedure able to convert the data in useful information for the updating, i.e. converting accelerograms into frequencies and mode shapes. In this report the algorithm called OKID/ERA is used to reach structural identification through the dynamic information. The data required for the identification by OKID are the input exciting forces and the output responses. The data sets can be information of velocity, displacement and time. For our purpose data deriving from acceleration are used. The OKID can reach the frequencies of the modes and Mode shapes information in the point where the sensors are positioned. Those output data sets become the measurements to use for the model updating through the Sensitivity analysis. Solve the time domain equations to compute the Markov parameters from the input and output data. Requires to invert an input matrix that is particularly large. The algorithm directly computes the Markov parameters of a steady-state Kalman filter from experimental data.

The OKID/ERA, rather than identifying the system Markov parameters that may exhibit a slow decay, it uses an asymptotically stable observer: it is an artifice to compress the data. The user has to define the decay rate of the observer.

Before continuing to explain how the OKID/Era works it is necessary to explain what are a steady-space and the Markov parameters. The Markov parameter sequence for a state-space model is a kind of matrix of impulse response. A real system is a continuous system; in the analysis with OKID/ERA it

is replaced by a discrete. The state-space representation is especially powerful for multi-input, multi-output (MIMO) linear systems, and also for time-varying linear systems. State-space models are also used extensively in the field of control systems. Here it is explained the relationship between the input and output histories in terms of Markov parameters. The impulse response of the state-space model can be summarized as:

If we describe the dynamic equation of motion for a system with 1 degree of freedom, we can write the following:

$$m\ddot{y} + c\dot{y} + ky = u \qquad [2.1]$$

$$\ddot{y} = -\frac{c}{m}\dot{y} - \frac{k}{m}y + \frac{1}{m}u \qquad [2.2]$$

Where y is the free coordinate of the system. *u* is the input exciting force, m is the mass, k is the stiffness value and c is the damping factor.

If we assume that $\mathbf{y} = \mathbf{x_1}$ and $\dot{\mathbf{y}} = \dot{\mathbf{x}}_1 = \mathbf{x_2}$, we can rewrite the previous equation as:

$$\ddot{y} = -\frac{c}{m}x_2 - \frac{k}{m}x_1 + \frac{1}{m}u \qquad [2.3]$$

But we also know that $\dot{\mathbf{y}} = \mathbf{x_2}$, so $\ddot{\mathbf{y}} = \dot{\mathbf{x}}_1$. And we can write a linear system on the two unknowns:

$$\begin{cases} \dot{x_1} = x_2 \\ \dot{x_2} = -\frac{k}{m}x_1 - \frac{c}{m}x_2 + \frac{1}{m}u \end{cases} \quad [2.4]$$

These equations are easily solvable in the unknowns x1 and x2. This equation is controllable and the space in which it is defined is called state-space. If we describe the dynamic equation of motion for a system with N degrees of freedom we can write:

$$[\mathrm{M}]\ddot{\mathrm{y}} + [\mathrm{C}]\dot{\mathrm{y}} + [\mathrm{K}]\mathrm{y} = \mathrm{u} \quad [2.5]$$

Where: M∈NxN; y∈Nx1; u ∈ Nx1.

Solving a second order differential equation is not simple from a numerical point of view. We introduce thus two new vectors, using the same approach used with one degree of freedom:

$$\mathrm{x} = \begin{bmatrix} \mathrm{y} \\ \dot{\mathrm{y}} \end{bmatrix} \text{ and } \dot{\mathrm{x}} = \begin{bmatrix} \dot{\mathrm{y}} \\ \ddot{\mathrm{y}} \end{bmatrix} \quad [2.6]$$

thus:

$$\begin{cases} \dot{\mathrm{x}} = \begin{bmatrix} 0 & 1 \\ -\mathrm{M}^{-1}\mathrm{K} & -\mathrm{M}^{-1}\mathrm{C} \end{bmatrix}\mathrm{x} + \begin{bmatrix} 0 \\ \mathrm{M}^{-1} \end{bmatrix}\mathrm{u} \\ \ddot{\mathrm{y}} = [-\mathrm{M}^{-1}\mathrm{K} \quad -\mathrm{M}^{-1}\mathrm{C}]\mathrm{x} + \mathrm{M}^{-1}\mathrm{u} \end{cases} \quad [2.7]$$

The matrices and vector in the [2.7] are called Markov parameters and are to be determined through the input and output data sets. X and its derivative are now two vectors with the size that is double than the one given by the [2.4]. A

continuous state-space system is characterized by continuous variable, thus:

$$\begin{cases} \mathbf{x} = \mathbf{A}_c\mathbf{x} + \mathbf{B}_c\mathbf{u} \\ \mathbf{y} = \mathbf{C}_c\mathbf{x} + \mathbf{D}_c\mathbf{u} \end{cases} \quad [2.8]$$

$$A_c = \begin{bmatrix} 0 & 1 \\ -\mathbf{M}^{-1}\mathbf{K} & -\mathbf{M}^{-1}\mathbf{C} \end{bmatrix}$$

$$B_c = \begin{bmatrix} 0 \\ \mathbf{M}^{-1} \end{bmatrix}$$

$$C_c = [-\mathbf{M}^{-1}\mathbf{K} \quad -\mathbf{M}^{-1}\mathbf{C}]$$

$$D_c = \mathbf{M}^{-1}$$

The subscript ''c'' indicates that the matrices are continuous. With the experimental data we acquire inputs and outputs in a discrete form, so, we can rewrite the [2.7] using discrete expression:

$$\begin{cases} \mathbf{x(i+1)} = \mathbf{Ax(i)} + \mathbf{Bu(i)} \\ \mathbf{y(i)} = \mathbf{Cx(i)} + \mathbf{Du(i)} \end{cases} \quad [2.9]$$

The relationship between the discrete matrix and the continuous one is:

i.e. $B = \int_0^T e^{A_c(t-\tau)} B_c u(\tau) d\tau$ [2.10]

Where x(i) is a state nx1 vector at time i. u(i) is the mx1 inputs vector, y(i) is the qx1 outputs vector. If we assume zero initial condition we can write:

u(i)=1 for i=0; u(i)=0 otherwise. Also in the initial condition x(0)=0.

Thus from the equation [2.8]:

for i=0;

$$\begin{cases} x[1] = B \\ y[0] = D \end{cases}$$

for i=1;

$$\begin{cases} x[2] = AB \\ y[1] = CB \end{cases}$$

for i=2;

$$\begin{cases} x[3] = A^2B \\ y[0] = CAB \end{cases}$$

And in conclusion for i=n-1;

$$\begin{cases} x[n] = A^{n-1}B \\ y[n-1] = CA^{n-2}B \end{cases} \quad [2.11]$$

So, summarizing:

$$y = Y \cdot U \quad [2.12]$$

Where each component are:

$$y = [y(0)\ y(1)\ y(2) \quad y(n-1)\ ] \quad [2.13]$$

It is the outputs data matrix of dimension qx*l*, where *l* is the number of samples. Then:

$$Y=[D \quad CB \quad CAB \quad CA^{n-2}B] \quad [2.14]$$

is the number of inputs. Its dimension is *qXml* where q the number of inputs, m the number of outputs and l the number of samples. The Y matrix contains all the Markov parameters D, CB, CAB, …, $CA^{n-2}B$ to be determined. The matrix U is an upper triangular block which dimensions are *mlXl*.

From this equation it is possible to solve and obtain the Markov parameters as:

$$Y = y \cdot U^{-1} \qquad [2.15]$$

Sometimes, the problem is ill-conditioned and, sometimes the solution appears to be not unique, but with some mathematical equations it is still possible to obtain a unique and stable solution. For more information read the paper of Juang and Phan. (Juang, Phan, Horta, Richard Longman Nasa Center al., 2011)
The measured structural outputs, Y(t), is related to the state vector, x(t), and to the input vector, u(t), through the system's matrix A, the input matrix B, and the output matrices C and D. The last two matrices depend on the types of measurements available (displacements, velocities, or accelerations). The system's matrix as well as the input and output matrices can be obtained from the singular value decomposition of the Hankel matrix containing the system's Markov parameters. However, for lightly damped systems, the number of the system's Markov parameters needed to provide a reliable representation of the system becomes too large and this introduces substantial numerical error that impairs a correct estimation of the system's matrices. The insight of Juang and Phan solves the problem of ill condition and numerical error when the matrix U is large. Instead of solve the Markov parameters of the real system, a fictitious observer with high damping factors is used as first to determine the system and then used to retrieve the system's Markov parameters. Such parameters are then included in the Hankel matrix and used to obtain a first-order system representation.

To better explain how the OKID/ERA input-output works a simple shear type system is shown.

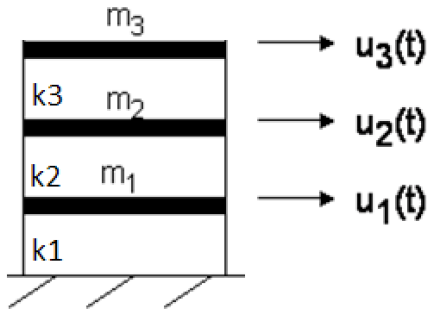

Image : Shear type system.

This numerical model explains how the OKID/ERA works. If we assume that the inter-story stiffness, the masses and the damping factors are known it is possible to obtain, from the eigenvalue decomposition, the natural frequencies and the mode shapes. This numerical result are the one that we have to obtain also from the OKID/ERA to identify the system.

So:

k_i=3500 kN/m;

m =2000 kg.

the damping is assumed to be proportional to the to the stiffness and mass values.

The frequencies and mode shapes get are:

Frequencies: [2.9631; 8.3023; 11.9972]

Mode shapes:

Λ_1: [-0.2319; -0.4179; -0.5211]

Λ_2: [0.5211; 0.2319; -0.4179]

Λ_3: [-0.4179; 0.5211; -0.2319]

In order to compute the OKID/ERA it is necessary to have inputs and outputs time series data sets, so also fictitious accelerograms are created. These accelerograms

are built both for the exciting forces and for the output responses. Since we know [K], [M] and [C], we can directly obtain the matrix A,B,C,D used to simulate the state space. So, it is possible to get the outputs signal directly from the equation [3.6]. As input signals it is used a Random Gaussian Signal. in the outputs also the 10% of noise is introduced. The outputs can be displacements, velocities and accelerations. In this case are used acceleration outputs. The outputs are dependent by the type of the structures and their expressions is strictly related to the mass and stiffness properties. The outputs depend by the dynamic system used and by the input signal. In the first example we assume to have exciting forces on every story and sensor on every story. It means that the we have three input accelerograms and three outputs accelerograms.

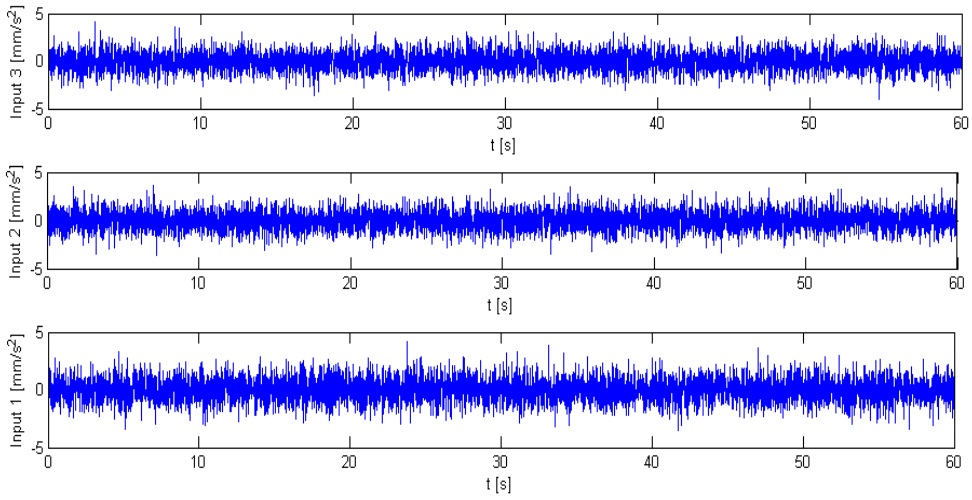

Image : input signals

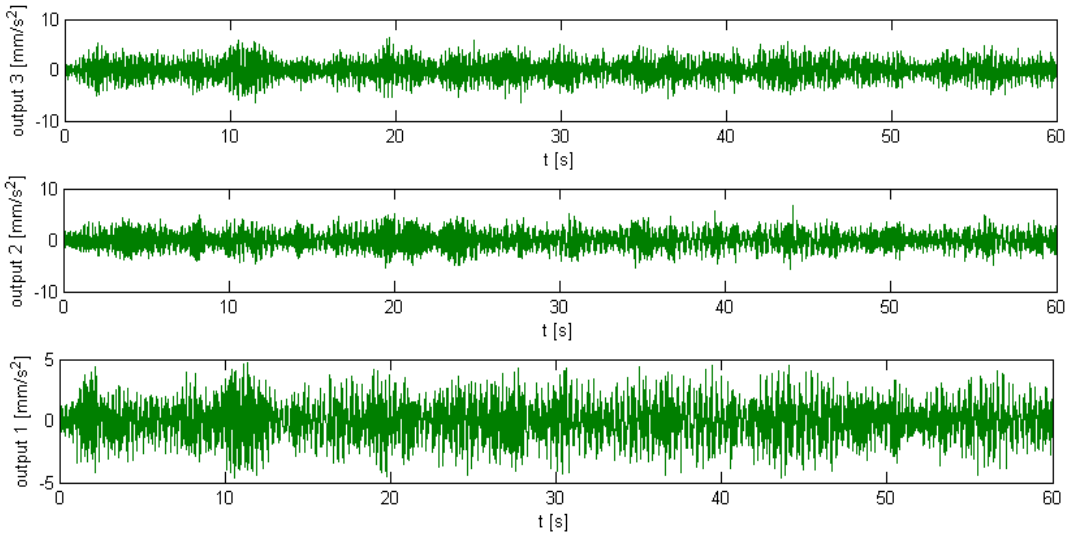

Image : outputs signals.

These six accelerograms are used as data to obtain the dynamic identification of the system. The dynamic identification gives information about frequencies and mode shapes of the system.

From the analysis with OKID/ERA, we get:

Frequencies estimated: [2.9627; 8.3028; 11.9995]

Mode shapes estimated:

Λ_1: [-0.2218; -0.5000; -0.3973]

Λ_2: [-0.4012; -0.2223; 0.50000]

Λ_3: [-0.5000; 0.39950; -0.2207]

Now we show a different configuration of input signals. We basically simulate the effect of a ground motion. A ground motion produce translations in the degrees of freedom as well. The only things that change are:

- The exciting force is proportional to the mass matrix;

· The input signal is applied at the base of the structure.

For these two reasons the expressions [3.4] and [3.6] change. The exciting force is not still u, but:

$$\begin{bmatrix} m_1 & 0 & 0 \\ 0 & m_2 & 0 \\ 0 & 0 & m\_3 \end{bmatrix} \begin{Bmatrix} 1 \\ 1 \\ 1 \end{Bmatrix} \ddot{a}(t)_g \qquad [1.16]$$

Where the exciting force at the base works as an inertia force. The mass matrix gives the value of the mass for every degrees of freedom, the vector gives the dynamic participation factor for every degree of freedom. Since the whole horizontal displacements are involved, the vector is a unit vector. For this reason the equation [3.4] and [3.6] changes their expressions and:

$$[\mathrm{M}]\ddot{\mathrm{y}} + [\mathrm{C}]\dot{\mathrm{y}} + [\mathrm{K}]\mathrm{y} = [\mathrm{N}]\{\mathrm{i}\}\ddot{\mathrm{a}}(\mathrm{t})_{\mathrm{g}} \qquad [1.17]$$

And from the [3.6] we get:

$$B = \begin{bmatrix} 0 \\ M^{-1} \end{bmatrix} M\{i\}\ddot{a}(t)_g = \begin{bmatrix} 0 \\ \{i\} \end{bmatrix} \ddot{a}(t)_g \qquad [1.18]$$

$$D = M^{-1}M\{i\}\ddot{a}(t)_g = \{i\}\ddot{a}(t)_g \qquad [1.19]$$

Here the accelerograms used.

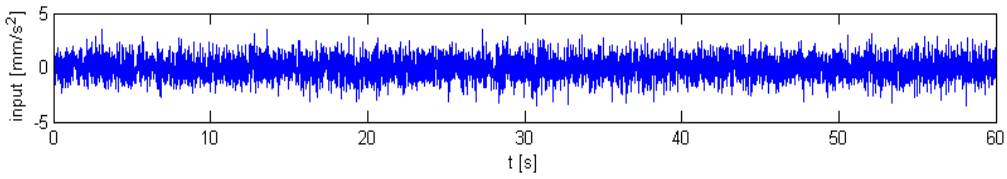

Image : the input signal is only the ground motion applied at the structure

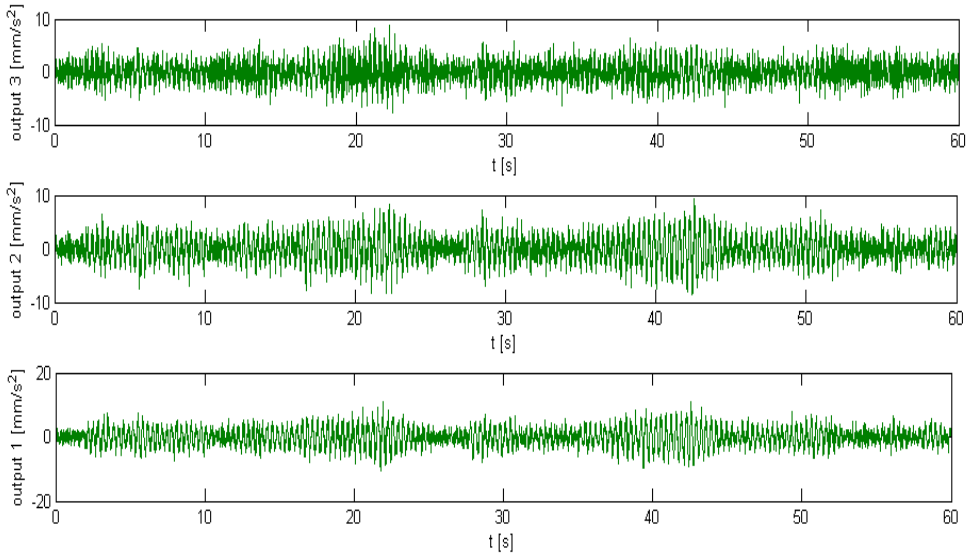

Image : outputs from the structure with ground motion.

From this configuration we get:

Frequencies estimated: [2.9631; 8.3024; 11.999]

Mode shapes estimated:

Λ_1: [-0.2239; -0.5000; -0.4068]

Λ_2: [0.4004; -0.2239; 0.50000]

Λ_3: [0.5000; 0.4020; -0.2279]

Comparing the result we get:

Percentage variation in frequencies [%]			
OKI/ERA results	f1	f2	f3
1	0.013	0.006	0.019
2	0.000	0.001	0.015

Table 2.1: Variation in frequencies respect to the real ones

The variation is less than the 0.1%. if we plot the mode shapes the result looks similar as well.

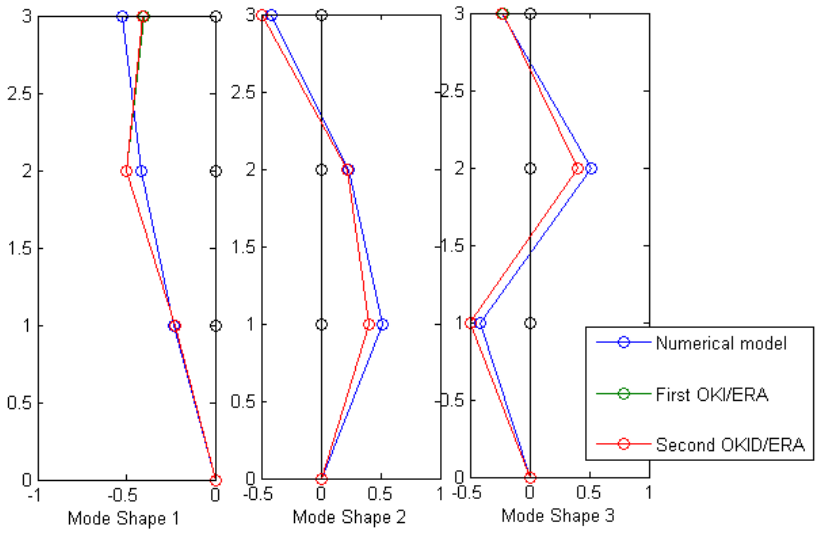

Image : mode shapes comparison

The mode shapes collected look very similar and it is worth to use them in the calibration procedure. It is usually like a rule of thumb, that the frequencies are gotten with higher precision ten rather than the mode shapes. If information based on covariance are available, the y can be used as weights in the updating procedure.

The mode shapes and the frequencies are used in the algorithm developed for the model updating. The system with exciting forces on every degrees of freedom is called *case 1*, while the system with ground motion is called *case 2*. We also assume the mass coefficients constant and the only ones subjected to update are the stifnesses. The results got are:

	K1	K2	K3
	[N/m]	[N/m]	[N/m]
Case 1	3498	3505	3480
Case 2	3512	3507	3497

Table 2.2: Model identified with OKID/ERA algorithm

Before apply the algorithm to experimental data sets it is worth to analyze how it works when there is a high number of degrees of freedoms. This check is done using a numerical structure. The input and output time histories have been simulated in a state space with 10% of noise and then processed in Matlab®. The structure is excited in each Dof and a scenario with full instrumentation is assumed. Thus the input accelerograms are 14 and the outputs are 14 as well.

To look also for the reliability with an high number of coefficients is contemporaneously subjected to update. The degrees of freedom are the vertical translations -the displacements along the z axis-. The response of the structure is simulated in each Dofs and the number of coefficients subjected to update are only the stifnesses -14 stifnesses coefficients-. For each bar of the structure only one value of stiffness is assumed. The masses values are $1.25*10^5$kg and stiffnesses of

$7.123*10^7$ N/m. For the finite element model updating the mass matrix is assumed to be diagonal and the stiffness matrix not fully populated, but with the correct shape. Due to the numbering order the [K] matrix results being diagonal with the first, second and the third diagonals are non-null.

Thus:

Degrees of freedoms:

$$\{U_{z_1};\ U_{z_2};\ U_{z_3};\ U_{z_4};\ U_{z_5};\ U_{z_6};\ U_{z_7};\ U_{z_8}\}; \qquad [2.20]$$

The calibration procedure leads to this table:

Coefficients detected [10^5N/m]									
k_1	k_2	k_3	k_4	k_5	k_6	k_7	k_8	k_9	k_{10}
7.129	7.060	7.150	7.139	7.139	7.110	7.142	7.139	7.099	7.110

Table 2.3: Stiffness detected

Percentage variation respect to the theoretical values [%]									
k_1	k_2	k_3	k_4	k_5	k_6	k_7	k_8	k_9	k_{10}
0.09	-0.88	0.37	0.23	0.23	-0.18	0.26	0.22	-0.33	-0.18

Table 2.4: Percentage variation

Chapter 3

Finite element model updating techniques

· *Description of mathematical model*: basically a real structure can be represented as infinite degrees of freedoms. Due to a high computational cost for the representation of a structure as continuous one, it is better to approximate it with a discrete model. This is done by introducing the structure masses, stiffness and damping factors. This model is the analytical model and may be expressed with square matrices of stiffness [K], mass [M] and dumping factor [L].

· *Numerical simulation*: the more the nodes in a structure, the better the precision of the model to represents the real structure. But the computational cost becomes higher. A good model is able to predict the behavior of the principal nodes, without being affected by the common problem in finite element method.

- *Experimental Validation*: the last step is the comparison between the experimental and the analytical results. This step represents the most important step in the analysis because it can tell if the model is capable to represent the real structure.

The objective of finite element model updating is to minimize the residual between the experimental and analytical outputs by changing the masses and/or stiffness and/or damping factors. Different techniques may be used for the updating, but all of these follow the same principal steps: (Mallano T., et al., 2014)

- *The choice of the residuals:* the choice of the output data to be compared should be done from analytical and experimental information. For static measurements due to self-weight or well-defined loads, displacements, stresses are chosen. For dynamical measurements frequencies and mode shapes are chosen.
- *The choice of parameters:* the parameter subjected to update are those who are uncertain. For example, it is well known that the elastic modulus of concrete changes with time due to aging and the moment of inertia can change as well due to cracking; it may happen also that due to inappropriate construction procedure some parameters changes.
- *The choice of the objective function:* the objective function is the function that is used to compare the analytical and experimental outputs. Usually, the objective function is a difference between them.
- *The choice of the boundary condition:* usually for the updating of the model it is necessary to fix some conditions on the variation of the

parameters. It is possible to fix the mass matrix [M] and do the update only on the stiffness parameters, it is possible to fix the boundary of variation of some parameters. It is possible to define a small range of variation to decrease the search space, in this way the convergence is much faster.

- *The choice of the optimization methods:* in literature there are a lot of updating techniques; some of those are based on the using of nonlinear searcher, some on the information of the Jacobean of the function. The difference in these approaches is usually not only the method used to do the update, but also the computational cost. The more convoluted is the algorithm, the slower is the time of analysis.

3.2 LIMITS

Every finite element model updating method has the target to calibrate the model built with finite elements, as similar as possible, to the real structure, which is usually solved with an optimization algorithm. Thus the value of an objective function that express the residuals between the measurements and analytical outputs of a system is going to be minimized after a certain number of steps. This is an inverse problem. An inverse problem is a general framework that is used to convert observed measurements into information about a physical object or system. This is useful because it generally tells us something about a physical parameter that we cannot directly observe. Thus, inverse problems are some of the most important and well-studied mathematical problems in science and mathematics. Inverse problems arise in many branches of science and mathematics, including computer vision, natural language processing, machine learning, statistics, statistical inference, geophysics, medical imaging (such as computed axial tomography and EEG/ERP), remote sensing, ocean acoustic tomography, nondestructive testing, astronomy, physics and many other fields. In structural field, proprieties as moments of inertia, elastic modules and damages could be detected with this approach, trying to minimize the differences with those information. Comparing the outputs to find a physical system, many times, can lead to solutions that are not unique which can be caused by:

· The presence of errors in measurements; every time that an experimental test is done or some data set are recorded during a survey on a real structure, the measurements are affected by errors. When the data set is affected by great

uncertainties there is also an uncertainties when the inverse problem is solved. It means that the solution related to the minimum of the objective function could be not the only one able to represents the real structure and many good solutions can be found instead of one only model. (Mallano T., et al., 2014)

· The incompleteness of measurements; when not all modal information are recorded during a survey due to the impossibility to put on the structure a sensor or due to the availability of a few number of it, the measurements can be considered incomplete. When the data set obtained is incomplete it is possible that solving an inverse problem could lead to multiple solution.

· Not enough steps; when a multi-step method based on iterative procedure is used, the number of steps run could be not enough to reach the solution, and if you try to do the same calibration starting from a different configuration of parameters, another solution can be found.

The inevitable presence of different kinds of errors exists during the research of the solution. The way in which they can appear is very random. Some of those are involved with measurements since the beginning, depending on the sensitivity of instruments. Some others appear during the analytical realization of the model; doing some assumption can lead to a solution that is not good at all or that is not very close to the real one due to a misunderstanding of a dynamical behavior. Some others are generated during the numerical calibration and are related to the solution of the second or first order differential equations. When all of those errors occur it is possible that a solution which is not appropriate can be reached. A good engineer is able to reduce the magnitude of errors changing the assumption for a finite element model, using the sensors in a condition that is at least with controlled noise. The errors are classified in the introduction. Here we

consider three commonly encountered forms of model error which may give rise to inaccuracy in the model prediction:

- *e1 model structure errors*, which are liable to occur when there is uncertainty concerning the governing physical equations and might occur typically in the modelling of non-linear behavior in certain systems;
- *e2 model parameter error*, which would typically include the application of inappropriate boundary conditions and inaccurate assumptions used in the order to simplify the model;
- *e3 model order errors*, which arise the discretization of complex system and can result in a model of insufficient order. The model order may be considered to be a part of the model structure.

Usually those error occur together and the result is an error.

$$e_{tot} = e_1 + e_2 + e_3 \qquad [3.1]$$

The reader should perhaps be reminded that errors are associated not only with numerical models but also with experimental testing. It is well known that the dynamic of structure, may be affected by masses and stiffness of equipment used to excite or measure the vibrations. Errors in natural frequencies due to the mass of roving accelerometer are especially common in modal analysis. Transverse motion and base bending of accelerometers, and accelerometer cable noise, are common sources of error in test data. Thus:

$$x_{real} = x_{measure} + e_{measure} \qquad [3.2]$$

$$x_{real} = x_{model} + e_{model} + e_{measure} \qquad [3.3]$$

$$x_{real} = x_{model} + e1 + e2 + e3 + e_{measure} \quad [3.4]$$

Where x_{real} is the real value, that is the target, and it is linked through the expression [3.2] and affected also by errors. The errors cumulated during this process are not separable.

$$| xmeasure - xmodel | = | xmeasure - xreal + xreal - xmodel | \quad [3.5]$$

$$| xmeasure - xmodel | = | - emeasure + e1 + e2 + e3 + emeasure | = | e1 + e2 + e3 | \quad [3.6]$$

It is possible to reduce independently these errors introducing more accurate way to take into account measurements with more pricise sensors or doing finite element approximation with best assumption.

Since these errors always exist in the experimental data and in the outputs of the numerical analysis, we have to manage these quantities using good correlation instruments. In literature there are different instruments of correlation. We are showing one related to mode shape information. The MAC (modal assurance criteria) was introduced by Allemang and Brown in 1982 (Randall J. Allemang al., 1982) which is an natural number:

$$MAC_{ik} = \frac{\left|\{\Phi_{m_i}\}^T\{\Phi_{a_k}\}\right|^2}{\{\Phi_{m_i}\}^T\{\Phi_{m_i}\}\{\Phi_{a_k}\}^T\{\Phi_{a_k}\}} \quad [3.7]$$

It indicates the correlation between two mode shape vectors to match two mode shapes.

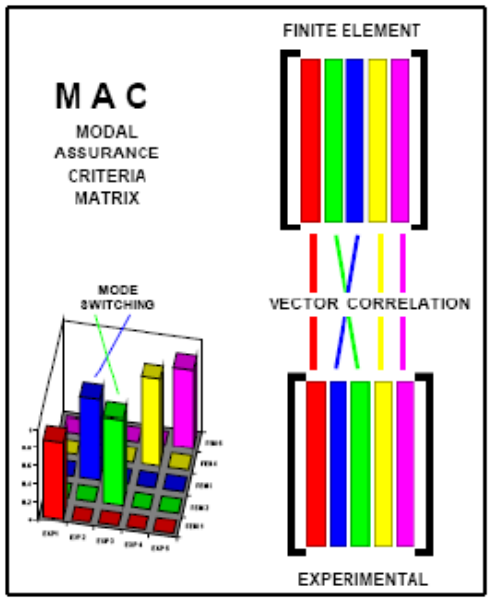

Image 1: explanation of the MAC

MAC equal to 1 indicates a good correlation with the parameter, while a MAC verging to 0 indicates a bad correlation between the mode shapes. The experimental and analytical mode shapes must contain the same number of elements. Note that complex mode shapes may be correlated using the MAC so long as the transpose is taken to be conjugate transpose. If the modes pair in numerical order, then the Mac matrix will have values close to 1 on the diagonal and values close to 0 elsewhere. With the MAC information it is possible to order the frequencies and the mode shapes to collect a good approximation of the parameters.

3.3 DETERMINISTIC APPROACH

The calibration of a model could be done also based on equations that represents the behavior of the model. In this way it is possible to calibrate a model trying to minimize an equation or an objective function that can express the differences between the numerical and experimental data. In this way we can define a first class of model updating methods called *deterministic methods*. These methods can be divided into two groups:

- Direct method ;
- Parametric method.

The first ones are usually known as one-step method, because they are non-iterative methods. Those can reach the solution applying the variation of parameters directly on the matrices that represents the problem. The second ones are usually known as multi-step method, because they iteratively modify the parameters' values introducing a variation until the convergence is reached. (Mallano T., et al., 2014)

3.3.1 DIRECT METHODS

It is well known that the finite elements are based on the material properties, such as Young's modulus, Poisson's ration, mass density, etc., and the physical dimensions of the real system. Certain updating schemes provide no opportunity for the user to select parameters for updating. These methods are known as 'direct' methods and the entire stiffness and mass matrices are updated in a single step. Consequently any physical meaning, which the initial finite element model might have possessed is lost in the updating process. The direct methods are the simpler and quick ones. It's simple because it doesn't require any iterative procedure and the time of evaluation is rapidly reduced. The drawback of these methods is that sometime the solution found has not any physical meaning, and it is impossible to find out what kind of variations are applied to the initial matrices. The direct methods are able to find a solution that perfectly matches the experimental data set. It looks like that the calibration target is reached easily and quickly with a very small residual; but actually, even if it is the target of the calibration procedure it would be necessary to check if the parameters have a physical meaning.

3.3.1.1 METHOD OF THE LAGRANGE MULTIPLIERS

The Lagrange multiplier method is simply and convenient for minimizing a function subjected to well-defined constraints on the independent variables.

REFERENCE-BASIS APPROACH

The model updating methods based on the Lagrange multipliers are indeed the most important based on this approach. According to these methods, the reference basis, which must be one parameter set taken from other masses, stiffness or measured modes, is considered to be inviolate. The two remaining parameter sets are then updated separately by minimizing an objective function, which constraints imposed through Lagrange multipliers. It should be recalled that, in constrained minimization, Lagrange multiplier methods result in the strict imposition of the constraints, whereas penalty methods allow flexibility to a degree which is controlled by the penalty number.

Baruch and Bar Itzhack (Baruch, M. et al., 1984) obtained updated eigenvector data by minimizing the mass-weighted norm of distance between the analytical and observed vector. In some works the norm that included the completely stiffness matrix [K] and mass matrix [M] is used and, as result, what has been get is a new configuration of [K] and [M]. In this work Lagrange multipliers are used to enforce satisfaction of the analytical mass and stiffness symmetry. The model reference basis approaches have been the focus of considerable attention in structural dynamics research. Some authors such as Berman and Nagy minimized the objective function:

$$J_M = \left\| M_A^{-\frac{1}{2}}(M - M_A)M_A^{-\frac{1}{2}} \right\| + \sum_{i=1}^{m}\sum_{j}^{m}\lambda_{ij}(\Phi^T M\Phi - I) \qquad [3.1]$$

Where λ_{ij} is the Lagrange multiplier used to enforce the orthogonally of the vectors with respect to the updated masses. The minimization procedure results in the expression for the updated mass:

$$M = M_A + M_A\Phi m_a^{-1}\left(I - \Phi^T M_A\Phi \quad\right)\left(\Phi^T M_A\Phi\right)\Phi^T M_A \qquad [3.2]$$

$\Phi\epsilon R^{P\times M}$ and is an incomplete modal matrix because M<P and P is the order of the analytical and updated models. Following the computation of **M**, also the **K** array can be determined by minimizing a further objective function:

$$J_M = \left\| M^{-\frac{1}{2}}(K - K_A)M^{-\frac{1}{2}} \right\| + \sum_{i=1}^{m}\sum_{j=1}^{m}\lambda_{K_{ij}}(K\Phi - M\Phi\Lambda)_{ij} + \sum_{i=1}^{m}\sum_{j=1}^{m}\lambda_{O_{ij}}\left(\Phi^T K\Phi - \Lambda\right)_{ij} + \sum_{i=1}^{m}\sum_{j=1}^{i}\left(K - K^T\right)_{ij} \qquad [3.3]$$

Where: Λ represents the spectral matrix. Here the Lagrange multipliers are used to enforce the equations of motion, orthogonally and stiffness symmetry. The stiffness updating equations can be written as:

$$K = K_A + (\Delta - \Delta^T) \qquad [3.4]$$

Where Δ is obtained with the equation below:

$$\Delta = \frac{1}{2} M\Phi\left(\Phi^T K_A \Phi + \Lambda\right)\Phi^T M - K_A \Phi\Phi^T M \qquad [3.5]$$

It should be noticed that although $M^{-1/2}$ appears in the objective function J_M and J_K its computation is unnecessary since it is absent from the updating equations of M and K. Regarding the performance of the algorithm, the measured eigenvalues are reproduced exactly. It is possible to expand the modal reference basis technique by introducing additional Lagrange multiplier constraints to account for rigid body mass information, such as centre of gravity, total mass and moment of inertia.
In addition to the *reference-basis* methods there are also others called *matrix mixing*, *eigenstructure assignment*, and *inverse eigenvalue methods*.

3.3.1.2 MATRIX MIXING APPROACH

This approach is very common, as the reference bases are. This approach can be used only if the mode shapes information are known in every degree of freedom. The result and the calibration is done starting from the assumption of the orthogonality of the mode shapes:

$$\Phi^T M \Phi = I \qquad [3.6]$$

$$\Phi^{T^{-1}}\left(\Phi^T M \Phi\right)\Phi^{-1} = \Phi^{T^{-1}} I \Phi^{-1} \qquad [3.7]$$

$$M = \Phi^{T^{-1}}\Phi^{-1} \qquad [3.8]$$

And $M^{-1} = \Phi\Phi^T = \sum_{i01}^{m} \Phi_i \Phi_i^T$ [3.9]

And then the same for the stiffness matrix.

$$\Phi^{T}K\Phi = \Lambda \quad [3.10]$$

$$\Phi^{T^{-1}}(\Phi K\Phi)\Phi^{-1} = \Phi^{T^{-1}}\Lambda\Phi^{-1} \quad [3.11]$$

$$K = \Phi^{T^{-1}}\Lambda\Phi^{-1} \quad [3.12]$$

$$\text{And } K^{-1} = \Phi\Lambda^{-1}\Phi^{T} = \sum_{i01}^{m}\frac{1}{\omega i^{2}}\Phi_i\Phi_i^{T} \quad [3.13]$$

When happens that some experimental mode shapes are missed on some degrees of freedom of the structure it is possible to integrate those with the analytical one; in this case, again, *m* is the number of measured mode shapes and *p* is the number of degrees of freedom. The problem with assembling mass and stiffness matrices from data is that the number *m* of measured eigendata is usually significantly smaller than the order *p* of the required model. Structural matrices assembled on the basis of m<p eigenmodes are incomplete. The matrix mixing approach uses finite element modes where test data are unavailable. Thus:

$$M^{-1} = \sum_{i=1}^{m}\Phi_{T_i}\Phi_{T_i}^{T} + \sum_{i=m+1}^{p}\Phi_{A_i}\Phi_{A_i}^{T} \quad [3.14]$$

$$K^{-1} = \sum_{i=1}^{m}(\Phi_{T_i}\Phi_{T_i}^{T})/\omega_{T_i}^{2} + \sum_{i=m+1}^{p}\Phi_{A_i}\Phi_{A_i}^{T}/\omega_{A_i}^{2} \quad [3.15]$$

Where the subscript A and T denote analytical and test data, respectively. The matrix mixing method generally returns full mass and stiffness matrices which bear little relation to physical connectivity.

3.3.1.3 EIGENSTRUCTURE ASSIGNEMNT APPROACH FROM CONTROL SYSTEM

The eigenstructure assignment approach for model updating was developed by Minas and Inman. (C. Minas, D. J. Inman, et al., 1991) As the name suggested the method reproduces the measured eigenvalues and eigenvectors. If the eignenvalues alone are assigned then the method is often called pole placement. The method is very powerful in the control system design context.

In control engineering, system are often analyzed using the state space representation, which is the equation of motion is written as a first order ordinary differential equation. In structural dynamics the equation of motion is more often written as a second order ordinary differential equation incorporating the mass, damping and stiffness matrices. In this approach, state feedback is used to represents the right side of the dynamic equation of motion in terms of displacement and velocity states. The problem then reduces to determine the terms in the feedback gain matrix such that the eigenvalues and eigenvectors of the closed loop system are identical to the measured eigendata. The result is that modifications are made to the stiffness and damping terms but the analytical mass matrix remains unchanged. The equation of motion in terms of displacement is:

$$\mathbf{M\ddot{x} + C\dot{x} + Kx = B_0 u} \qquad [3.16]$$

Where /m, C, K are the positive matrices. The vector u is the input of control force

vector. The matrix B0 distributes the exciting force to the correct displacement degrees of freedom. Often it is not possible to measure all the displacement variables. Also the state space representation allows the measurement of the velocity. Sometimes the measurement is a combination of velocity and displacement vectors. y the is the measured vector that contains information of displacement and velocity:

$$\mathbf{y} = \mathbf{D_0 x} + \mathbf{D_1 \dot{x}} \qquad [3.17]$$

In control engineering the matrices B0, D1 and D0 are given, whereas in model updating these matrices have been chosen. And the problem is to find a control law able to express the problem. If we chose a law $u=Gy$ where G is the gain matrix, the one that gives the closest eigenvalues and eigenvectors in the end of a loop, can represents the equation of motion:

$$\mathbf{M\ddot{x}} + \mathbf{C\dot{x}} + \mathbf{Kx} = \mathbf{B_0}(\mathbf{D_0 G x} + \mathbf{D_1 G \dot{x}}) \qquad [3.18]$$

$$\mathbf{M\ddot{x}} + (\mathbf{C} - \mathbf{B_0 G D_1})\dot{\mathbf{x}} + (\mathbf{K} - \mathbf{B_0 G D_0})\mathbf{x} = \mathbf{0} \qquad [3.19]$$

The gain matrix G has provided perturbations on the damping and stiffness matrices given by the product of the second terms in the parenthesis. These perturbed matrices give updated matrices which can reproduce the measured eigenstructure. For our purpose it is sufficient to comment that, for a given system, there may not be any gain matrix G that reproduces a given set of eigenvalues and eigenvectors.

The updated stiffness and damping arrays are given by the follow:

$$K=K_A+B_0GD_0 \quad [3.20]$$

$$C=C_A+B_0GD_1 \quad [3.21]$$

Where B0 is an input distribution matrix, D0 and D1 are the matrices relating the outputs and states, and G is the feedback gain matrix. The matrices B0, D0 and D1 are derived from the excitation positions and the location and type of measurement. The matrix B0 may be chosen arbitrarily, and C0 and C1 must be chosen such that the sum $D1\Phi\Lambda+D0\Phi$ is nonsingular, it means that it is possible to obtain the inverse matrix. The terms in the matrix G are determined by eigenstructure assignment method. The matrices Φ and Λ contain the incomplete measured eigenvectors and eigenvalues. The eigenstructure assignment method requires the measurements of only $m<p$ eigenvector terms. This aspect is considerable useful, since the rotational and internal degrees of freedom, which are present in the finite element models, are largely unmeasurable in the experimental modal analysis. The unmeasured mode shape terms are recovered by using the finite element model which, for this purpose, must be a good representation of the structure under test. The issue of eigenvector expansion is central to all of the representation model techniques. This approach to be used requires the Lagrange multipliers. To find the Lagrange multipliers is computationally expensive, involving the calculation of the eigenvalues of a *pm x pm matrix*. Smith and Beattie considered quasi-Newton methods for stiffness updating which preserve the structural connectivity of substructures in frequency domain structural synthesis. (C. Minas, D. J. Inman, et al., 1991)

3.3.2 PARAMETRIC METHODS

The parametric method are developed and studied and used in the realization of this thesis. The correlation is determined by penalty function involving the mode shapes and eigenvalue data: often the sum of squares of difference between the measured and the estimated eigenvalues is used. These methods allow a wide choice of parameters to be updated and both the measured data and the initial analytical parameter estimates may be weighted. This requires engineering skills to provide correct weights. With the study of this approach is possible to get solution in a parametric way. It means that everything is done iteratively. This approach is also called multi-step method for its nature. The most important differences with the direct methods are listed in the following part. As first, the parametric methods try to find an accurate solution not scanning the matrices of mass and stiffness only, but also trying to find out the real physical parameters that affect the finite element problem, in this way it is possible to discover and show directly if the solution found has a physical meaning. Those parameters can be the elastic modules, the inertia moments, the geometry, the mass, the polar moments of inertia etc. The other difference is that these methods are quick and easy to be applied and the solution found matches pretty well with the experimental data set. The parametric methods were introduced to correct the weakness of the direct methods. The object of this methods based on a penalty function is to minimize the correlation between the measured and the analytical modal model. these methods allow a wide choice of parameters for updating, but the requirement to optimize a non-linear penalty function implies an iterative procedure, with the possible attendant convergence problems. Also, an iterative scheme requires the

evaluation of the analytical modal model at every iteration. When the change in the parameters between successive iterations is small, a good estimate of the modal model is available and may be used to improve the eigensystem calculation and efficiency. The input information for this method are eigenvalues (equivalent to the natural frequencies and damping ratios) and mode shapes. It is important that during the comparison between the experimental and analytical data the information must correspond in right position.

There are three major possible problems to compare the measured data and the corresponding analytical estimates.

- First, the natural frequencies and mode shapes in the experimental and theoretical data must be relate to the same mode: they must be paired correctly. Arranging the natural frequencies in the ascending order of magnitude is not sufficient, especially when two modes have close frequency values. Another problem in mode pairing is that not all the experimental modes may be measured accurately, usually because the force excitation or the accelerometer is placed close to a node of a particular mode shape. Mode shape pairing is easily solved using the modal assurance criteria MAC.
- The second problem is the mode shape scaling. Usually the analytical eigenvector are mass normalized. Because the mass distribution of the finite element model and the real structure may be different, the mode shapes may not be scaled consistently. It is possible to divide consistently all the rows of mode shapes matrix through one row of each, in this way it is possible to study the ratio between the mode shapes (not use as reference row a row with a nil value); or it is possible to use also a modal scale factor (MSF):

$$MSF = \frac{\Phi_i^T \Phi_{mi}}{\Phi_{mi}^T \Phi_{mi}} \qquad [3.22]$$

Multiplying by the modal scale factor it is possible also to solve the mode shapes that are 180 out of phase.

· The third problem is the damping. If damping is not present in the finite element model, then just the measured natural frequencies are included in the definition of measured and predicted response. When damping is included in the finite element model, the complex eigenvalues and mode shapes could be used in the measurement vector.

3.3.3.1 PENALTY FUNCTION METHODS

The penalty functions are generally nonlinear functions of the parameters, and so an iterative procedure is required with the possible associated convergence problems. Also an iterative procedure, due to the nature of the cost function, requires the evaluation of modal model at every iteration. If the change in parameters in successive iterations is small, a good estimate of the parameter is done. It means that the convergence of the solution has been reached.

3.3.3.2 SENSITIVITY ANALYSIS APPROACH

The methods generally are based on the use of a truncated Taylor series of the modal data as a function of the unknown parameters. This series is often truncated to produce the linear approximation. Both natural frequencies and mode shapes may be used in the updating procedure. Until now, the mode shape data was not generally used for updating for two reasons: the mode shapes often contain significant measurements errors, and it has to be normalized for consistency with the analytical model. Although the general shape of the mode shape vector is likely to be reasonable, elements of the vector may be up to 20% errors. In contrast, the natural frequencies can be measured to much better accuracy than 1% and can be used with confidence. The development of scanning laser Doppler measurements may improve the quality and the quantity of mode shapes data. These system are able to scan large areas of the structure quickly and give the mode shape at a large number of locations, without introducing errors by modifying the structure. Although the quality of each individual entry in the mode shape vector may not be improved, the increased number of elements with similar variance gives an overall increase in the quality of the data available. Mode shape data then becomes more significant in the updating process. When natural frequencies alone are used to update the analytical model the mode shape data is still required to pair the measured and the analytical natural frequencies. The usual method to achieve this match is the MAC. Distinguishing different modes by using the MAC may be difficult if the measurement locations on a structure are poorly selected. To produce a linear approximation usually the Taylor series expansion is often limited to the first two terms.

When there are more measurements than parameters, the matrix equation linearized provides more algebraic equations than unknowns, and the set of simultaneous equations is over determined. In many practical cases, the number of unknown parameter exceeds the number of measured data points. The set of equation is under-determined and there are an infinite number of sets of parameter which will satisfy the equation. In this case it is difficult to say which is the best solution for the problem, because everyone satisfies the numerical equations. In general the individual parameters may have magnitudes that differ considerably, for example the Young's modulus. The parameters should be normalized so their initial value is 1 to improve the numerical conditioning in the problem.

3.3.3.3 MINIMUM VARIANCE METHODS

Minimum variance method may be regarded as a penalty function methods in which the weighting matrices change in a particular way from one iteration to the next. The root of this approach are in the Bayesian method and these statistical techniques are most useful when the amount of data is large. What happens in the model updating field is that the amount of data is small, and can be regarded as a sample from the limited measurement data, because it provides a rational way to weight the measured and theoretically estimated data. Information that is possible to get from this method is the quality of the update of the single parameters since the variance is estimated. The minimum variance methods assume that both the measured data and the initial parameters estimates have errors that may be expressed in terms of variance matrices. Collins (Collins et al. 1974) introduced the minimum variance method on the assumption that the parameter estimates and measured data are statistically independent.

3.3.4 METHODS USING FREQUENCY DOMAIN DATA

The methods measured FRF data optimize a penalty function involving the FRF data directly. Extracting natural frequencies and mode shapes for structures with close modes or high modal density can be difficult. The FRF data may be used directly without extracting the natural frequencies and mode shapes. In this method the damping must be included in the finite element model. Since damping is so difficult to model accurately, usually proportional damping is used.

3.4 PROBABILISTIC APPROACH

The approach used is different respect to the one seen until now. The calibration or the model has become a statistical problem. The parameters subjected to update are not treated with direct formulation or with multi-step problem. During the calibration procedure of the model the presence of errors are taken into account. Some authors such as Beck and Katafygiotis(J. L. Beck, L. S. Katafygiotis et al., 1998) says that is worth to define probabilistic classes for the explanation of the variability of the parameters. In this case at the end of the analysis the result is a model in which each parameters has a statistical probability density function and error related to its estimation.

MONTE CARLO METHODS

Monte Carlo methods are a class of computation algorithm that rely on repeated random sampling to obtain the numerical results. Typically one runs simulations many times in order to obtain the distribution of an unknown probabilistic entity. This method are used when it is difficult or impossible to get a closed-form expression, or infeasible to apply a deterministic algorithm. The Monte Carlo's approach is similar to the genetic algorithm, but it is less efficient. In latter one, the generation of model has a valid criteria: only the strongest models are collected (called parents) and are the only ones able to produce valid alternative (sons) based on their ''generic'' information. The Monte Carlos approaches follow a particular pattern:

1. Define a domain of possible inputs;
2. Generate inputs randomly from a probability distribution over the domain;
3. Perform deterministic computation on the inputs;
4. Aggregate the results using a probabilistic function.

The deterministic computation is a set of equation that gives the result for that input. In this way it is possible to understand which inputs determine the defined outputs.

For more information on the Monte Carlo's approach applied to invers problems consul the Mares work.(C. Mares, J. E. Mottershead, M. I. Friswell et al., 2006)

3.5 MULTIPLE MODEL APPROACH

The previous methods have as only purpose the calibration of the model, trying to fix as better as possible the experimental data. Usually if the number of equation is bigger than the number of the unknowns the solution is unique. Classical methods focus on identifying the global minimum of this objective function, not identifying other minima with similar performance. Meanwhile, one of these local minima might represent the optimal solution for the problem. During this decade method based on a multiple solution have been developed. The purpose of these methods is to find solutions that are still located in minima of the objective function, but which parameters are able to show a valid alternative for the updating. The reasons why this method are used is the heavy uncertainties that usually the experimental data get during the surveys.

The method proposed by Smith and Saitta (Smith, Saitta et al., 2007) is based on the multiple models approach. The important aspect of this methodology is the generation of a population of candidate models. The development of this new approach is based onto the idea that a large number of models might predict responses that reasonably match the observations; therefore, procedures that match measured and predicted responses might lead to the identification of the wrong model. This is compounded by inevitable errors in modeling assumptions and inaccuracies during measurements. Now, these possible behaviors are taking into account with the generation of a population of candidate solutions in the feasible domain whose objective function values lie below a threshold. As in the other approaches the models are identified through matching measurements data with

model predictions. The calibration procedure involves the reduction of the residual between the experimental and the analytical solution; This assumption is valid only if we are sure that the measurements are correct. There are several factors that could influence the results. Errors influence the reliability of the algorithm.

The first step is the realization of the model. During this step the model composition makes possible to seek for models containing varying numbers of degrees of freedom. There is no need to formulate an optimization in which the number of variables is fixed a priori. For modeling the behavior of a structure this method use different fragments to generate a complete model. These fragments are got from libraries defined by an user and that are able to define only models compatible.

The second step is the optimization procedure. In this methodology is used a stochastic global search and optimization algorithm for the selection of a population of candidate models whose outputs match the measurements as closely as possible. Mathematical optimization techniques that make use of derivatives and sensitivity equations are not used because search is performed among sets of model classes that contain varying numbers of parameters and multiple local minima have been observed in the search space. A stochastic global search called PSGL is used to minimize the cost function that evaluates the difference between measurements and model prediction. PGSL performs global search through sampling the solution space using a probability density function.

Chapter 4

Classic sensitivity based finite element model updating

The algorithm described in the following is based on the classic sensitivity based finite element model updating method. Generally the two matrices [K] and [M] of the model are studied in a different way: the mass matrix is the one whose terms are almost well known and trying to update these terms may lead to values similar to those detected from experiment, with another approach. To save the cost of the optimization, especially the time of calibration, stiffness matrix is the only one worth subjecting to update.

4.1 Generation of models

The first step of the algorithm developed is represented by the random generation of N_m sets of parameters, representing N_m models. A set of parameters is the array of the coefficients that are going to be updated. The parameters that identify the structure are such as the Young's modulus, mass density and Poisson's ratio. It is necessary to fix boundaries in which the parameters can vary. These boundaries need engineering insight. For the realization of these parameters different approaches are used:

- Generation from a uniform distribution, and it is the only distribution that gives initial models the same probability in the range defined at the beginning;
- Generation of the parameters using the permutation theory, that divides the domain in equal bricks.

For the first case, if we assume that the range of variation of a parameter *x* is [a;b], and then:

$$f(x) = \frac{1}{a-b} \quad \forall x \epsilon [a;b] \qquad [4.1]$$

$$F(x) = \frac{x-a}{b-a} \quad \forall x \epsilon [a;b] \qquad [4.2]$$

Where f(x) indicates the probability density function and F(x) the cumulative distribution function. The probability density function is independent from the variable and its value is constant throughout the domain. The bigger is the domain, the lower is the probability to extract a certain value. N_m is often chosen to be as

large as possible so that more possible combinations can be reached, but at the same time not so large to avoid a huge computational cost during the processing of the algorithm. Usually it depends on the dimension of the range [a; b] and on the number of parameters subjected to updating. N_m might be chosen as following:

$$N_m \approx 10 \cdot N_p \cdot \frac{a-b}{\text{magnitude(a or b)}} \qquad [4.3]$$

N_p indicates the number of parameters subject to updating. The uniform distribution is the best one to be used when only the range of parameters variation is known exactly; in this way we are not focusing the attention around a starting model, but we are spreading the search space.

The second approach uses the theory of permutation. With the permutation theory the search space is divided into uniformly bricks. The starting points are widespread in the whole range [a; b] considering all the mathematical combinations. The only information necessary to give as input is the number of step in which the user wants to divide the domain [a; b].

For example, given a vector **V**= [A, B, C, D], all the possible couples of this vector are:

AA, AB, AC, AD, BA, BB, BC, BD, CA, CB, CC, CD, DA, DB, DC, DD;

Basically it means 2^4.

In general:

$$\mathbf{N_m = N^n} \qquad [4.4]$$

For a vector **V** of *n* dimension, we can realize N_m permutations using N for each realization. The vector **V** is a vector that spreads the range [a; b]. Since the algorithm is rapidly convergent to a reliable solution, it is suggested to not choose a thick step into the range [a; b] otherwise the computational cost increase exponentially.

For example if:

[a; b]= [1; 3]; step=0.5; N=3;

$$N_m = 3^{\frac{3-1}{0.5}} = 81;$$

If step=0.25

$N_m = 3^{\frac{3-1}{0.25}} = 6561$; That is a great number of possible sets of parameters as starting point.

4.2 Sensitivity analysis

In the second step of the algorithm, the procedure aims to reach the calibration of these models. From these initial models, generated in the step one, the algorithm tries to minimize the objective function through the updating of the parameters, whose bounds are well-defined at the beginning of the analysis. It is necessary to fix the upper and lower bounds for the existence of the coefficients, because it might happen that a combination of the parameters gives a minimum for the error function but the values don't have any physical meaning and the model obtained can't be used to represent the real structure. (Mottershead, Friswell et al., 2013)

Let's take into account a nonlinear function *F* in [4.5]. The problem to be solved in inverse problem: from the known parameters {z} we have to find out, recursively, which are the {θ} parameters that gives the specific {z} outputs. Due to its nature, it is very hard to investigate and manage easily the research of a minimum if we don't involve a first order approximation. Given this function:

$$\{\mathbf{z}\} = F\{\boldsymbol{\theta}\} \qquad [4.5]$$

In which {**z**} is a vector of output responses such as natural frequencies, mode shapes and displacements, and a vector of input parameters {**θ**} such as stiffness and mass parameters. It's preferred to study its linear approximation. In a small interval of the hypothetical correct input parameters {$\boldsymbol{\theta}_m$} it is possible to linearize the analytical function through the Taylor series expansion stopped at the first order.

If F$\in R$ and dim{θ}=1,

$$F(\vartheta) = F(\vartheta_m) + \frac{dF}{d\vartheta}(\vartheta - \vartheta_0) + \cdots + \frac{d^n F}{d\vartheta^n}(\vartheta - \vartheta_m)^n + o(\vartheta - \vartheta_m)^{n+1} \quad [4.6]$$

The sensitivity analysis theory uses the first derivative $\frac{dF}{d\vartheta}$ of the function respect to the parameter {θ}. The mathematical meaning of the derivative is the slope assumed by the function at a certain point. If F$\in R^n$ and the dimension of the inputs {θ} is *n* and the dimension of outputs {z} is m, the first order derivative is represented by a function of mx*n* dimension. Sensitivity Based are the most used methods. The sensitivity matrix is a matrix that shows the variation of the function F due to a variation of each parameter. The bigger is the influence of parameters into the function F, the bigger is the value of the sensitivity coefficient. Mathematically the first derivative it is the Jacobean of the non-linear function. Thus, in an interval of $\{\boldsymbol{\theta}_m\}$ it is possible to apply a small perturbation to this vector and obtain an expression shown in the following:

$$\{\partial z\} = [S]\{\partial\theta\} \quad [4.7]$$

Where:

$$\{\partial z\} = \{z_a\} - \{z_m\} \in \mathbb{R}^m \quad [4.8]$$

$$\{\partial\theta\} = \{\theta_a\} - \{\theta_m\} \in \mathbb{R}^p \quad [4.9]$$

Where [4.8] identifies the difference between the analytical and experimental data and [4.9] indicates the infinitesimal difference between the hypothetical model that gives the output array $\{z_m\}$ and the mathematical model subjected to update. Using the same notation of [4.7], [S]$\in \mathbb{R}^{mxp}$. This matrix is called sensitivity matrix and it indicates mathematically the Jacobean of the function F. Every i-th column of the matrix expresses the variation in the output vector, due to an

infinitesimal variation of the i-th parameter:

$$S(:,j) = \frac{\{z_a\} - [\{z_a\} + \{dz_a\}]}{d\theta_j} \quad [4.10]$$

To obtain a solution that can be considered as correctly updated the terms on the left and on the right of [4.7] must be equal. With this assumption it is possible to consider as objective function the residual between the two terms of [4.7]. Using this hypothesis a very common function to minimize is represented with the classical least square function:

$$J = (\{dz\} - [S]\{d\theta\})^T(\{dz\} - [S]\{d\theta\}) \quad [4.11]$$

Whose minimum can be found as following:

$$\frac{dJ}{d\theta} = [S]^T\{dz\} - [S]^T[S]\{d\theta\} = 0 \quad [4.12]$$

$$\{d\theta\} = ([S]^T[S])^{-1}[S]^T\{dz\} \quad [4.13]$$

During the initial iterations it is suggested to use another equation to avoid a local minimum. The first to introduce this equation was Tikhonov (Mottershead, Friswell et al., 2013) who introduced a regularization factor α in the equation:

$$\{d\theta\} = ([S]^T[S] - \alpha[I])^{-1}[S]^T\{dz\} \quad [4.14]$$

It is suggested to use a value of α not so big to provide a jump outside a possible global minimum, but not so small to not jump outside a local minimum. There are in literature a lot of heuristic studies about the magnitude to give to this α coefficient.

When the input data sets are obtained with different techniques and different

instruments, the reliability of each of those could change drastically, so it is necessary to give much influence to the data that are more reliable. To do that in the expression [4.6] it is possible to introduce a weight matrix W:

$$J = (\{dz\} - [S]\{d\theta\})^T W(\{dz\} - [S]\{d\theta\}) \quad [4.15]$$

$W \in R^{mxm}$. Usually the weight matrix is obtained inverting the Covariance matrix C, which is a matrix in which the information of the standard deviation are stored for each of measurements data set. From experimental data sets Friswell and Mottershed said that the uncertainty related to frequencies and mode shapes is different. (Mottershead, Friswell et al., 2013) They assumed usually a 1% error for frequencies and 10% error for mode shapes at the best. Thus the mode shape data is less reliable than the natural frequency data, and higher frequencies are not measured as accurately as the lower frequencies.

$$[W] = [C]^{-1} \quad [4.16]$$

$$[C] = \begin{bmatrix} \sigma_{11}^2 & \cdots & \sigma_{1m} \\ \vdots & \ddots & \vdots \\ \sigma_{m1} & \cdots & \sigma^2_{mm} \end{bmatrix} \quad [4.17]$$

Thus:

$$\frac{dJ}{d\theta} = [W][S]^T\{dz\} - [S]^T[W][S]\{d\theta\} = 0 \quad [4.18]$$

$$\{d\theta\} = ([S]^T[W][S])^{-1}[S][W]^T\{dz\} \quad [4.19]$$

$$\{d\theta\} = ([S]^T[W][S] - \alpha[I])^{-1}[S]^T[W]\{dz\} \quad [4.20]$$

Either vectors [4.14] or [4.19] of the parameters' variation have to be applied to the initial set of parameters to obtain a model that minimizes the residual within the numerical and experimental data. Thus:

$$\{\theta\}_{new} = \{\theta\}_{old} + \{d\theta\} \quad [4.21]$$

4.3 Candidate Selection

During every iteration the multiple sets of parameters –deriving from the iterations- are stored. At the end of the updating procedure the result is a different configurations of parameters for each starting model. Several of these configurations are very far from the target model. Taking into account all of them for the further steps can bring through an incorrect solution. Thus, it is necessary to select rationally only those models with physical meaning. For each sets of parameters the objective functions are stored too. From the way in which this objective function is built in [4.15] and [4.11] we can say that the smaller is the value the more consistent is the fitting within the inputs and outputs. For this reason taking into account only the models associated with the smallest values of the objective functions is an objective criteria. So, if we start from N_m models, at the end of the updating we end up with N_m models with parameters updated. For each of these models the objective functions are stored as well.

The next step of the algorithm is the selection of the candidates able to represent the problem with physical meaning. This updating procedure is effective only in a small region of the initial point, because we are trying to update a vector $\{\theta\}$ with a variation $\{d\theta\}$. Aiming to reach a solution that can fit the experimental data with all the models generated is impossible, especially when the range of variations is very wide. Then the models updated are sorted from the one associated with the smallest value of the objective function to the one associated with the highest minimum. In this way the models are sorted from the one that fits the outputs in the best way to the one that fits the outputs relatively badly. From experience it is

very difficult to know a proper value of threshold. The user can choose models worth to collect for solving the problem. This can be done easily looking at the value assumed by the objective function. In fact after the updating of each starting models and the sorting, the values of the objective functions are plotted. The user can choose the subjective number of models to keep.

4.4 Data Mining

The fourth step that follows the selection of reasonable candidates is the one based on the Data Mining techniques. Generally to treat a huge amount of data an engineer can get lost, so usually Data mining techniques are used. In literature author have tried to manage these information using PCA (principal component analysis) and cluster techniques using score functions or error functions to decide which one is the correct numbers of clusters. (smith et al., 2007)

The purpose of using a cluster technique is trying to divide an amount of solutions in clusters, in this way a few number of centroids –models per each subpopulations- can express the dispersion of the data giving a reasonable set of possible solutions. In the literature there are a lots of algorithms that use the clustering methods such as k-means; but for this one, the number of cluster is a prerogative input to be fixed a priori. In this algorithm the number of clusters and the clusters are an output of the analysis. Thus a hierarchical approach is necessary. A general cluster algorithm that is hierarchical starts from one cluster and then, if an hypothesis is not respected, the population of data is split in two subpopulation and so on until the hypothesis is respected. In scientific field many score functions are used to get the reasonable number of clusters, some of this are based on a score function that gives information related to the distance between the clusters.

In this finite element model updating algorithm *G*-means function is used for the clustering. When clustering a dataset, the right number *k* of clusters to use is often not obvious, and choosing *k* automatically is a hard algorithmic problem. The G-means algorithm (Hamerly, Elkan et al., 2004) is based on a statistical test for the hypothesis that a subset of data follows a Gaussian distribution. G-means runs k-means with increasing k in a hierarchical fashion until the test accepts the hypothesis that the data assigned to each k-means center are Gaussian. Additionally, G-means only requires one intuitive parameter, the standard statistical significance level α for the Anderson Darling test. Center-based clustering algorithms (in particular k-means and Gaussian expectation maximization) usually assume that each cluster adheres to a unimodal distribution, such as Gaussian. With these methods, only one center should be used to model each subset of data that follows a unimodal distribution. The G-means algorithm starts with a small number of k-means centers, and grows the number of centers. Each iteration of the algorithm splits into two those centers whose data appear not to come from a Gaussian distribution. Between each round of splitting, we run k-means on the entire dataset and all the centers to refine the current solution. We can initialize with just $k = 1$, or we can choose some larger value of k if we have some prior knowledge about the range of k. The k-means algorithm implicitly assumes that the data points in each cluster are spherically distributed around the center. Less restrictively, the Gaussian expectation-maximization algorithm assumes that the data points in each cluster have a multidimensional Gaussian distribution with a covariance matrix that may or may not be fixed, or shared. The Gaussian distribution test that we present below are valid for either covariance matrix assumption. To specify the G-means algorithm fully we need a test to

detect whether the data assigned to a center are sampled from a Gaussian. The alternative hypotheses are:

• H_0: The data around the center are sampled from a Gaussian.
• H_1: The data around the center are *not* sampled from a Gaussian.

If we accept the null hypothesis H_0, then we believe that the one center is sufficient to model its data, and we should not split the cluster into two sub-clusters. If we reject H_0 and accept H_1, then we want to split the cluster. The test we use is based on the Anderson-Darling statistic. This one-dimensional test has been shown empirically to be the most powerful normality test that is based on the empirical cumulative distribution function (ECDF). Given a list of values x_i that have been converted to mean 0 and variance 1 –with a normalization procedure-, let x(i) be the i-th ordered value. Let zi = F(x(i)), where F is the N(0, 1) cumulative distribution function. Then the statistic is:

$$A^2(Z) = -\frac{1}{n}\sum_{i=1}^{n}(2i-1)[\log(z_i) + \log(1 - z_{n+1-i})] \qquad [4.25]$$

The value of [4.25] must be compared to the critical values A_c related to the problem that we want to solve. If the value of [4.25] is smaller than the critical value A_c the test passes and we accept the hypothesis H_0, then is not necessary to split the starting population by increasing the number of clusters.

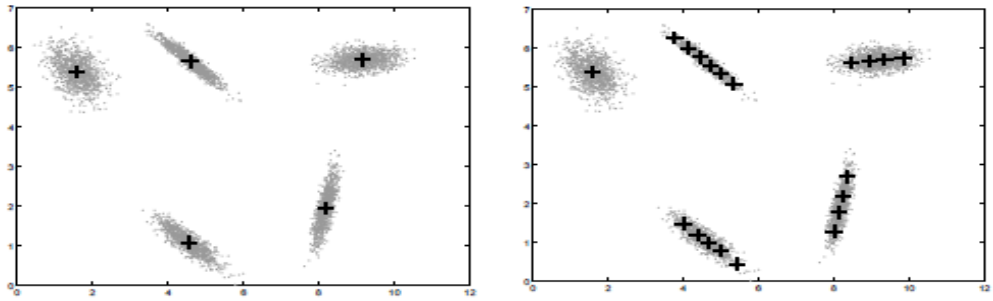

Image 4.2: comparison between G-means and k-means algorithm

It is possible to notice how the two algorithm differs when the distribution is not spherical and Gaussian. After G-means, if the solution is unique the algorithm gives only one finite element model that fits the input data, otherwise more than one finite element models are got as solution. It depends the user's ability to choose which finite element models can represent a good solution when multiple solution appears.

4.5 Flow-chart

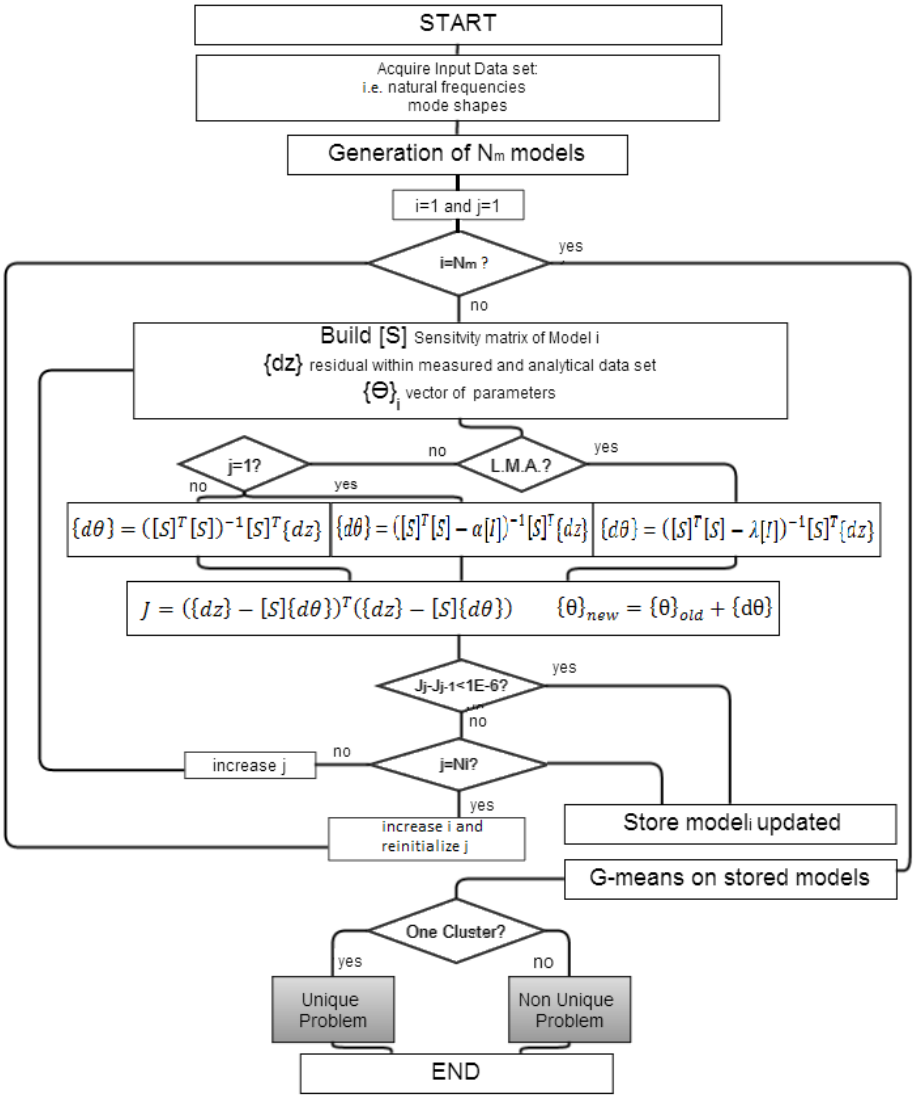

Image 4.3: Flow chart of the algorithm developed

Chapter 5

SENSITIVITY BESED RECURSIVE MULTI-MODEL UPDATING

In this chapter, the new method different from the classic sensitivity based FEM updating method is explained. The main difference between these two methods is: not all the parameters are updated at every single iterature, but only part of the parameters are updated. The parameters are divided into different subsets depending on theirs sensitivity to the system responses. (The details of the division is explained in the following.) In this way, the time consuming and the amount of calculation will be reduced. The most sensitive parameters are firstly updated so that the discrepancy is minimized quickly, and then the less sensitive parameters

are updated so that the discrepancy will be further minimized. Obviously this is more tricky because the classic method calculate sensitivity of all the parameters and update them in every single iterature of the process which needs more time consuming and calculation. (Bianco et al., 2011)

The division of the parameters is very important in this method. The most important factors are:

- The number of the subsets to be divided in
- The division node of every subset
- The number of iteratures of each subset

Obviously, the sensitivity analysis should be made, then depending on the distribution of the parameters the division nodes should be selected. It's important to distinguish the level of sensitivity of the parameters and put the parameters with same level of sensitivity into the same subset. Otherwise the recursive method will lose the meaning. This is the critical factor of the new method.

5.1 Sensitivity analysis and division of subsets

The parameters are the input of model updating which can be adjusted during the procedure, many factors can be used as the model parameters, such as material parameters(Young's modulus and density), moments of inertia, spring stiffness and mass. The responses are the output of model updating, such as natural frequencies, mode shapes or displacement. In this paper, the natural frequencies and mode shapes are chosen as the responses. Specifically, the diagonal of MAC calculated from the mode shapes are used. The sensitivity is simplified by the linearization of the relationship between responses and parameters which is usually nonlinear.

$$\varepsilon = z_m - z(\theta) \tag{5.1a}$$

ε represents the difference between the measured outputs z_m and analytically predicted outputs $z(\theta)$. Thus the goal is to minimize ε, so that the analytical model can produce the same output as the real structure.

Using the Taylor series expansion truncated after the linear term:

$$z(\theta) \cong z_i + S_i(\theta - \theta_i) \tag{5.1b}$$

$$\varepsilon = z_m - z(\theta) \cong z_m - (z_i + S_i(\theta - \theta_i)) = r_i - S_i(\theta - \theta_i) \tag{5.1c}$$

$r_i = z_m - z_i$, represents the residual at the ith iteration, and the linearization is carried out at θ_i.

$$\{\delta z\} = [S]\{\delta\theta\} \tag{5.2}$$

z represents the responses, and θ represents the model parameters, meanwhile, the matrix [S] represents the sensitivity matrix.

5.1.1 Sensitivity analysis with local sensitivity method

For the sensitivity analysis, the local sensitivity method LSM is used, which involves taking the partial derivative of every responses with respect to each parameter. The input parameters are allowed to vary within a small interval of fractional variation around a nominal value to compute the partial derivatives numerically.

The sensitivity matrix S is given by:

$$S_i = \left[\frac{\partial z_j}{\partial \theta_k}\right]_{\theta=\theta_i} \tag{5.3}$$

Where j=1,2,…,q denotes the output data points and k =1,2,..,p is the parameter index. The sensitivity matrix S_i is computed at the current value of the complete vector of parameters $\theta = \theta_i$. The error is assumed to be small for parameters in the vicinity of θ_i.

At each iteration, Eq. (2.1) is solved for

$$\Delta\theta = \theta - \theta_i$$

And the model is then updated to give

$$\theta_{i+1} = \theta_i + \Delta\theta$$

This procedure continues until consecutive estimates θ_{i+1} and θ_i are sufficiently converged.

5.1.2 Division of the parameters

In the sensitivity matrix $[S]$, each column contains the sensitivities of one parameter. Sum up all these sensitivities of each parameter:

$$\{sumS\}_j = \sum_{i=1}^{n} |S_{ij}| \tag{5.4}$$

n is the number of the parameters.

So sumS is the sum of the sensitivities to all the responses of a parameter, the

Then two limits are found:

$$maxS = max(\{sumS\}) \tag{5.5a}$$

$$minS = min(\{sumS\}) \tag{5.5b}$$

Then, from the original vector $\{sumS\}$ and the two limits $maxS$ and $minS$, a new vector of sensitivity indicator $\{diffS\}$ is realized with the value range between 0 and 1, following the relation:

$$\{diffS\}_j = \frac{\{sumS\}_j - minS}{maxS - minS} \tag{5.6}$$

In this way, even if the parameters have comparable value, the program is capable to divide the parameters into subsets. The domain [0, 1] divided into the

preselected number of intervals the same as the number of subsets of the parameters. For each parameter, if the sensitivity indicator $\{\mathrm{diffS}\}_j$ is located within the subinterval, then the parameter belongs to the subset. The subsets with larger sensitivities will be updated in prior. In this way, the process will arrive in convergence earlier than the traditional sensitivity method.

In the research domain, multi-models are built at the beginning of the procedure, for each model, the sensitivity analysis are performed. Different models correspond to different points in the search domain, so that each model has different matrix of sensitivity S. Naturally, the division of subsets are also different between different models.

In the whole research domain, the model parameters have uncertain importance in the process of updating. In the traditional sensitivity method, before the process of updating, it is difficult to decide which parameters to be ignored, because in each model the sensitivity of parameters are different. Instead, in the new recursive method, the parameters are divided into preselected number of subsets according to their sensitivity. The importance of the parameters in the process of updating depends on the sensitivity of the parameter. The larger the sensitivity, the earlier the subset will be updated, and even more, the updating will repeated more times for the subsets with higher sensitivity. The detail of the procedure will be

explained in the following chapter. For this, the new recursive method is more efficient with respect to the traditional sensitivity method which endows the same importance to all the parameters during the process of model updating.

5.2 PROCEDURE OF UPDATING

5.2.1 Order of Updating

Before the procedure of updating, the model parameters are divided into a preselected number of subsets. As explained in precedence, if the sensitivity indicator $\{diffs\}_j$ is located within the subinterval, then the parameter belongs to the subset.

The strategy of the new method, is firstly to update the most sensitive parameters, so that the discrepancy is minimized significantly at the very first iterations, after that, updating the less sensitive parameters the discrepancy can be further minimized. The order of updating is quite crucial and there are many choices, and each one has its advantage and disadvantage, in the new method, the following technique based on a triangle matrix is used.

The selection of subset to be updated during each iteration is based on the following triangle matrix (Suppose the preselected number of subsets is 3):

$$\begin{bmatrix} 1 & & \\ 2 & 1 & \\ 3 & 2 & 1 \end{bmatrix} \tag{5.7}$$

The single elements of that matrix is generated, and memorized in the vector according the following relationship:

$$\{\text{updses}\}_k = i - j + 1 \tag{5.8}$$

If for each subset, Niter iterations should be executed. Firstly, Niter iterations of model updating will be executed on the first subset. Then, Niter iterations will be executed on the second subset, after that, Niter iterations will be executed again on the first subset. The order will be this way until the termination of the iterations.

5.2.2 Operation of Updating

Once the sensitivity analysis is performed at the beginning of the procedure of iteration, the algorithm starts to process the updating of the individual parameters in the base of the choice of the users. In every iteration, the subset is selected, and a new sensitivity matrix is obtained based on the current parameters. The objective is to minimize the residual containing the difference between analytical and measured structural behavior. The objective function is:

$$J(\{\delta\theta\}) = \varepsilon^T\varepsilon \tag{5.9}$$

Given the linearization from the function (2,2), the objective function becomes:

$$J(\{\delta\theta\}) = (\{\delta z\} - [S]\{\delta\theta\})^T(\{\delta z\} - [S]\{\delta\theta\}) \tag{5.10}$$

In the case when fewer measurements are available, namely, the measurements are fewer than the parameters, the system is underdetermined. The solution for an underdetermined system is not unique. Conversely, if the number of measurements is larger than the number of parameters, the system is overdtermined. In this case, minimize J with respect to $\delta\theta$ to give an improved parameter:

$$\{\delta\theta\} = ([S]^T[S])^{-1}[S]^T\{\delta z\} \tag{5.11}$$

In the present work, the natural frequencies and MAC are used as responses of the

system. The frequencies and the MAC are weighted according to the use of the model and the importance of the modal modes.

5.2.3 The regularization strategy of tikhonov

Ill-conditioning usually exists in the sensitivity based method due to the large difference of sensitivity , overdetermined condition and noisy system. (Mottershead, Friswell et al., 2013)

For example, in the overdetermined condition, if there are two parameters parallel parameters with the same sensitivities, then

$$[S]^T[S] = 0$$

The procedure of updating will be blocked and the convergence can will not be achieved.

Tikhonov regularization is one of the most ideal tool to deal with the ill-conditioning problems. The objective function (3.4) is extended to meet the requirement of a minimized parameter changes:

$$J(\{\delta\theta\}) = (\{\delta z\} - [S]\{\delta\theta\})^T(\{\delta z\} - [S]\{\delta\theta\}) + \alpha * \{\delta\theta\}^T\{\delta\theta\} \quad (5.12)$$

Where $[S]$ is the sensitivity matrix, and $\{\delta z\}$ is the discrepancy between the measured data and simulated response, $\{\delta\theta\}$ is the parameter changes, and α is the regularization parameter in the range between 0 and 0.3.

$$\{\delta\theta\} = ([S]^T[S] + \alpha * I)^{-1}[S]^T\{\delta z\} \tag{5.13}$$

$$[S]^T[S] + \alpha * I \neq 0$$

This wil permit the procedure of updating unobstructed and the ill-conditioning will be solved.

How to choose the regularization parameter α is very important for the model updating. When the ill-conditioning is not too strong $\alpha = 0.05$, and when the matrix $[S]^T[S]$ is strongly ill-conditioned $\alpha = 0.3$. The higher the value of α, the more iteration steps are needed for convergence.

Chapter 6

Validation with Numerical and Experimental Application

In this paragraph different numerical models and experimental applications are shown. For each model a critical problem is explained. In the following four different structures are chosen to explain how the algorithm works and what are the decisions that the user has to make before every calibration.

6.1 Shear type system

Usually in the finite element model updating applications the stiffness matrix [K] is the one more affected by uncertainty rather than the mass matrix [M]. The engineer, instead of updating contemporaneously the mass and stiffness parameters, can choose a different way to do the calibration; the only coefficients that is worth to update are the stiffness ones.

The mode shapes information are not usually so easy to get, especially with the mass normalized values and, they are affected by huge uncertainty, Friswell and Mottershead (Mottershead, Friswell et al., 2013) said around 10% for mode shapes and 1% for natural frequencies, so the calibration of the model becomes slightly inaccurate. During an experimental test it is easy to identify the different magnitude of the modal displacements rather than the exact values expressed as mass normalized terms, so a tester uses a ratio of mode shapes instead of the real value. For example he can decide to divide the eigenvectors respect to the first row and get the ratio. The user should realize that if the ratio for the experimental data is taken, also the ratio of mode shapes for the FEM model has to be taken to have consistent data sets.

$$V = \begin{bmatrix} 1 & 1 & 1 \\ \frac{v_{21}}{v_{11}} & \frac{v_{22}}{v_{12}} & \frac{v_{23}}{v_{13}} \\ \frac{v_{31}}{v_{11}} & \frac{v_{32}}{v_{12}} & \frac{v_{33}}{v_{13}} \end{bmatrix} \quad [6.1]$$

In the following example we are trying to use this approach. To reach the target solution. The targets stiffness coefficients of this structure are:

$$k_i = \{2; 1; 1\} \frac{N}{m} \quad [6.2]$$

That are the coefficients for each inter-story stiffness. From the first to the third. In this analysis the lumped masses are known exactly and the values from the first to the third floor are shown in the next vector.

$$m_i = \{1; 1; 0.5\}\ kg$$

$$\theta_1 = k_1; \quad \theta_2 = k_2; \quad \theta_3 = k_3;$$

Using in the sensitivity analysis the all set of natural frequencies and the mode shapes expressed by their ratio we get:

Models detected [N/m]		
k_1	k_2	k_3
2.00	1.00	1.00

Table 6.1: Models detected during the analysis

As shown in table 6.1 the solution obtained coincides with the one assumed as target. The solution is consistent with the one got during the validation. The

important thing is being consistent with pairing the input data set with the analytical data set: in this case the ratio of the mode shape as been used, so also the ratio of the analytical mode shape must be used for the calibration.

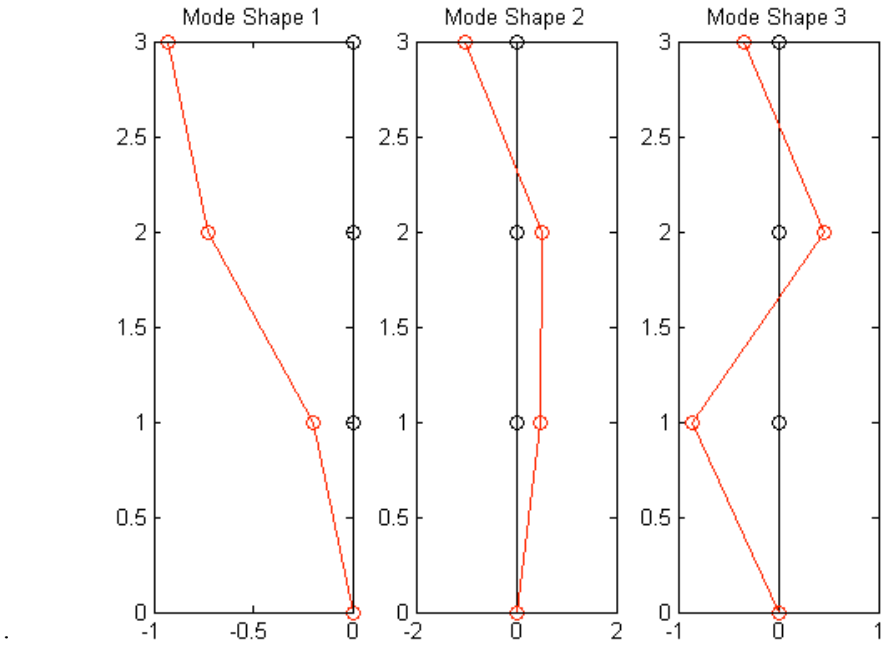

Image 6.1: Mode shapes for the numerical application 1

6.2 Steel cantilever beam

The beam is fixed on the left edge and free on the others, assumed to be uniaxial undeformable. The beam has been analyzed as an element in the three dimensional space and for its slenderness it is considered mono-dimensional. In a three dimensional space the degrees of freedom are the displacements along the axes and the rotation around the axes, so basically it is a problem with six degrees of freedom. In the finite element model for this structure four parameters for the realization of the structure are chose, the displacements along the x and y axes called respectively U_x and U_y, and the rotation around the x and y axes called respectively θ_x and θ_Y. In the following two pictures are shown the profile of the beam in the yz plane and the section of the beam in the xy plane.

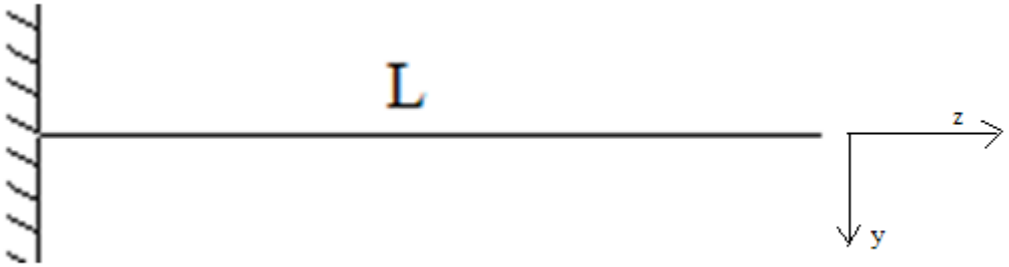

Image 6.2: Representation of the cantilever beam

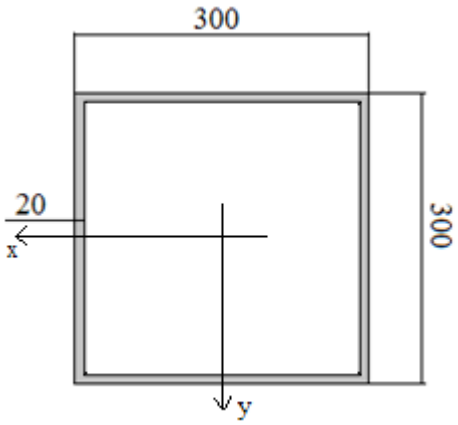

Image 6.3: Representation of the section of the beam. The measurements are in millimeters

Here are shown the geometry of the structure and the length and the moments of inertia. The length of the structure is L=6m. The mass of the structure is supposed to be m=1055 kg, due to a mass density equal to ρ=7850 kg/m^3. The elastic modulus of the steel is E=1.999*10^{11} N and the moment of inertia in both the direction is the same due to the symmetry. The values of the moments of inertia is $I_x=I_y=2.94*10^{-4}m^4$.

The degrees of freedom are sorting starting from the displacements and terminating with the rotations. The stiffness and mass matrix are built respecting this order.

$$\text{Dofs: } \{U_x; U_y; \theta_x; \theta_Y\} \qquad [6.3]$$

The stiffness are gotten applying the Euler-Bernoulli theory and the values are:

$$k_{11} = \frac{12EI_x}{L^3};$$

$$k_{14} = -\frac{6EI_y}{L^2};$$

$$k_{22} = \frac{12EI_x}{L^3};$$

$$k_{23} = \frac{6EI_x}{L^2};$$

$$k_{33} = \frac{4EI_x}{L};$$

$$k_{44} = \frac{4EI_y}{L} \qquad [6.4]$$

$$K = \begin{bmatrix} k_{11} & 0 & 0 & k_{14} \\ 0 & k_{22} & k_{23} & 0 \\ 0 & k_{23} & k_{22} & 0 \\ k_{14} & 0 & 0 & k_{44} \end{bmatrix} \qquad [6.5]$$

For the mass matrix the only non-null terms are on the diagonal.

$$diag(M) = \left\{m, m, \frac{mL^2}{3}; \frac{mL^2}{3}\right\} \qquad [6.6]$$

Generally the choice for the updating parameters should be done carefully, otherwise it is possible the solutions don't represent the real structure even if the values are obtained according to the algorithm written. If we assume that the unknowns are contemporaneously the stiffness and the mass, it might be possible to cause some problems. In this case the choice of the updating parameters are:

$$\theta_1 = EI_x; \quad \theta_2 = EI_y; \quad \theta_3 = m; \qquad [6.7]$$

With this choice it's impossible to find an unique model, that can express problem due to the presence of a sort of scalar factor. To explain this phenomenon we assume a single degrees of freedom structure with *k* as stiffness and *m* as mass. According to the general solution for a dynamic system in free motion it's simple to write:

$$\omega^2 = \sqrt{\frac{k}{m}} \qquad [6.8]$$

Where ω is the natural frequency for the previous system expressed in rad/s^2. If we assume another single degree of freedom structure with $\alpha \cdot k$ as stiffness and $\alpha \cdot m$ as mass, we get the same frequency of [6.22] $\forall \alpha \in \mathrm{R}$. In fact if we run the calibration of the algorithm, the solution is not unique. The centroids detected are very different one form each other and every term of each centroid has the same percentage variation respect to the target one: It means that there is a sort of scalar factor between the coefficients, that in the simple degree of freedom structure we have called α. In fact these results are got:

Models detected		
I_x [10^7 m^4]	I_y [10^7 m^4]	M [ton]
5.77	5.77	1.04
5.75	5.75	1.03
5.54	5.54	0.99
5.39	5.39	0.97
4.93	4.93	0.89
4.27	4.27	0.77
2.90	2.90	0.52

Table 6.2: Centroids detected with scalar factor

Percentage variations		
%	%	%
2	2	2
2	2	2
4	4	3
6	6	6
8	8	8
16	16	16
27	27	27
51	51	51

Table 6.3: Percentage variation

To solve this problem is necessary to fix some of those parameters. The mass matrix is usually known with high confidence and we can fix it, but if we are not sure about the real value of *m*, we can basically update a different configuration: the stiffness and mass parameters are divided by the values of mass *m*. In this way the issue of the scalar factor doesn't occur. The parameters to be updated become:

$$\theta_1 = \frac{EI_x}{m}; \qquad \theta_2 = \frac{EI_y}{m} \qquad [6.9]$$

And the diagonal of [M] becomes:

$$\mathrm{diag(M)} = \left\{1,1,\frac{1L^2}{3};\frac{1L^2}{3}\right\} \qquad [6.10]$$

Once the updating is done and the mass information is well-defined with other techniques, the stiffness parameters are multiplied by this mass factor. Physically the ratio k/m is in the International System of measurements=[$1/s^2$] , it indicated the decay of the stiffness term by effect of the mass: it is a damage information.

Models Detected	
$EI_x/m*10^7$ [$1/s^2$]	$EI_y/m*10^7$ [$1/s^2$]
5.57	5.57

Table 6.4: Centroid detected with scalar factor

6.3 3D Steel Frame

In this other numerical application it is explained a numerical problem that can occur during the calibration. The structure is a three dimensional steel frame. It has one bay in the x direction and one bay in the y direction. If we assume as degrees of freedom the translations along the x and y axes and the rotation around the z axis for each floor, we get an amount of six degrees of freedom. These degrees of freedom are indicated as: $\{U_{x1}, U_{y1}, \theta_{z1}, U_{x2}, U_{y2}, \theta_{z2}\}$, where the first floor is indicated with number 1 ant the second floor with the subscript number 2. The section of the frame is a typical steel section: a double T section with the geometry represented in the picture 6.6 below. The slab is made by steel. The assumptions are:

- Non-deformable slab on each floor; In both the direction x and y the slab behaves as a rigid body.
- Axially non-deformable columns. The axial deformation of the columns is smaller than the deformation of the columns due to the bending moment, so it can be disregarded.

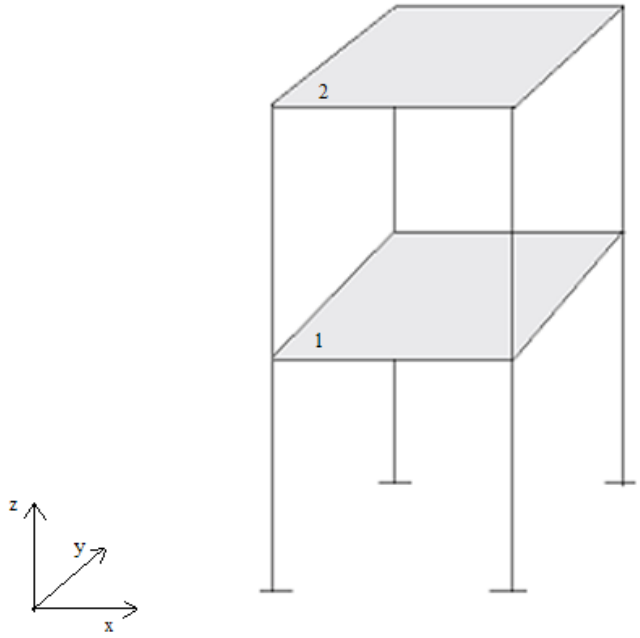

Image 6.5: 3D representation of the frame.

The sections of the columns are the same and in the following image there is a brief description:

The geometrical characteristics of the frame are:

The length is the same for every stories. L=3m;

The mass of the first floor m_1=5628kg. The mass of the second floor m_2=3320kg.

The moment of inertia along the x direction is equal for each floor and the value is $I_{x1}=I_{x2}=1.44*10^{-4}$ m^4. The moment of inertia along the y direction is equal for each floor and the value is $I_{y1}=I_{y2}=4.05*10^{-5}$ m^4.

In this paragraph, to not forget that the target of the updating procedure is the calibration of the parameters, we assume that we know how to build the stiffness matrix and the mass matrix of a 3D frame and we focus the attention only on the

updating of the parameters. For more information on how to build the mass matrix and the stiffness matrix of a 3D frame look at the Appendix B. The centroids of the stiffness coincide with the centroids of the masses due to the symmetry, so basically the mass and stiffness matrices are diagonal and tri-diagonal. The [K] and [M] matrices are as follow:

If we assume the degrees of freedom sorted as follow:

$$\{U_{x1}U_{y1}\theta_{z1},U_{x2},U_{y2}\theta_{z2}\} \quad [6.11]$$

The stiffness coefficient are shown in the follow:

$$k_{11} = \frac{48E(I_{x1}+I_{x2})}{L^3};$$
$$k_{14} = -\frac{48EI_{x2}}{L^2};$$
$$k_{22} = \frac{48E(I_{y1}+I_{y2})}{L^3};$$
$$k_{25} = -\frac{48EI_{y2}}{L^3};$$
$$k_{33} = \frac{12E(I_{x1}+I_{x2}+I_{y1}+I_{y2})}{L};$$
$$k_{36} = -\frac{12E(I_{x2}+I_{y2})}{L};$$
$$k_{44} = \frac{48E(I_{x2})}{L^3};$$
$$k_{55} = \frac{48E(I_{y2})}{L^3};$$
$$k_{66} = \frac{12E(I_{x2}+I_{y2})}{L^3}; \quad [6.12]$$

$$K = \begin{bmatrix} k_{11} & 0 & 0 & k_{14} & 0 & 0 \\ 0 & k_{22} & 0 & 0 & k_{25} & 0 \\ 0 & 0 & k_{33} & 0 & 0 & k_{36} \\ k_{14} & 0 & 0 & k_{44} & 0 & 0 \\ 0 & k_{25} & 0 & 0 & k_{55} & 0 \\ 0 & 0 & k_{36} & 0 & 0 & k_{66} \end{bmatrix} \quad [6.13]$$

The mass matrix is diagonal and the masses are supposed to be lumped and concentrated in the centroids of gravity. The polar moment of inertia for each floor is:

$$I_{01} = \frac{1}{12} m_1 (L^2 + L^2)$$

$$I_{02} = \frac{1}{12} m_2 (L^2 + L^2) \quad [6.14]$$

$$\mathrm{diag}(M) = \{m_1, m_1, I_{01}, m_2, m_2, I_{02}\} \quad [6.15]$$

Since there is the problem shown in the §6.2 to avoid the presence of a scalar factor it is necessary to fix some coefficients before doing the calibration. We can decide to fix the mass values and update only the stiffness

N_m=360;

N_i=20;

The ratio respect to the first non-null value of the mode shape is used.

$$\theta_1 = \frac{EI_{x1}}{m_1}; \quad \theta_2 = \frac{EI_{x2}}{m_1}; \quad \theta_3 = \frac{EI_{y1}}{m_1}; \quad \theta_4 = \frac{EI_{y2}}{m_1}; \quad [6.16]$$

The model detected are shown in the following table:

Models detected			
EI_{x1} [Nm^2]	EI_{x2} [Nm^2]	EI_{y1} [Nm^2]	EI_{y2} [Nm^2]
28421	28421	8892	8892
8892	8892	28421	28421

Table 6.5: Models detected

Apparently two models are detected with the moments of inertia I_{x1} and I_{y2} inverted. Basically due to the symmetry of the structure the magnitude of displacements respect to the first and second floor is constant. So, it is not possible to determine which is the correct orientation of the sections if we use the ratio of the mode shapes. If it was a real structure, it would have been to check directly the structure to see which is the correct orientation of the sections and decided which one is the good oriented model.

6.4 Experimental Application of the masonry arch bridge

The 1:2 scaled model of the masonry arch bridge shown in figure 1 was built in the laboratory of the Department of Structural, Building and Geotechnical Engineering at the Politecnico di Torino consisting of a twin-arch bridge with a length of 5.90m, a width of 1.60m and it is 1.75m high. The two arches are segmental arches with a radius of 2.00m and an angular opening of 30°. Each span is 2.00m long between the supports and the thickness of the arch is equal to 0.20m. The model was built with handmade clay bricks also scaled to 130x65x30mm to respect the adopted modelling scale law. Low compressive strength elements were chosen and a mortar with poor mechanical properties was used to bound them in order to reproduce the typical materials of historical constructions. (**Ruocci G.; Quattrone A.; De Stefano A. (2011))**

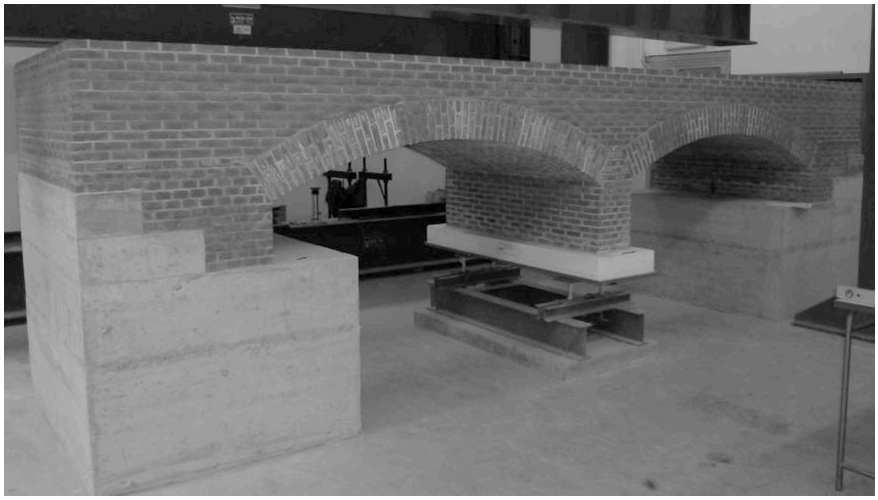

Figure 1. The scaled masonry bridge: notice the settlement application device under the central pier.

The mid-span masonry pier, which was cut at a hypothetical middle-height section to allow the insertion of a settlement application system, is imagined to be placed inside the streambed and subjected to the scour of its foundation.
Foundation settlements and rotations were applied on the bridge model by means of the four independent screws installed at the extremities of the settlement application system. The spherical plain bearings placed at the head of the screws allow the rotations of the plate which supports the central pier about axes parallel to the longitudinal and transversal directions of the bridge.

The experimental study involved three different testing campaigns. The first campaign regarded the undamaged structure: an extensive set of dynamic tests was

carried out on the bridge model in order to characterise its “healthy” state. The second campaign started after the application of additional masses on the central pier, in order to take in account the weight of the missing part of the pier. In the same campaign the first four settlement steps were applied on the upstream side of the pier. Dynamic tests were conducted in correspondence of each settlement step. During the third campaign five further settlement steps were applied (11 mm total settlement).

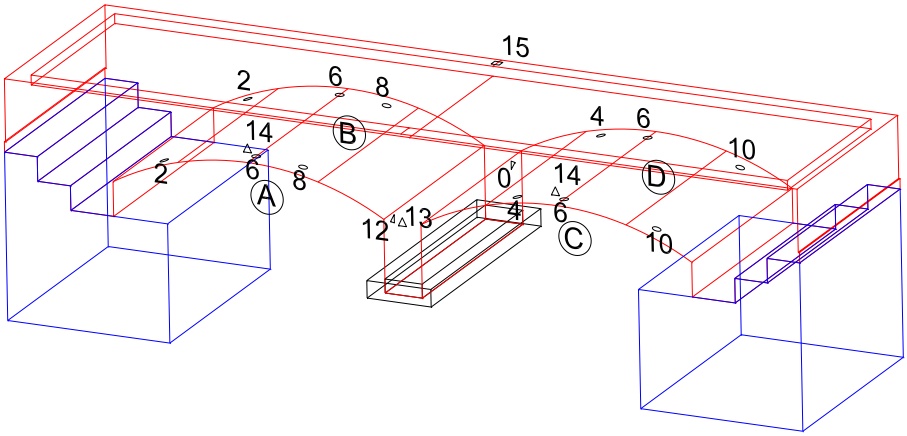

Figure 1. Shaker application in positions 9A and 6C (right), experimental setups for vibration tests (left).

Measuring points were selected in order to achieve a sufficient mode shapes resolution. The arch barrels were subdivided in 11 segments whose ends were assumed as measuring points for both the edge and the middle lines. Other 6 positions at the springing sections of the pier were materialised to capture the longitudinal displacements. The 4 mid-span sections of the arch barrels lateral

faces and the 2 pier frontal faces were considered for the lateral and torsional modes. Finally, the 2 positions on the longitudinal spandrel walls at the middle section of the deck were added to identify the vertical modes.

Forced vibration tests were performed by using a shaker TIRA TV 51220, capable to supply a rated peak force of 200 N. The force applied was acquired by using a mechanical impedance sensor PCB Piezotronics 288D01 (measurement range ±222.4 N pk). Figure 1 shows both the location where the shaker has been applied and the accelerometers dislocation on the structure.

Through a first linear identification, at each damage step, the modal frequencies were identified, in order to plan the forced vibration tests. In fact, at each modal frequency it has been applied a harmonic excitation using different force levels, usually 33 N, 66 N and 100 N for one minute. Both the force and the acceleration input to the system were acquired. Using the accelerometers, dynamic measurements were collected at 18 different locations, as shown in figure 2.

Model without mass

Eight parameters are chosen for the process of model updating.

E1, E2, E3: The elastic module of the spring at the end to the central pier;

E4: The Young's module of the masonry parapet;

E5: The Young's module of the masonry arch;

E6: The Young's module of the backfill material;

E7: The Young's module of the concrete slab;

E8: The density of the backfill material;

The first three modes are chosen for updating, the objective function values of every iteration are showed in the following figure.

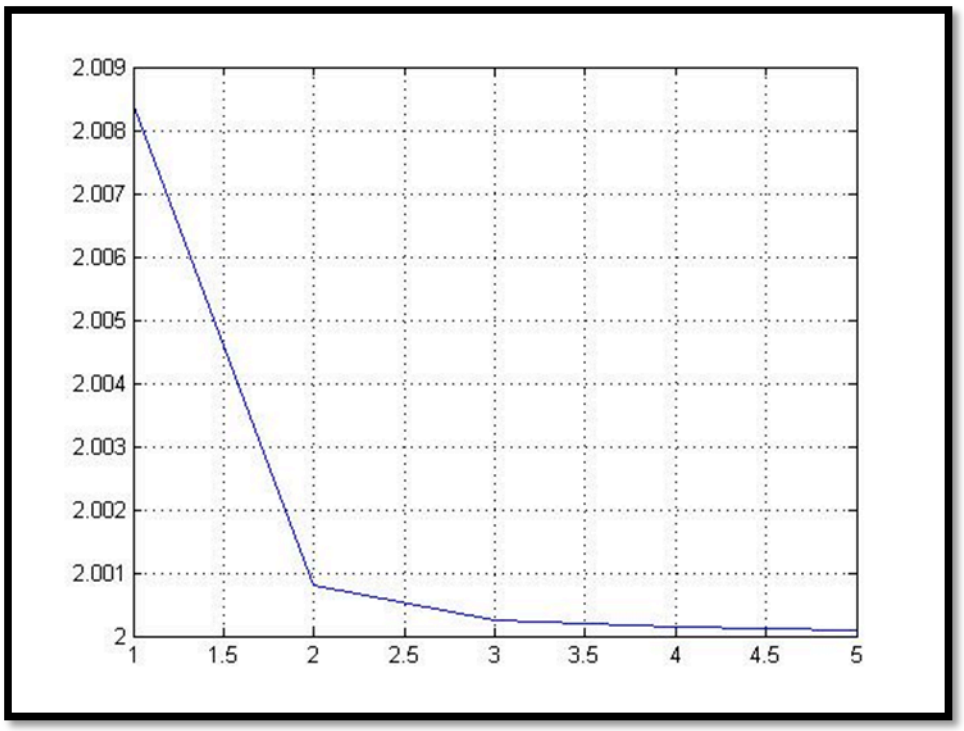

The comparison of the first 3 identified and updated modal frequencies are performed:

	ID	FEM	%
1	32,63000	32,36916	-0,799
2	34,30000	34,34440	0,129
3	36,84000	36,95197	0,304

The updated values(the nominal values are set to 1) are:

E1	0,9431
E2	1,2061
E3	1,1981
E4	1,0880
E5	0,7237
E6	0,7611
E7	1,1704
E8	1,3336

This model possess enough fitting capabilities and sufficient physical meaning as a reliable representation of the benchmark building structure.

Model with mass

4 steel masses are added on top of the bridge, and the vibration tests are performed at the beginning fase without damage.
The comparison of the identified and updated modal frequencies are performed:

	ID	FEM	%
1,00	19,33	19,53	1,04
2,00	29,55	28,87	-2,29
3,00	36,27	35,18	-3,02
4,00	41,10	41,25	0,38
5,00	48,93	50,13	2,44
6,00	52,08	55,22	6,02

The first six modes are chosen for updating, the objective function values of every iteration are showed in the following figure.

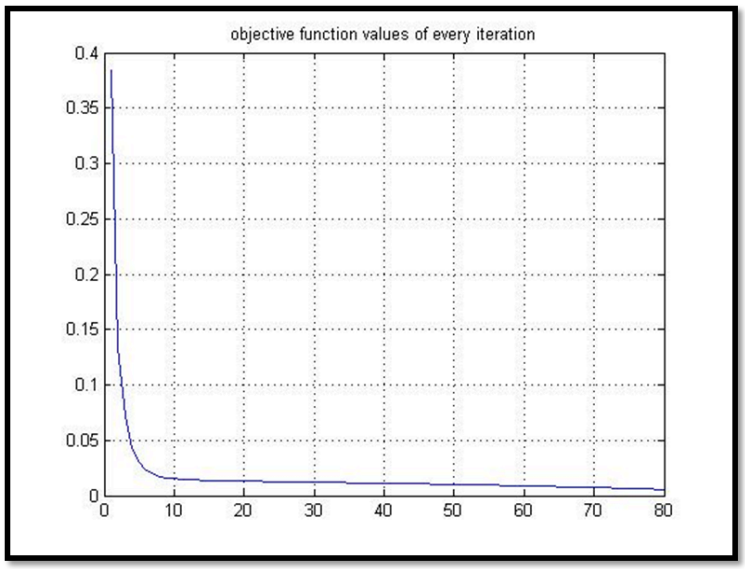

The updated values(the nominal values are set to 1) are:

E1	1,2417
E2	1,0380
E3	0,2687
E4	1,2567
E5	0,8300
E6	0,9479
E7	0,1395
E8	2,4004

This model possess enough fitting capabilities and sufficient physical meaning as a reliable representation of the benchmark building structure.

Chapter 7

Critical analysis with classic methods

The precedent chapter, proved the validation of the new method, but what is the difference between the new method and the classic methods. The critical analysis is performed comparing the new recursive method and the classic one with reference to a precedent results of genetic method made by Emiliano Matta(Matta.2010).

Different parameters are used for updating and different cases are discussed to find the drawbacks and the advantages of the new method. Obviously, when the parameters have similar sensitivity, it's not quite useful to use the new method, because it loses the affects of some important parameters in the first iterations and the convergence are slow respect to the classic method.

The sensitivity analysis should firstly made and respect to the distribution of the sensitivity, the number of groups and the nodes of the division should be chosen in a proper way, so that the recursive method should have sense, otherwise, it may leads to a insine result.

If the sensitivity of the parameters have the similar sensitivities, only one group should be enough, but when the sensitivities of the parameters are distributed with quite large differences with each other, the division of the groups should be made. The principle is to divide the parameters with similar sensitivities into the same group.

7.1 Test structure

The test structure is a large-scale (2:3) model of a two-storey steel frame building with composite steel-concrete floors. The steel structure, consisting of columns and beams orthogonally interconnected into a regular (doubly-symmetrical) three dimensional frame with one bay in both directions and two rectangular floors (level 1 and 2), is mounted on a rigid horizontal base (level 0), resting on two sliding guides and connected to a dynamic hydraulic actuator which can impart the desired mono dimensional excitation to the structure. Four HE140B equal columns, fixed to the base, extend continuously to the top floor. Eight IPE180 lateral beams, welded to the columns, support the two composite floors, made up of concrete slabs cast on coffer profiled steel sheeting. The columns free length is 4.00m, divided into two 2.00m inter storey heights. The beams length is 4.00m in the along-excitation (longitudinal) direction and 3.00m in the across excitation (transverse) direction. The floors thickness is larger than expected because of the sagging effect occurred during concrete casting. (Matta, E, De Stefano, et., 2011)

In order to house the dissipating devices during tests on the controlled structure,

four vinverted braces, crowned with gusset plates, are bolted at both storeys, parallel to the longitudinal direction.
With the aim of model characterization, various dynamic tests were conducted on the structure, the sliding guides being locked, ranging from ambient noise excitation to hammer impact tests to ground motion induced by operating a nearby shaker, and subsequent vibration was measured using a whole of 15 mono-directional accelerometers, deployed in the most significant observation points: two at the ground level; four at the base level; four at the first level; four at the second level; and one to the gusset plate atop one of the two lower V-inverted braces.

During testing, concrete blocks were placed on the first and second floors as additional rigid lumped masses in order to improve dynamic characterization. The resulting three mass configurations are distinguished as follows: the basic configuration(BC) of the bare frame, with no additional masses; the non-symmetric configuration(NC, with two blocks at the first and two at the second storey, placed along the same longitudinal side; the symmetric configuration (SC), with four blocks at each storey.

The accelerometers set-up and the additional masses location are depicted in figure 1. Table 1 reports mass and eccentricity of each concrete block.

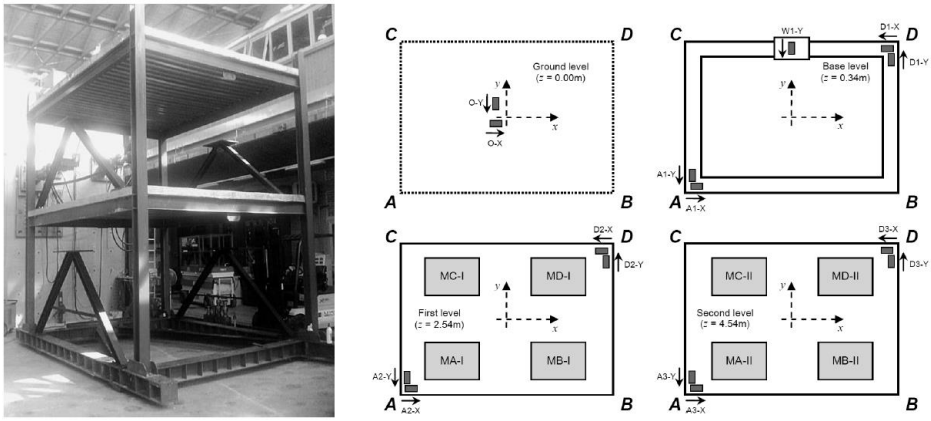

Figure 1. The structural prototype: The overall view and the location of the accelerometers and additional blocks

Table 1: Properties of the additional masses

Block	Ievel	Corner	Mass(kg)	e_x	e_y	BC	NC	SC
MA-I	I	A	338	-0.95	-1.00	No	Yes	Yes
MB-I	I	B	340	0.95	-1.00	No	Yes	Yes
MC-I	I	C	336	-0.95	1.00	No	No	Yes
MD-I	I	D	336	0.95	1.00	No	No	Yes
MA-II	II	A	336	-0.95	-1.00	No	Yes	Yes
MB-II	II	B	340	0.95	-1.00	No	Yes	Yes
MC-II	II	C	338	-0.95	1.00	No	No	Yes
MD-II	II	D	330	0.95	1.00	No	No	Yes

The experimental data acquired during tests under the various excitation scenarios and for each mass configuration have been recently made kindly available to the Authors by partner Unites directly involved in the experimental campaign. These data, and the brief introduction above, are the starting point of the present note.

In what follows, such data will be processed in order to calibrate a representative FE model of the test structure. Even in case a more elaborate numerical model should finally be preferred, the results of the present note will hopefully help at least in the estimation of plausible inertia properties of the building. Also, the performed experimental modal identification will highlight some intriguing issues of unexpected coupled dynamics, showing the potentially significant role of secondary elements in the overall response of dynamic systems.

The experimental modal is identified on the basis of ambient vibration tests. Three classical output-only methods are used to extract frequencies and mode shapes, respectively working in the time-domain, in the frequency-domain and in the time-frequency domain: ERA,FDD and TFIE. The V-inverted braces attached to the first storey works as a TMD, which produces the coupling effect to the fourth mode. The current updating relies on the left five modes. (Matta, 2011)

7.2 The numerical model

In this section, the 3-D FE numerical model of the JETPACS frame structure is formulated which will undergo experimental calibration in subsequent sections. Two alternative modelling approaches have already been implemented by partner Units, together with corresponding model calibration strategies.

In precedence, a 6-Degree-Of-Freedom (6-DOF) FE model, with two translational DOFs and one rotational DOF for each storey. Both mass and stiffness matrices are there obtained starting from a wholly-flexible model with 72 DOFs(6 DOFs for each of 12 nodes: 8 beam-column nodes, 2 central nodes and 2 eccentric nodes), clamped at the base level, in which Euler-Bernoulli flexibility formulation and lumped mass representation are adopted for columns and beams; columns' and beams' axial rigidity and floors' in-plane rigidity are enforced through 50 linear kinematical equations; and finally the 16 rotational DOFs at the beam-column nodes are eliminated through a Guyan reduction. At last, the stiffness matrix of the resulting condensed 6-DOf model is parameterized under the simplifying assumption of identical columns at both storeys and identical beams at both storeys for each direction. In the subsequent updating procedure, inertia properties of both storeys are first identified based on the change in modal frequencies between the BC and the SC mass configurations, under the simplifying assumption of co-linearity between respective modeshapes, using an asymptotic technique; then the unkown stiffness parameters are updated based on the obtained mass matrix through matching simulated with identified modal properties.

In the present note, a 6-DOFs FE model is condensed in MATLAB according to exactly the same procedure described in the last paragraph but for minor variations in deriving the system mass matrix. A simplified model in MATLAB language is here preferred to a more detailed one developed through commercial software, being the former more suitable for the subsequent iterative model-updating procedure. (Matta, E, De Stefano, et., 2011)

The main modelling assumptions are briefly summarized as follows.
Stiffness and mass matrices, respectively K and M, are condensed to the six translational and rotational displacement components of the first and second floors' geometrical centres, included in the vector $\eta = \{dx1 \;\; dy1 \;\; d\theta1 \;\; dx2 \;\; dy2 \;\; d\theta2\}^T$, under the hypotheses of axial rigidity of Euler-Bernoulli type colums and beams, in-plane rigidity of floor slabs, and lumped mass formulation for columns and beams. Columns are supposed to be clamped at their base(i.e. no dynamics attributed to the base level), the V-inverted braces deprived of any dynamics of their own, and no connection is explicitly recognized between the floor slab and the steel beams.

In order to simulate the floors' sagging effect, the slab thickness at the i-th level, ti, is modelled not as a constant value but as a 4th order polynomial function of x and y, according to the following expression:

$$ti(x,y) = si + fi[1-(2x/Lx)^2|1-(2y/Ly)^2]$$

Where Lx and Ly are the slab dimensions along x and y axes, si is the uniform

thickness at the i-th level, fi I s the mid-span deflection of the i-th floor. Accordingly, the slab mass mi and the slab polar inertia Joi are obtained respectively as:

$$mi = \int_A \varrho cti(x,y)dA = \varrho cLxLy(si + \frac{rfi}{9})$$

$$Joi = \int_A \varrho cti(x,y)(x^2 + y^2)dA = \varrho cLxLy(Lx^2 + Ly^2)(si - 12 + fi/45)$$

Where obviously the integral operator preserves the linearity between the two inertia properties and the two thickness parameters at each floor.

Each of the concrete blocks deployed in the NC and in the SC configurations is individually accounted for as a translational inertia rigidly attached to the floors, and enters the system mass matrix with its own mass, static moment and polar inertia.

For simplicity's sake, a unique mean value is attributed to all the blocks' masses, averaged over the values given in Table 1, and equal to 336.75 kg.

With the previous assumptions, for each mass configuration the nominal FE model is obtained through equaling each geometrical and mechanical parameter to its expected (nominal) value. The following table lists the nominal parameters of such nominal model.

symbol	Description	Value	Unit
lx	Distance	4.00	m
ly	Distance	3.00	m
h	Inter-storey	2.00	m
Lx	Slab width	4.14	m

Ly	Slab width	3.14	m
hp	Column	0.5	m
E	Young's	206000	N/mm^2
V	Poisson's	0.3	-
ϱs	Steel mass	7850	Kg/m^3
ϱc	Composite slab	2500	Kg/m^3
s1	Lower slab	0.10	m
s2	Upper slab	0.10	m
f1	Lower slab	0.02	m
f2	Upper slab	0.02	m
m1	Lower slab	3539	kg
m2	Upper slab	3539	kg
J01	Lower slab	7702	kg m^2
J02	Upper slab	7702	kg m^2
Δmi	Individual	336.75	kg
exi	Additional	± 0.95	m
eyi	Additional	± 1.00	m
Icx1	Lower	$1.509 \cdot 10^{-5}$	m^4
Icx2	Upper	$1.509 \cdot 10^{-5}$	m^4
Icy1	Lower	$0.550 \cdot 10^{-5}$	m^4
Icy2	Upper	$0.550 \cdot 10^{-5}$	m^4
Ibx1	Lower x-	$1.317 \cdot 10^{-5}$	m^4
Ibx2	Upper x-	$1.317 \cdot 10^{-5}$	m^4
Iby1	Lower y-	$1.317 \cdot 10^{-5}$	m^4
Iby2	Upper y-	$1.317 \cdot 10^{-5}$	m^4
Ict	Columns'	$2.000 \cdot 10^{-7}$	m^4
Ibxt1	Lower x-	$0.480 \cdot 10^{-7}$	m^4
Ibxt2	Upper x-	$0.480 \cdot 10^{-7}$	m^4
Ibyt1	Lower y-	$0.480 \cdot 10^{-7}$	m^4
Ibyt2	Upper y-	$0.480 \cdot 10^{-7}$	m^4

This table deserves a few comments. First, slab thickness parameters are assumed as si=0.10m and fi=0.02m, as approximately suggested by visual inspection. No effort is put in correctly guessing their values at this point, since at all events subsequently adjusted through experimental reconciliation. For the same reason, mass density of the composite floor slab is assumed as $\varrho c = 2500\ kg/m^3$, roughly accounting for the contributions from concrete, reinforcement and coffer steel sheet. Also, no mass from V/inverted braces is explicitly included in the nominal model, so their contribution will be parceled out from the overall inertias of the updated model. Finally, no flexural stiffening effect is explicitly recognized to the floor slab in the nominal model, i.e. beam-s bending stiffness is equaled to its nominal value. The model parameters for the process of updating are the slab mass, the slab polar inertia, the lower column's bending inertia, the upper column's bending inertia, the lower column's bending inertia and the upper column's bending inertia.The following figure shows the finite element model, and the potential updating parameters and the their correspond position in the structure.

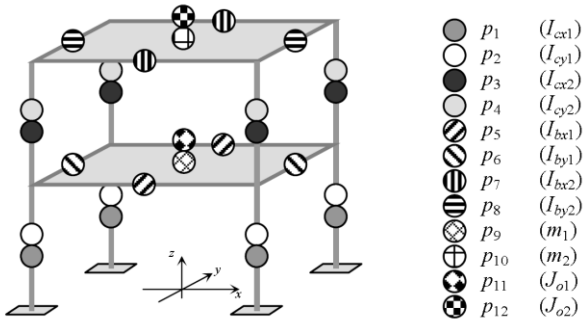

Figure 2. The FE model with the 12 potential updating parameters

7.3 The experimental modal analysis

Identification of structural modal properties from experimental data is the first step towards vibration/based model calibration. Many techniques exist nowadays to process dynamic response measurements in order to catch the dynamic behaviour of a mechanical system, their applicability and success depending on a variety of factors, such as the character of the excitation, the type of the measurement apparatus, the properties of the mechanical system itself, including the extent of non-linearity, the noise level, and so on. In the mere scope of linear methods, dynamic identification may be mainly performed through time-domain, frequency-domain, or time-frequency-domain techniques. The simultaneous use of multiple methods is generally recommended to enhance robustness, as well as the running of several successive identification sessions, performed on different signal fragments and through varying the set-up of the identification parameters. (Matta, E, De Stefano, et., 2011)

In the present case, the dynamic characterization experiments conducted on the JETPACS frame comprised ambient vibrations, impact excitations and base shaking induced by operating a nearby laboratory machine. All the tree mass configurations were tested using a consistent set of 15 accelerometers to measure the structural response.

In this study, only ambient vibrations tests are used, since the only type of tests to have been repeated for all the three mass configurations. Measurements data are processed to extract structural natural frequencies and mode shapes, which will be

used in the subsequent model-updating procedure. As a by-product, structural modal damping is obtained as well.

Three different output-only modal analysis techniques, corresponding to respectively time-domain, frequency-domain and time-frequency-domain methods, are used and the respective results averaged to increase robustness: ERA(Eigen system Realization Algorithm(, FDD(Frequency Domain Decomposition), TFIE(Time-Frequency Instantaneous Estimators). Furthermore, FREs(Frequency Response Functions) are evaluated at the ground level to the accelerations measured at the other locations, in order to confirm the spurious character of certain frequency components corresponding to the external excitations.

Without entering into the details of each technique, results are shown in what follows. Figures 3-5 plot the singular value curves obtained using the FDD technique where the structural natural frequencies are identified through peak/peaking (red circles), for respectively the BC, the NC and the SC mass configurations.

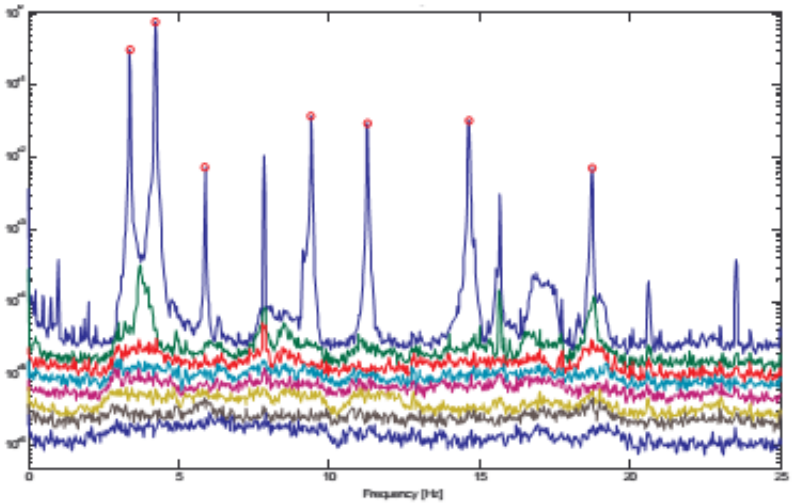

Figure 3. FDD method. Singular value curves in the BC configuration

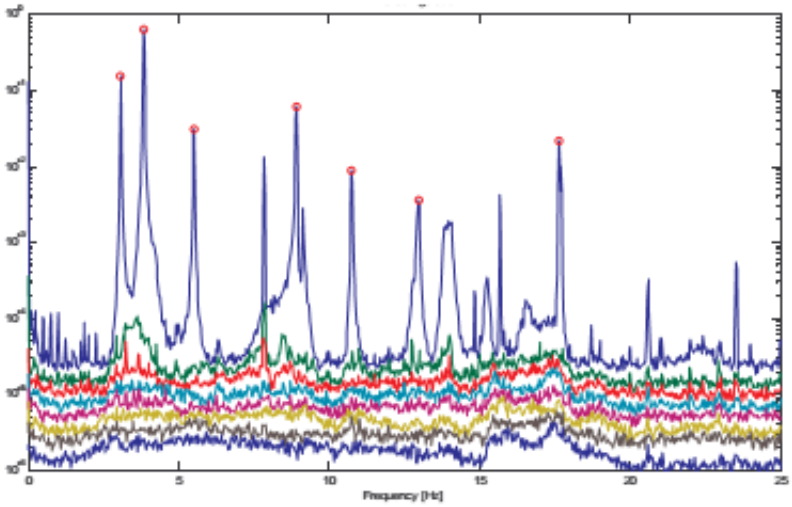

Figure 4. FDD method. Singular value curves in the NC configuration

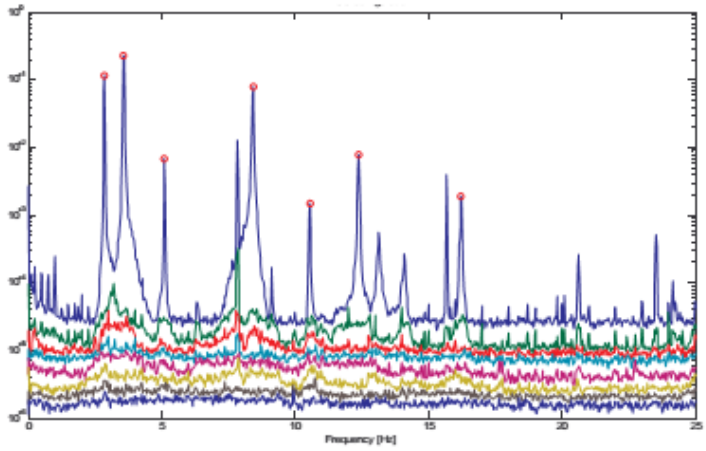

Figure 5. FDD method. Singular value curves in the SC configuration

Figure 6-8, again referred to respectively the BC, NC and SC cases, show the standard deviations of the phase difference provided by the TFIE method. The red circles identify the modal frequencies. Please note that 7 natural frequencies have been circled in Figures 3-8. This aspect will be clarified later.

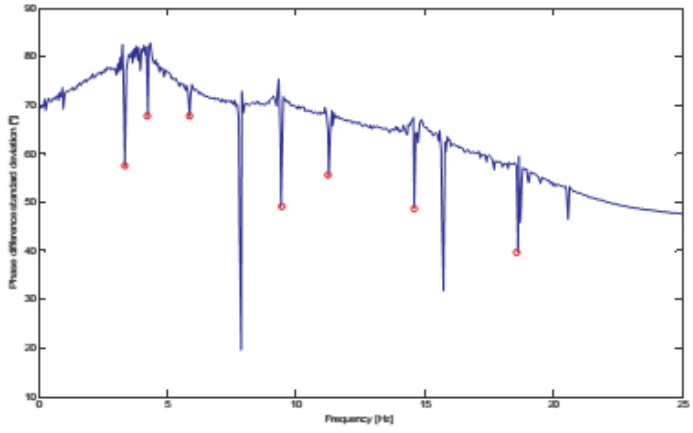

Figure 6. TFIE method. Phase difference standard deviation in the BC configuration

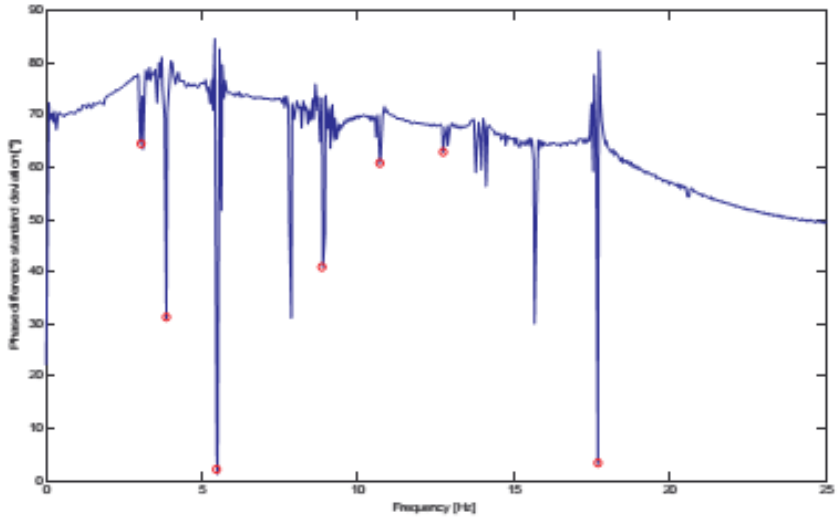

Figure 7. TFIE method. Phase difference standard deviation in the NC configuration

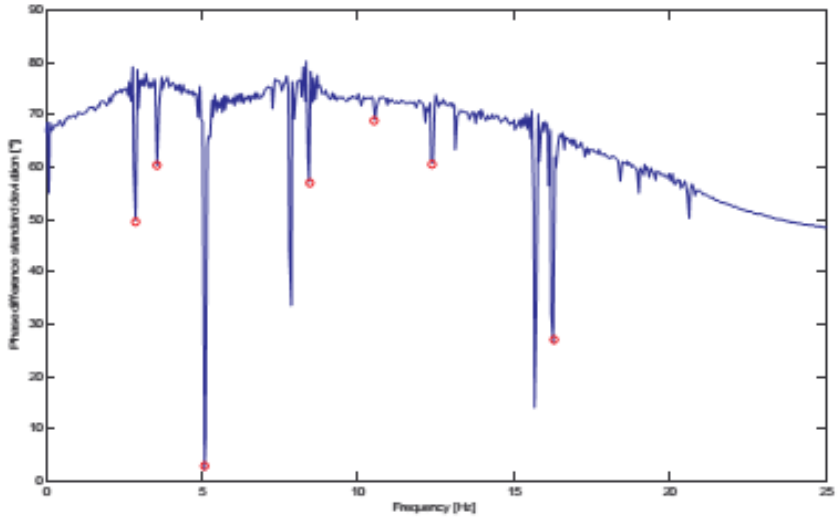

Figure 8. TFIE method. Phase difference standard deviation in the SC configuration

Figure 9-11, again referred to respectively the BC, NC and SC cases, contain the FRFs from the acceleration at the ground level to the acceleration at respectively the first and the second floors (average over the two channels at each floor).

Through applying ERA, FDD and TEIE techniques on several fragments of ambient vibration tests, a considerable number of experimental modal models is deduced, each consisting of a set of identified modes, where every mode is described by a natural frequency, a mode shape and a damping ratio. Each identified mode shape initially possesses as many components as the number of sensing channels, and particularly the rigid in-plane motion of the two composite floors is provided by 8 channels(two at two opposite corners at each storey).

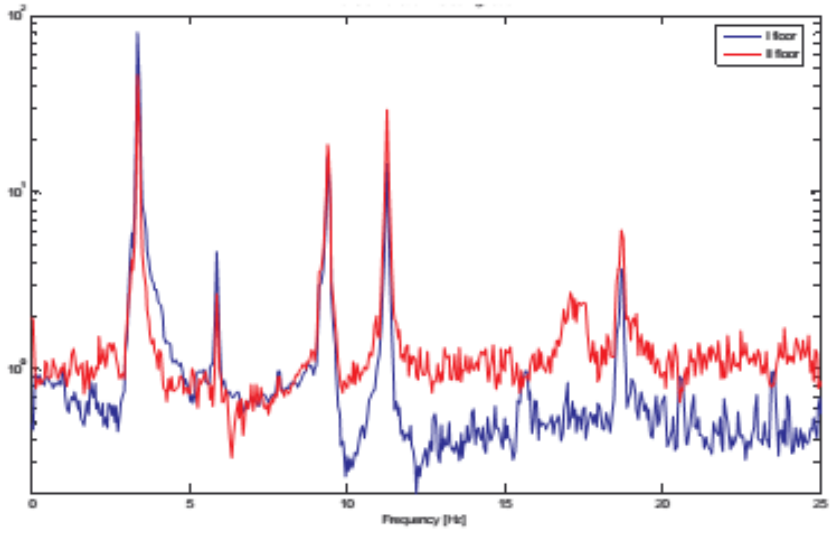

Figure 9. FRFs from the ground to the two storey levels in the BC configuration

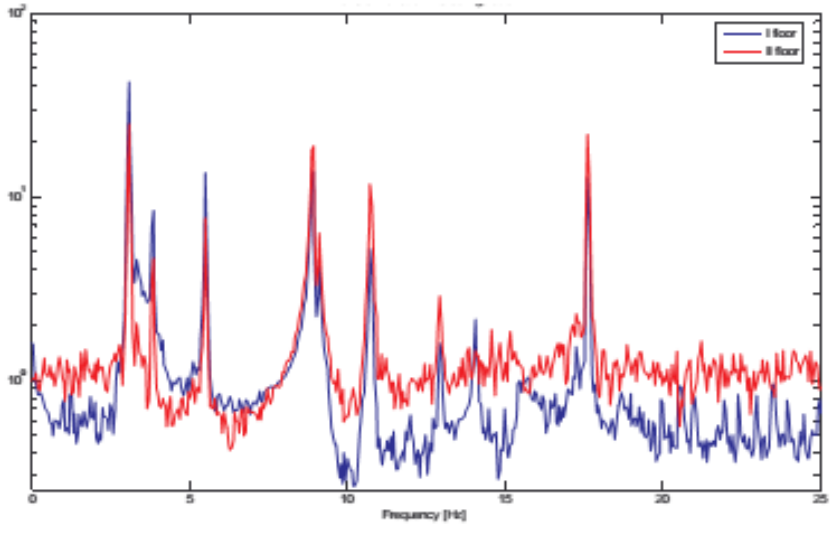

Figure 10. FRFs from the ground to the two storey levels in the NC configuration

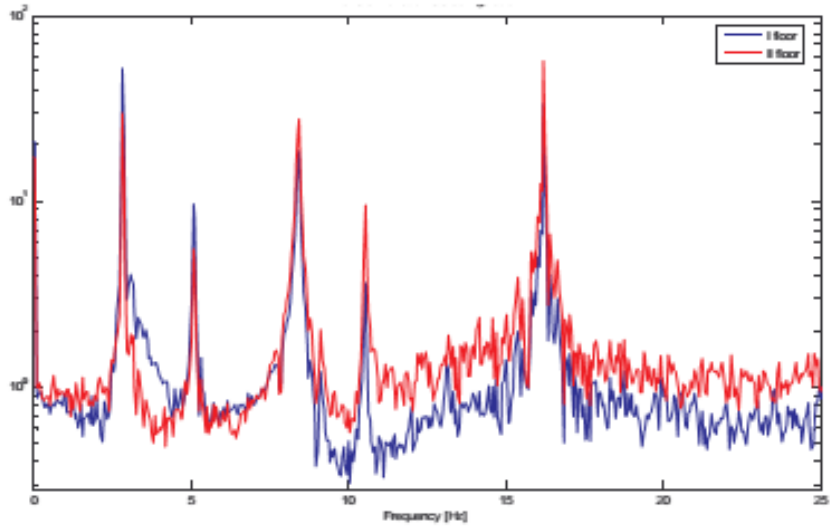

Figure 11. FRFs from the ground to the two storey levels in the SC configuration

By reducing in a least-square sense such 8 redundant components to the 6 DOFs of the analytical model and by further excluding the channels which measure unmodelled dynamic (ground level, base level and brace gusset plate), 6-components eigenvectors are finally synthesized. Through averaging over the whole of the obtained experimental modal models, the mean values and the standard deviations (expressed as a percentage of the mean values) for the natural frequencies and for the mode shape are obtained as reported in Tables 3 and 4, where each mode shape is normalized so as to have unit norm(i.e. unit Euclidean length) and is represented in each column through its components $\phi 1i,..,\phi 6i$(ordered as the elements in the displacement vector η). Not reported in

Tables 3 and 4 since still deserving further verifications, modal damping around 0.2-0.3% has been roughly calculated for the different modes. Identification from impact tests measurements is recommended to improve damping estimation accuracy.

The peculiar and unexpected feature of Tables 3 and 4, easily recognizable in Figures 3-8 as well, is the occurrence of two distinct experimental modes, denoted as 4a and 4b, instead of a single fourth mode, having relatively close frequencies and very similar mode shapes, clearly incompatible with the 6-DOF representation adopted in the FE numerical model. Such weird couple of modes will be reconsidered later in this paper, where an explanation will be provided for their existence.

Table 3. Mean values for the experimental modal properties

Experimental modal properties for the BC configuration (mean values)							
i (# mode)	f_i (Hz)	ϕ_{1i}	ϕ_{2i}	ϕ_{3i}	ϕ_{4i}	ϕ_{5i}	ϕ_{6i}
1	3.37	-0.009	0.507	0.001	-0.005	0.862	0.004
2	4.23	0.445	-0.004	-0.002	0.895	0.006	0.000
3	5.89	0.057	0.053	0.478	0.054	-0.011	0.873
4a	9.39	0.026	0.777	0.006	-0.038	-0.627	-0.029
4b	11.28	-0.031	0.913	0.006	-0.020	-0.405	-0.010
5	14.65	0.876	0.000	0.004	-0.483	0.005	-0.005
6	18.74	-0.006	-0.071	0.828	-0.006	0.011	-0.555

Experimental modal properties for the NC configuration (mean values)							
i (# mode)	f_i (Hz)	ϕ_{1i}	ϕ_{2i}	ϕ_{3i}	ϕ_{4i}	ϕ_{5i}	ϕ_{6i}
1	3.08	-0.004	0.510	0.005	-0.007	0.860	0.004
2	3.85	0.448	-0.004	0.027	0.892	0.002	0.049
3	5.51	-0.120	0.010	0.470	-0.276	-0.032	0.829
4a	8.90	0.012	0.825	0.000	0.004	-0.565	-0.017
4b	10.75	0.020	0.927	0.011	0.022	-0.372	-0.020
5	12.95	0.868	-0.081	0.084	-0.475	0.027	-0.082
6	17.63	-0.247	-0.011	0.806	0.196	0.021	-0.501

Experimental modal properties for the SC configuration (mean values)							
i (# mode)	f_i (Hz)	ϕ_{1i}	ϕ_{2i}	ϕ_{3i}	ϕ_{4i}	ϕ_{5i}	ϕ_{6i}
1	2.85	-0.004	0.505	-0.001	-0.004	0.863	0.005
2	3.57	0.447	-0.002	-0.001	0.894	0.007	-0.001
3	5.11	-0.005	0.012	0.495	0.019	-0.015	0.868
4a	8.43	0.003	0.840	0.002	-0.004	-0.542	-0.012
4b	10.54	-0.001	0.944	0.001	-0.006	-0.329	-0.011
5	12.38	0.880	-0.005	0.002	-0.474	0.002	-0.004
6	16.23	-0.016	-0.062	0.851	0.022	0.008	-0.520

For the time being, such issue set aside, Tables 3 and 4 can be easily explained as follows.

From Table 3, in the symmetric BC configuration, modes 1, 4a and 4b appear as purely flexural modes long y, modes 2 and 5 as purely flexural modes along x, modes 3 and 6 as torsional modes. In the NC configuration, due to the eccentricity of the additional masses, a weak lateral/torsional coupling arises, so that rotational

components appear in modes 2 and 5 and flexural components in modes 3 and 6. Also, due to the increased mass, frequencies generally decrease. In the SC configuration, thanks to the recovered symmetry, lateral-torsional coupling disappear, and frequencies get even smaller

In table 4, the percentage standard deviation in the experimental modal properties is quite small for the natural frequencies(never larger than 0.7 per thousand), and considerably fluctuating for the mode shapes components. As expected, the larger the component-s mean value, the smaller its percentage standard deviation. The deviations represented in bold type in Table 4, corresponding to the two most important components for each mode shape, range from some per-thousand to some percent, up to a maximum of 8.4% for the second important component of the third mode in the BC configuration.

Table 4. Standard deviations for the experimental modal properties

Experimental modal properties for the BC configuration (percentage standard deviations)							
i (# mode)	std[f_i] (%)	std[ϕ_{1i}] (%)	std[ϕ_{2i}] (%)	std[ϕ_{3i}] (%)	std[ϕ_{4i}] (%)	std[ϕ_{5i}] (%)	std[ϕ_{6i}] (%)
1	0.03	72.2	0.6	90.9	240.7	0.2	86.6
2	0.06	0.2	39.6	15.8	0.0	47.8	101.4
3	0.02	126.1	97.3	8.4	110.9	392.8	0.7
4a	0.06	155.8	2.7	302.0	214.2	3.1	91.2
4b	0.02	230.4	1.0	214.4	210.8	6.9	303.7
5	0.01	0.5	2328.1	92.7	1.5	110.5	41.9
6	0.01	873.4	73.3	3.0	820.3	271.9	4.1

Experimental modal properties for the NC configuration (percentage standard deviations)							
i (# mode)	std[f_i] (%)	std[ϕ_{1i}] (%)	std[ϕ_{2i}] (%)	std[ϕ_{3i}] (%)	std[ϕ_{4i}] (%)	std[ϕ_{5i}] (%)	std[ϕ_{6i}] (%)
1	0.05	280.4	0.9	98.3	229.4	0.3	112.8
2	0.07	0.3	66.6	35.0	0.1	94.1	35.8
3	0.06	7.4	117.6	1.2	8.8	20.6	0.8
4a	0.04	142.7	0.5	2496	1042	1.0	46.2
4b	0.01	194.6	0.7	126.3	276.7	2.3	53.4
5	0.03	2.0	110.0	44.5	5.8	64.0	29.4
6	0.00	5.5	159.8	0.8	9.8	67.4	1.0

Experimental modal properties for the SC configuration (percentage standard deviations)							
i (# mode)	std[f_i] (%)	std[ϕ_{1i}] (%)	std[ϕ_{2i}] (%)	std[ϕ_{3i}] (%)	std[ϕ_{4i}] (%)	std[ϕ_{5i}] (%)	std[ϕ_{6i}] (%)
1	0.05	217.3	0.6	814.2	546.2	0.3	69.2
2	0.06	0.4	132.4	76.2	0.1	78.0	36.2
3	0.01	1101.5	272.7	3.9	412.0	275.5	1.8
4a	0.04	617.2	0.5	196.0	356.1	0.9	64.2
4b	0.01	210.8	0.8	1753	210.8	6.5	81.0
5	0.02	0.7	127.8	256.2	2.4	191.9	212.7
6	0.01	133.9	61.9	1.2	191.7	338.8	2.4

Let us now go back to the couple of modes 4a and 4b, and try to explain them. The first question arises if they are real(physical) or spurious(computational) modes. The spurious modes is actually inherent in the external input and not representative of intrinsic structural dynamics, as will be also easily inferred from the auto-spectrum of the ground measurements. In fact, several circumstances

proclaim modes 4a and 4b as real. First, they are confirmed by virtually all identification sessions and for all mass configurations, even though the peak at the higher frequency appears less pronounced in the NC and SC cases than in the BC case. In particular, they both exist no matter how large the vibration level of the individual signal fragment, so they are unlikely the effect of nonlinearities. Second, they undergo the same trend of frequency reduction that can be appreciated in Table e for any other mode, as the structural mass increases from the BC to the SC configurations. Third, looking at the auto-spectrum of the accelerations measured at the base level, no abnormal energy appears to enter the structure at frequencies close to those attributed to these two modes. To sum up, modes 4a and 4b must be real modes. But what-s their origin then?

To answer this question, let us consider Figures 12/14, where the auto/spectral densities are plotted, respectively in the BC, NC and SC mass configurations, for the accelerations in the y direction measured at the ground level, at the base level, at the first and second floor levels and at the gusset plate atop one of the lower V-inverted braces(those attached to the base level of the prototype).

Looking at the figures 12-14, first a confirmation is obtained on what anticipated earlier about the real character of the couple of modes: the two correspondent peaks, migrating leftwards as the structural mass increases, are evident for the two storey levels(and larger at the first floor as it is typical for a second flexural mode) whilst virtually absent for the ground and base levels, contrary to the small peak around 7.8Hz, almost identical for all the spectra and independent on the mass configuration, and already identified as a spurious mode. But a new ingredient,

above all, enters these figures, which has been overlooked so far: the braces transverse dynamics.

With respect to the global behaviour of the benchmark structure, braces could be classified as secondary structural elements. Their mass is relatively small, their connection to the main steel frame is made uncertain by the degree of restraint provided by their bolted connection to the composite floor and to the lateral beams, their transverse (along-y) behaviour is of little interest in the final (controlled) structural configuration, when a seismic action will be applied in the longitudinal(along-x) direction and the braces will be connected to the floors through the control prototypes. For these reasons, in the simplified 6-DOF model derived in last section their dynamics was completely ignored.

Figures 12-14 remind that, contrary to expectations, braces' dynamics might play a non-negligible role in the global behaviour of the structure. A coupling effect can in face be appreciated between the brace's spectrum and the first and second storeys' spectra: on the on hand, modes 4a and 4b induce large peaks on the brace's spectrum, and on its turn the brace induces small but distinct effects on the structural spectra(a protuberance to the left of mode 4a resonance in Figure 12, a bifurcation centred on mode 4a resonance in Figure 13, a small peak between the two resonnances in Figure 14).

Such interation is even more remarkable in that it regards one of the lower braces(the only instrumented one, unfortunately), i.e. those connected to the base of the frame, a base which should be approximately working as a rigid boundary for the

2-storey frame(and as such modelled in the 6-DOf simplification). The said interaction must essentially rely on the torsional deflection of the lateral beam of the base horizontal frame on which the brace is attached, and through that on the rotation of the base of the columns, so as to reach the two storeys, since it occurs without any intervention of along-y acceleration at the base level(no coupling appears between the brace's spectrum and both the ground and the base spectra).

But Figures 12-14 provides another precious element of information to characterize braces' dynamics: the natural frequency of the lower brace is close to modes 4a and 4b, namely approximately equal to 9Hz.

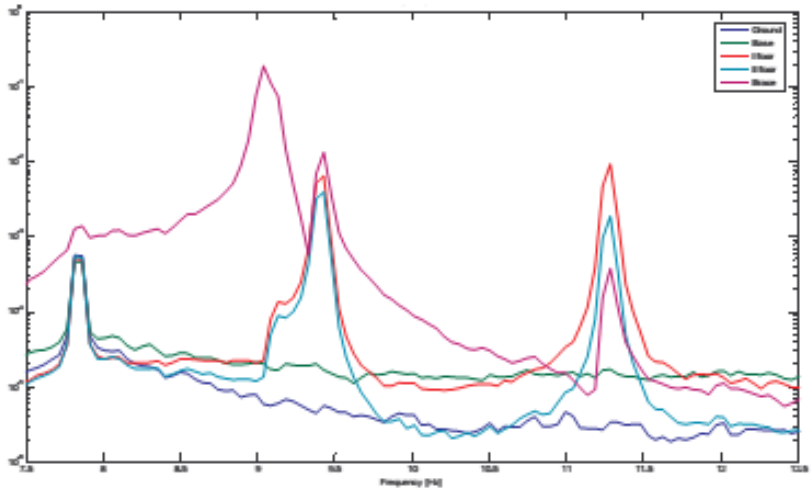

Figure 12. Auto-spectral densities in the along-*y* direction – BC configuration

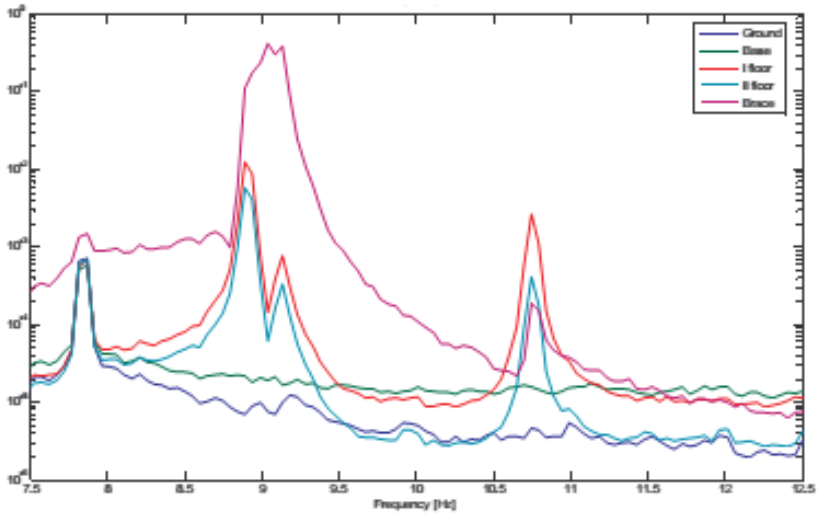

Figure 13. Auto-spectral densities in the along-*y* direction – NC configuration

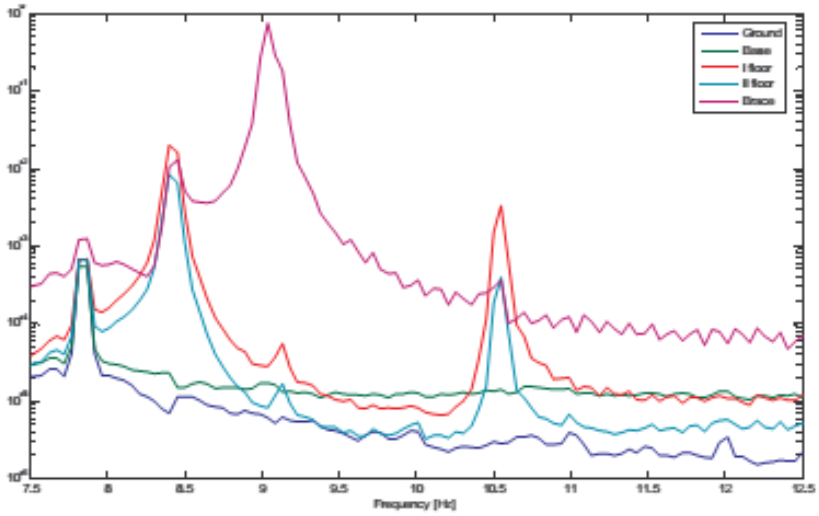

Figure 14. Auto-spectral densities in the along-*y* direction – SC configuration

These findings allow for the following explanation of modes 4a and 4b, which the

explanation require a basic knowledge of the principles of Frahm's Vibration Dynamic Absorber(VDA) and Den Hartog's Tuned Mass Danoer(TMD). The VDA and the TMD are well-known passive control devices working as SDOF appendices of the main system to be controlled, their only difference resting on the VDA being an undamped mass-spring system whereas the TMD is a damped mass-spring-dashpot system. The optimal choice of the device's frequency ratio rc(the ratio of the device's frequency over the structural frequency), generally very close to one, and for the TMD of the damping coefficient as well, assure that, under the effect of an external dynamic input, part of the structural vibratory energy is transferred to the device. A typical transfer function from ground acceleration to structural acceleration in the presence of an under-damped TMD is given in figure 15, where the device's mass is 5% the structural mass, both strucutre's and device's damping ratios are 0.2%, and the device's frequency ratio is equaled to eigher 0.9 or 1.0 or 1.1. Interacting with the structural mode by virture of the frequency closeness, the controlled system clearly possesses two natural frequencies, on right below and one right above the original resonance. The smaller rc, the larger the second peak with respect to the first one, and vice versa. The smaller the device's damping ratio, the more pronounced two peaks.

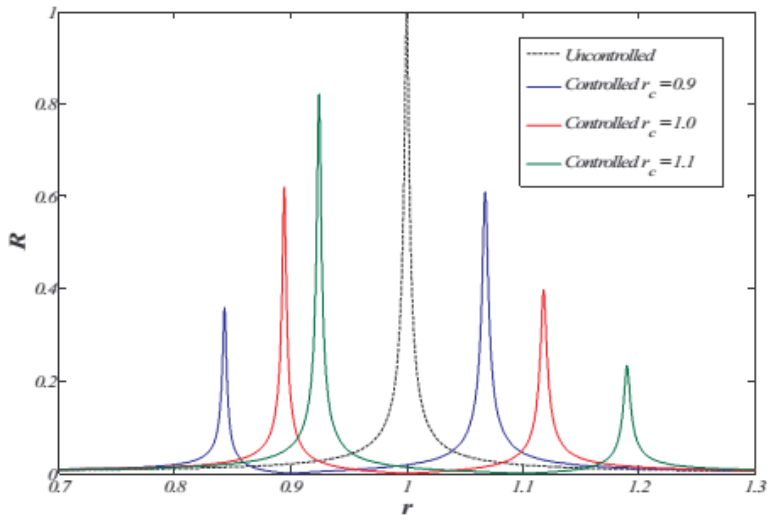

Figure 15. Structural FRF in the presence of an under-damped TMD

All the ingredients being set, the explanation is straightward. The two modes 4a and 4b are merely the result of the coupling of the fourth mode (the second flexural mode in the y direction) of the main structure with the dynamics of the upper V-inverted braces (those attached to the first floor), unexpectedly working as a couple of almost identical under-damped TMD's roughly tuned to the JETPACS prototype.

The total mass of the two TMDs, roughly including the two gusset plates atop and half the mass of the four HE100A, is around 140kg. This value, apparently small compared to the total mass of the building(which in the updated model obtained will approximate 6600kg), is indeed quite large compared to the modal mass o f the fourth mode(which in the updated model will equal to 413kg, 498kg and 583

kg, respectively for the BC, the NC and the SC mass configurations), and this aspect justifies the strong tuning interaction.

An interesting confirmation comes from the way the first and second storyes spectra in Figures 12-14 change due to the increase in the structural mass from the BC to the SC configurations. With the mass increase, the frame structural frequencies obviously decrease whilst the frequency of the couple of (unmeasured9 TMDs must remain unchanged. This corresponds to increasing the frequency ratio rc, and therefore(as clear in Figure 15) to augmenting the first FRF peak while decreasing the second peak. This very effect is recognizable in figures 12-14, where the ratio of the second peak amplitude to the first peak amplitude appears to progressively diminish from the BC to the SC configuration.

The foregoing TMD conjecture is based on the assumption that the two upper braces, unfortunately not instrumented during the characterization tests, roughly behave as the lower braces, one of which instrumented instead. In fact, it is very likely that the upper braces possess a frequency which is slightly higher than the 9 Hz identified for the lower instrumented brace, and approximately equal to 10.3 Hz, i.e. the mean value of the two resonant frequencies of modes 4a and 4b evaluated in the BC configuration (where in fact the two peak amplitudes are almost equal), which is also a rough approximation of the minima(anti-resonance frequency) of first and second floor spectra in Figures 12-14. This guess is left for future experimental verification, which shall merely require ambient vibration acquisition from a further accelerometer deployed on one of the upper braces.

With the forging explanation of modes 4a and 4b, the experimental modal analysis can be taken as fulfilled. Next section will use the identified models to finally step towards calibration of the FE numerical model.

7.4 Finite Element Model-updating

7.4.1 GENETIC ALGHORITHM

Basically, finite element modal-updating is the inverse problem of correcting uncertain parameters of a FE model in order to replicate test results. Many authors have addressed FE model-updating applications to structural dynamics in recent years.

The success of any FE model-updating procedure depends on a number of factors, including the selection of the updating parameters, the definition of the objective function, the choice of the optimization algorithm, the extent of modelling errors and of noise in the test data. If the experimental information is not rich enough to forbid noise from heavily biasing the objective function; if the optimization search is not capable to escape local minima; then, the calibrated model may be unacceptably far away from the real model. In order to avoid such circumstance, robustness should always be pursued in model-updating. To this purpose, some robust techniques are currently under development by Authors, inspired by multi-model approaches, and final aimed at providing not only the most plausible estimate of a model but an index of its reliability as well.

The JETPACS case will offer here the opportunity to show a basic implementation of the ongoing researches. In particular, the importance will be stressed of embracing an entire range of alternative models, each one corresponding to a specific combination of updating parameters. In fact, since large sets of parameters may lead to ill-conditioning, multiple combinations of relatively few parameters must be selected(and independently solved), the selection being governed by direct

a-priori knowledge, and/or by extensive simulation aimed at identifying all the possible condition states (or damage scenarios) for the system. A critical analysis of the resulting multiple solutions will finally enhance reliability of the calibration. In this section, the reference FE model derived in section 2 and the experimental modal model identified in section 3 are used to implement a simple version of multiple-model reconciliation. For each of the multiple models, the procedure is posed as an iterative minimization problem, its main constituents being a set of parameters(optimization variables), an objective function (depending on the parameters9, and an optimization algorithm(searching for the parameters minimizing the objective function).

In this study, the discrepancy between numerical and experimental eigenfrequencies and mode shapes is taken as the objective function. After a preliminary attempt at a Pareto multi-objective optimization to keep frequencies and modeshapes calibration separate, a single objective function is finally preferred which properly weighs the two contributions. The fourth mode is excluded from calibration and a reduced weight is assigned to torsional modes. If all the six modes were employed, the objective function would be as follows:

$$f_{ob} = \sqrt{\frac{\sum_{c=1}^{Nc=3}\sum_{i=1}^{Nm=6}\omega_i^2\left[\omega_f^2\left(\frac{f_{i,s}^c}{f_{i,e}^c}-1\right)^2+w_{\emptyset}^2\left(\sqrt{2(1-\sqrt{MAC_{ii}^c})}\right)^2\right]}{N_c N_m(w_f^2+w_{\emptyset}^2)(w_x^2+w_y^2+w_{\theta}^2)/3}}$$

Where $f_{i,s}^{c}$ and $f_{i,e}^{c}$ are respectively the simulated and the experimental frequencies in the c-th mass configuration; MAC_{ii}^{c} is the Modal Assurance Criterion evaluated between the i-th simulated modeshape and the i.th experimental modeshape in the c.th mass configuration; wf=10 and wϕ=1 are weights assigned to respectively frequencies and mode shapes; wi=wx=2 for i=2, 5 is the weight assigned to modes 2 and 5; wi=wy=2 for i=1,4 is the weight assigned to modes 1 and 4; wi=wθ=1 for i=3,6 is the weight assigned to modes 3 and 6; Nc=3 is the number of mass configurations(BC, Nc, SC); Nm=6 is the number of modes. Since, however, the fourth mode is exclude from the updating, objective function is rescast in the following form:

$$f_{ob} = \sqrt{\frac{\sum_{c=1}^{Nc=3}\sum_{i=1}^{Nm=6}\omega_i^2\left[\omega_f^2\left(\frac{f_{i,s}^{c}}{f_{i,e}^{c}}-1\right)^2 + w_{\emptyset}^2\left(\sqrt{2(1-\sqrt{MAC_{ii}^{c}}}\right)^2\right]}{N_c(N_m-1)(w_f^2+w_{\emptyset}^2)(w_x^2+w_y^2+w_{\theta}^2)/3}}$$

Where the inner summation is evaluated only for i=1, 2, 3, 5, 6, i.e. skips the fourth mode. This objective function represents the weighted error of the numerical model with respect to the experimental modal model.

As to the optimization variables, the overall set of potentially significant parameters is first chosen. Then a sensitivity analysis is used to remove uninteresting parameters.

Finally, from the remaining set of parameters different subsets are extracted, each providing a different model.

In particular, assuming as exactly know the geometry of the structure(except for the floor thickness), the properties E, v, ρs, ρc of the materials, the amount and position of the additional eccentric masses, and the torsional inertia of the columns (since negligibly small), the potentially significant parameters result to be the following 16 ones: columns' bending inertias; beams' bending inertias, slabs' masses and polar inertias; and beams' torsional inertias. (Matta, E, De Stefano, et., 2011)

A sensitivity matrix is then evaluated to show the influence of the 16 parameters on natural frequencies and mode shapes:

Table 5. Percentage sensitivity

	I_{cx1}	I_{cy1}	I_{cx2}	I_{cy2}	I_{bx1}	I_{by2}	I_{by1}	I_{bx2}	m_1	m_2	J_{a1}	J_{a2}	I_{bxt1}	I_{bxt2}	I_{byt1}	I_{byt2}
S_{f1j}	0.0	23.0	0.0	9.6	0.0	0.0	13.8	3.6	-9.4	-34.6	0.0	0.0	0.0	0.0	0.0	0.0
S_{f2j}	18.1	0.0	6.0	0.0	17.1	8.8	0.0	0.0	-7.2	-36.9	0.0	0.0	0.0	0.0	0.0	0.0
S_{f3j}	10.1	9.9	2.1	6.9	7.8	3.2	7.5	2.5	0.0	0.0	-7.0	-31.0	0.0	0.0	0.0	0.0
S_{f4j}	0.0	19.8	0.0	23.9	0.0	0.0	0.2	6.2	-34.0	-9.6	0.0	0.0	0.0	0.0	0.0	0.0
S_{f5j}	23.4	0.0	17.8	0.0	0.0	8.7	0.0	0.0	-36.3	-7.3	0.0	0.0	0.0	0.0	0.0	0.0
S_{f6j}	12.8	8.9	10.0	10.5	0.0	5.0	0.1	2.7	0.0	0.0	-29.8	-7.3	0.0	0.0	0.0	0.0
$S_{\phi 1j}$	0.0	15.1	0.0	10.5	0.0	0.0	1.1	3.5	4.3	4.4	0.0	0.0	0.0	0.0	0.0	0.0
$S_{\phi 2j}$	9.7	0.0	4.5	0.0	0.0	5.2	0.0	0.0	2.6	2.6	0.0	0.0	0.0	0.0	0.0	0.0
$S_{\phi 3j}$	6.3	5.9	1.9	5.4	0.1	2.6	0.4	1.7	0.0	0.0	2.9	3.0	0.0	0.0	0.0	0.0
$S_{\phi 4j}$	0.0	15.2	0.0	10.6	0.0	0.0	1.1	3.5	40.4	41.0	0.0	0.0	0.0	0.0	0.0	0.0
$S_{\phi 5j}$	9.8	0.0	4.5	0.0	0.0	5.2	0.0	0.0	35.0	35.6	0.0	0.0	0.0	0.0	0.0	0.0
$S_{\phi 6j}$	6.4	6.1	2.0	5.5	0.1	2.7	0.5	1.8	0.0	0.0	32.3	33.6	0.0	0.0	0.0	0.0

From Table 5 the modal response results very little influence by beams' torsional inertias which are therefore exclude from updating. A total of 12 variables remain.

According to the multi-model approach, three alternative combinations of parameters, i.e. three possible models, are selected. Each model is then separately solved several times and the statistics of the resulting solutions are analyzed to enhance reliability.

The first model updates only 6 out of the 12 variables indicated above, namely the lower columns' bending inertias Icx1, Icy1 and the slabs' masses and polar inertias m1, m2, Jo1 and Jo2.

The second model updates 8 variables out of 12, the same as for the first model plus the upper columns' bending inertias Icx2, Icy2.

The third model updates 8 variable out of 12, the same as for the first model plus two variable for the beams' bending inertias Ibx1=Ibx2, Iby1=Iby2.

Each time, the optimization is solved using a hybrid stochastic search algorithm consisting of a genetic algorithm(GA) followed by a nonlinear least-square solver(a subspace trust region method based on the interior-reflective Newton method. The GA, using exceeding large numbers of individuals and generations for the purpose of robustness, should grant a solution close to the global optimum. The nonlinear least-square solver, starting from that solution, should grant the convergence to the nearest minimum. For convenience's sake, prior to optimization each variable is normalized with respect to its nominal value. The resulting normalized variable is hereafter denoted with the superscript 'n'. For any individual in the initial GA population, each normalized variable is randomly

extracted in the interval [0.5 1.5].

For the first model, the optimization is run 5 times, and the corresponding solutions are given in Table 6, ordered from the best to the worst. The average model, whose parameters are set to the mean values over the 5 solutions, is reported as well, together with its corresponding objective function.

The mass properties corresponding to the best solution(solution #1) are given in Table 7, where the diagonal terms of the mass matrix M and the slabs' inertial properties (inclusive of the braces' inertias) are reported in the first row while the second row lists the inertial and the geometrical properties of the floors' slabs obtained through deducting braces' inertias (denoted through the star).

Table 6. Updating the first model – 5 runs and the mean value

i (# run)	I_{cx1}^n	I_{cy1}^n	m_1^n	m_2^n	J_{o1}^n	J_{o2}^n	f_{ob} (%)
1	0.756	0.792	0.887	0.716	0.830	0.694	0.827
2	0.750	0.787	0.884	0.713	0.827	0.691	0.827
3	0.743	0.782	0.876	0.710	0.820	0.688	0.829
4	0.771	0.803	0.899	0.723	0.841	0.703	0.829
5	0.785	0.815	0.909	0.730	0.850	0.711	0.834
Mean	0.761	0.796	0.891	0.719	0.833	0.697	0.827

Table 7. Updating the first model – Mass properties for the best solution

$M_{11} = M_{22}$ (kg)	$M_{44} = M_{55}$ (kg)	M_{33} (kg m^2)	M_{66} (kg m^2)	m_1 (kg)	m_2 (kg)	J_{o1} (kg m^2)	J_{o2} (kg m^2)
3673	2999	9154	7686	3140	2534	6394	5348

m_1^* (kg)	m_2^* (kg)	J_{o1}^* (kg m^2)	J_{o2}^* (kg m^2)	s_1^* (m)	s_2^* (m)	f_1^* (m)	f_2^* (m)
2906	2534	5735	5348	0.062	0.066	0.062	0.027

The discrepancy between the experimental and the numerical model is reported for the best solution in Table 8, where the contributions to the objective functions

from the different modes and the different mass configurations are kept separate. No comparison is conducted from the fourth mode, for obvious reasons.

Table 8. Updating the first model – Discrepancies for the best solution

Discrepancy between experimental and numerical modal properties									
	BC configuration			**NC configuration**			**SC configuration**		
***i* (mode)**	$\Delta f_i/f_i$ (%)	MAC_{ii}	f_{obi}^{BC} (%)	$\Delta f_i/f_i$ (%)	MAC_{ii}	f_{obi}^{NC} (%)	$\Delta f_i/f_i$ (%)	MAC_{ii}	f_{obi}^{SC} (%)
1	**0.44**	**1.000**	**0.45**	**-0.06**	**1.000**	**0.16**	**-0.44**	**1.000**	**0.45**
2	**0.45**	**1.000**	**0.47**	**-0.39**	**1.000**	**0.44**	**-0.40**	**1.000**	**0.43**
3	**-0.14**	**0.991**	**0.98**	**0.24**	**0.998**	**0.55**	**0.16**	**0.998**	**0.49**
5	**-1.09**	**0.999**	**1.13**	**1.80**	**0.991**	**2.03**	**-0.48**	**1.000**	**0.49**
6	**-0.70**	**0.994**	**1.05**	**-0.29**	**0.998**	**0.55**	**0.85**	**0.995**	**1.09**

Finally the updated numerical modal properties are reported for the best model in Table 9, which represents the numerical counterpart of Table 3.

The same layout is adopted for presenting the results corresponding to the second model(Tables 10 to 13) and to the third model (Tables 14 to 17).

From tables 6 to 18 the following considerations can be drawn

Table 9. Updating the first model – Modal properties for the best solution

Numerical modal properties for the BC configuration							
i (# mode)	f_i (Hz)	ϕ_{1i}	ϕ_{2i}	ϕ_{3i}	ϕ_{4i}	ϕ_{5i}	ϕ_{6i}
1	3.39	0.000	0.502	0.000	0.000	0.865	0.000
2	4.25	0.435	0.000	0.000	0.901	0.000	0.000
3	5.88	0.000	0.000	0.464	0.000	0.000	0.886
4	9.96	0.000	0.815	0.000	0.000	-0.579	0.000
5	14.49	0.861	0.000	0.000	-0.509	0.000	0.000
6	18.61	0.000	0.000	0.848	0.000	0.000	-0.529

Numerical modal properties for the NC configuration							
i (# mode)	f_i (Hz)	ϕ_{1i}	ϕ_{2i}	ϕ_{3i}	ϕ_{4i}	ϕ_{5i}	ϕ_{6i}
1	3.07	0.000	0.500	0.000	0.000	0.866	0.000
2	3.84	0.432	0.000	0.031	0.899	0.000	0.060
3	5.52	-0.136	0.000	0.440	-0.281	0.000	0.842
4	9.11	0.000	0.825	0.000	0.000	-0.565	0.000
5	13.18	0.866	0.000	0.075	-0.492	0.000	-0.042
6	17.58	-0.284	0.000	0.803	0.181	0.000	-0.491

Numerical modal properties for the SC configuration							
i (# mode)	f_i (Hz)	ϕ_{1i}	ϕ_{2i}	ϕ_{3i}	ϕ_{4i}	ϕ_{5i}	ϕ_{6i}
1	2.84	0.000	0.499	0.000	0.000	0.866	0.000
2	3.55	0.433	0.000	0.000	0.902	0.000	0.000
3	5.11	0.000	0.000	0.462	0.000	0.000	0.887
4	8.45	0.000	0.832	0.000	0.000	-0.554	0.000
5	12.32	0.875	0.000	0.000	-0.485	0.000	0.000
6	16.36	0.000	0.000	0.859	0.000	0.000	-0.512

Table 10. Updating the second model – 4 runs and the mean value

i (# run)	$I_{cx1}{}^n$	$I_{cy1}{}^n$	$I_{cx2}{}^n$	$I_{cy2}{}^n$	$m_1{}^n$	$m_2{}^n$	$J_{o1}{}^n$	$J_{o2}{}^n$	f_{ob} (%)
1	0.782	0.778	0.915	1.073	0.862	0.726	0.834	0.707	0.814
2	0.779	0.776	0.913	1.070	0.859	0.724	0.829	0.706	0.814
3	0.783	0.778	0.913	1.073	0.862	0.726	0.833	0.709	0.814
4	0.768	0.774	0.940	1.070	0.865	0.721	0.835	0.700	0.816
Mean	0.778	0.777	0.920	1.072	0.862	0.724	0.833	0.706	0.814

Table 11. Updating the second model – Mass properties for the best solution

$M_{11} = M_{22}$ (kg)	$M_{44} = M_{55}$ (kg)	M_{33} (kg m^2)	M_{66} (kg m^2)	m_1 (kg)	m_2 (kg)	J_{o1} (kg m^2)	J_{o2} (kg m^2)
3585	3033	9182	7786	3052	2568	6422	5448

m_1* (kg)	m_2* (kg)	J_{o1}* (kg m^2)	J_{o2}* (kg m^2)	s_1* (m)	s_2* (m)	f_1* (m)	f_2* (m)
2818	2568	5763	5448	0.067	0.068	0.044	0.025

Table 12. Updating the second model – Discrepancies for the best solution

Discrepancy between experimental and numerical modal properties									
	BC configuration			NC configuration			SC configuration		
i (mode)	$\Delta f_i/f_i$ (%)	MAC_{ii}	$f_{obi}{}^{BC}$ (%)	$\Delta f_i/f_i$ (%)	MAC_{ii}	$f_{obi}{}^{NC}$ (%)	$\Delta f_i/f_i$ (%)	MAC_{ii}	$f_{obi}{}^{SC}$ (%)
1	0.43	1.000	0.44	-0.06	1.000	0.12	-0.42	1.000	0.42
2	0.46	1.000	0.51	-0.35	0.999	0.44	-0.34	0.999	0.43
3	-0.20	0.991	0.99	0.24	0.998	0.54	0.23	0.998	0.51
5	-1.04	1.000	1.04	1.74	0.991	1.97	-0.61	1.000	0.62
6	-0.73	0.993	1.09	-0.28	0.997	0.61	0.88	0.995	1.11

Table 13. Updating the second model – Modal properties for the best solution

Numerical modal properties for the BC configuration							
i (# mode)	f_i (Hz)	ϕ_{1i}	ϕ_{2i}	ϕ_{3i}	ϕ_{4i}	ϕ_{5i}	ϕ_{6i}
1	3.39	0.000	0.508	0.000	0.000	0.861	0.000
2	4.25	0.427	0.000	0.000	0.904	0.000	0.000
3	5.87	0.000	0.000	0.465	0.000	0.000	0.886
4	10.18	0.000	0.820	0.000	0.000	-0.572	0.000
5	14.50	0.873	0.000	0.000	-0.487	0.000	0.000
6	18.60	0.000	0.000	0.850	0.000	0.000	-0.526

Numerical modal properties for the NC configuration							
i (# mode)	f_i (Hz)	ϕ_{1i}	ϕ_{2i}	ϕ_{3i}	ϕ_{4i}	ϕ_{5i}	ϕ_{6i}
1	3.07	0.000	0.507	0.000	0.000	0.862	0.000
2	3.84	0.425	0.000	0.031	0.903	0.000	0.059
3	5.52	-0.133	0.000	0.441	-0.282	0.000	0.842
4	9.31	0.000	0.829	0.000	0.000	-0.560	0.000
5	13.18	0.877	0.000	0.074	-0.472	0.000	-0.043
6	17.58	-0.290	0.000	0.804	0.176	0.000	-0.488

Numerical modal properties for the SC configuration							
i (# mode)	f_i (Hz)	ϕ_{1i}	ϕ_{2i}	ϕ_{3i}	ϕ_{4i}	ϕ_{5i}	ϕ_{6i}
1	2.84	0.000	0.506	0.000	0.000	0.863	0.000
2	3.56	0.425	0.000	0.000	0.905	0.000	0.000
3	5.12	0.000	0.000	0.463	0.000	0.000	0.886
4	8.62	0.000	0.834	0.000	0.000	-0.551	0.000
5	12.30	0.884	0.000	0.000	-0.467	0.000	0.000
6	16.37	0.000	0.000	0.860	0.000	0.000	-0.510

Table 14. Updating the third model – 4 runs and the mean value

i (# run)	$I_{cx1}{}^n$	$I_{cy1}{}^n$	$I_{bx1,2}{}^n$	$I_{by1,2}{}^n$	$m_1{}^n$	$m_2{}^n$	$J_{o1}{}^n$	$J_{o2}{}^n$	f_{ob} (%)
1	0.629	0.755	1.254	1.192	0.816	0.777	0.790	0.740	0.753
2	0.655	0.753	1.226	1.234	0.833	0.783	0.801	0.754	0.760
3	0.660	0.775	1.192	1.123	0.835	0.768	0.802	0.735	0.761
4	0.661	0.761	1.172	1.136	0.833	0.759	0.796	0.728	0.762
Mean	0.651	0.761	1.211	1.171	0.829	0.771	0.797	0.739	0.757

Table 15. Updating the third model – Mass properties for the best solution

$M_{11} = M_{22}$ (kg)	$M_{44} = M_{55}$ (kg)	M_{33} (kg m^2)	M_{66} (kg m^2)	m_1 (kg)	m_2 (kg)	J_{o1} (kg m^2)	J_{o2} (kg m^2)
3422	3214	8846	8039	2889	2749	6086	5700

m_1* (kg)	m_2* (kg)	J_{o1}* (kg m^2)	J_{o2}* (kg m^2)	s_1* (m)	s_2* (m)	f_1* (m)	f_2* (m)
2655	2749	5427	5700	0.063	0.068	0.042	0.037

Table 16. Updating the third model – Discrepancies for the best solution

Discrepancy between experimental and numerical modal properties									
	BC configuration			NC configuration			SC configuration		
i (mode)	$\Delta f_i/f_i$ (%)	MAC_{ii}	f_{obi}^{BC} (%)	$\Delta f_i/f_i$ (%)	MAC_{ii}	f_{obi}^{NC} (%)	$\Delta f_i/f_i$ (%)	MAC_{ii}	f_{obi}^{SC} (%)
1	0.20	1.000	0.23	-0.03	1.000	0.10	-0.22	1.000	0.23
2	0.21	1.000	0.29	-0.24	1.000	0.30	-0.02	1.000	0.18
3	-0.29	0.991	1.00	0.21	0.998	0.46	0.34	0.999	0.45
5	-0.86	1.000	0.86	1.69	0.991	1.93	-0.78	1.000	0.78
6	-0.65	0.993	1.05	-0.28	0.996	0.67	0.73	0.995	1.00

Table 17. Updating the third model – Modal properties for the best solution

Numerical modal properties for the BC configuration							
i (# mode)	f_i (Hz)	ϕ_{1i}	ϕ_{2i}	ϕ_{3i}	ϕ_{4i}	ϕ_{5i}	ϕ_{6i}
1	3.38	0.000	0.510	0.000	0.000	0.860	0.000
2	4.24	0.463	0.000	0.000	0.887	0.000	0.000
3	5.87	0.000	0.000	0.486	0.000	0.000	0.874
4	10.17	0.000	0.846	0.000	0.000	-0.534	0.000
5	14.52	0.874	0.000	0.000	-0.486	0.000	0.000
6	18.62	0.000	0.000	0.853	0.000	0.000	-0.522

Numerical modal properties for the NC configuration							
i (# mode)	f_i (Hz)	ϕ_{1i}	ϕ_{2i}	ϕ_{3i}	ϕ_{4i}	ϕ_{5i}	ϕ_{6i}
1	3.08	0.000	0.509	0.000	0.000	0.861	0.000
2	3.84	0.461	0.000	0.032	0.885	0.000	0.058
3	5.52	-0.140	0.000	0.462	-0.269	0.000	0.833
4	9.28	0.000	0.849	0.000	0.000	-0.529	0.000
5	13.17	0.874	0.000	0.074	-0.479	0.000	-0.045
6	17.58	-0.297	0.000	0.804	0.175	0.000	-0.485

Numerical modal properties for the SC configuration							
i (# mode)	f_i (Hz)	ϕ_{1i}	ϕ_{2i}	ϕ_{3i}	ϕ_{4i}	ϕ_{5i}	ϕ_{6i}
1	2.84	0.000	0.509	0.000	0.000	0.861	0.000
2	3.57	0.462	0.000	0.000	0.887	0.000	0.000
3	5.12	0.000	0.000	0.485	0.000	0.000	0.875
4	8.59	0.000	0.851	0.000	0.000	-0.526	0.000
5	12.28	0.878	0.000	0.000	-0.478	0.000	0.000
6	16.35	0.000	0.000	0.859	0.000	0.000	-0.512

First, among the three proposed models, the best calibration is obtained with the third one(fob=0.753%) and the worst with the first one(fob=0-827%), the second one resting in the middle (fob=0.814%). This was largely expected. As a matter of fact, the first model makes the stiffness matrix depending only on the lower columns' stiffness, so that a comparatively poor approximation is unavoidable. The second model too can't attain the best results, since it excludes the beams from updating.

It slightly improves the first model through the addition of two further variables, the upper columns' stiffness, but these two variables, although significant according to the sensitivity matrix in the Table 5, are not where the largest uncertainty actually resides: mere a-priori physical knowledge might have easily anticipated that their updated stiffness would have been close to their nominal stiffness(in Table 10 the change is only about 8%), because in the real structure upper columns and lower columns are a unique structural element and no uncertainty exists in their mutual connection. In fact, the improvement from the first model to the second one could be described as more seeming than real: it improves matching the experimental modal properties without actually improving the physical insight. In the end, the third model is superior, in that the two further variables, the beams' stiffness, although seemingly less significant than upper columns' stiffness according to the sensitivity analysis, appear more adequate to represent the actual discrepancies between real and numerical models.

Second, the improvement from the first to the second and up to the third models might appear small in absolute terms if considered in the light of the objective function: respectively from 0.827% to 0.814% to 0.735%. If only the first model

had been explored, an overall error less than 1% would have been easily accepted as correct. But look at the corresponding variations in terms of physical parameters. The mass of the first storey slab, m1, varies from 2906 kg to 2818 kg to 2655 kg. The normalized stiffness of the lower columns along x, lcx1, varies from 0.756 to 0.782 to 0.629. The normalized stiffness of the lower columns along y, Icy1, varies from 0.792 to 0.778 to 0.766. As to the beams, their normalized stiffness is not updated in the first and the second models and thus implicitly equal to 1, whereas for the third model it increases to Ibx1,2=1.252 and Iby1,2=1.192. It is clear, thus, that small absolute variations in the objective function may correspond to large variations in the domain of physical parameters. If, for instance, the 8 parameters on the first row of Table 14(the best solution of the third model) are increased by 10% or 20%, the corresponding objective function will pass from 0.753% to respectively 1.053% or 1.546% only. This fact has some important implications. First, even in simple cases such as the one here addressed, model-updating is not an easy task, and attaining a robust calibration requires a multiple-model approach, so as to depict at which extent results depend on the initial(arbitrary) choice of the set of updating parameters. Small absolute values of the objective function are not per se a reliable index of successful updating. Observing how the solution improves through enlarging the updating set may provide useful information on its optimal dimension. Improvement in the objective functions should always be judged in relative terms: passing from 0.827% to 0.753% may indeed represent a drastic improvement, corresponding to a completely different solution. Second, since small improvements in the objective function may be so important, every care must be taken to minimize all sort of possible errors, which could bias the operator's judgment in the selection of the

best solution. To this purpose, all operations should be repeated and statistically processed for the sake of robustness. Experimental identification should be faced through different techniques and for each techniques should be repeated several times and averaged in order to cancel out random noise. Intrinsically robust optimization algorithms should be chosen and run several times, initially on simulated cases for the sake of validation and only afterwards on the real case. And finally a statistical treatment of the whole solution should be performed.

At any rate, although trying further models should be in principle recommended, the best solution obtained with the third model will be regarded hereon as the final result of the calibration process, and as such proposed to partner Units as a possible model for future work.

Such model, completely defined by the first row of Table 14(and by all the other parameters being equaled to their nominal value, as in Table2), reveals a columns' stiffness which is less than nominal, so as to account for the imperfect clamp at its base, and a beams' stiffness which is larger than nominal, so as to apparently reveal a partial collaboration of the floor slabs. Mass properties are more conveniently read in Table 15, where those of the composite floor slabs are given by m1=2655 kg, m2=2749 kg.

Even in case a more elaborate FE model should finally be implemented through commercial software, the inertia properties found above could possibly be accounted for as a useful reference.

7.4.2 SENSITIVITY BASED METHOD

After having the results of the GA method, we will use the classic sensitivity based method and the new recursive method for the model updating. As told in the last part, the third model should made as a reference model for the further updating, in this part only the third model with 8 parameters are treated. The comparison of between the different methods will be made, and some further discussion of the new recursive method should also be performed.

7.4.2.1 Comparison with the GA methods

With multi-models generated within the research domain, process the new recursive sensitivity method to achieve the convergence. Then with the technics of data mining of all these optimal models, several models are created with their physical meaning. In the present work, the model with minimal objective function is chosen as the optimal model. The next table shows the optimal model obtained with genetic algorithm and the recursive method with 2 subsets.

The comparison of the optimal model between the different methods

	Icx1	Icy1	Ibx12	Iby12	m1	m2	Jo1	Jo2	Fob(%)
Sensitivity	0,6128	0,7572	1,2907	1,1929	0,8068	0,7831	0,7824	0,7451	0,7525
Genetic	0,6290	0,7550	1,2540	1,1920	0,8160	0,7770	0,7900	0,7400	0,7533

From table 1, the optimal value of the objective function obtained with the new recursive sensitivity method is 0.7525%, and the genetic method obtained the optimal value of 0.7533%, which means the new recursive method improves the fitting respect to the genetic method. The new method possess enough fitting capabilities and sufficiently sound physical meaning to be accepted as reliable representation of the benchmark building structure.

7.4.2.2 Critical Analysis with the classic sensitivity method

Now that the new method is validated again in this case, we will discuss the advantage and drawback of the new method. The following figures shows the objective function value in every step, in which five beginning points are selected as the model to be updated, and for each model, the classic method and the new recursive method with two subsets are adopted for the model updating.

1° Model

In this figure, the '1 group' indicates the classic sensitivity based method, all the parameters are updated together, and the '2 groups' indicates the new recursive method with the parameters divided into two subsets.

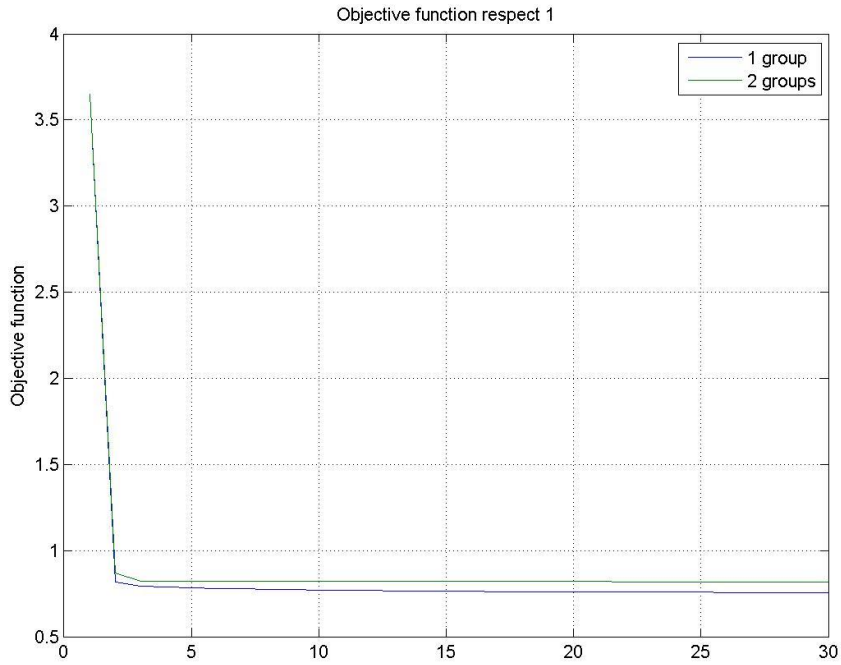

From the figure, we can see the new recursive method can produce equal good results as the classic method. As we proposed in the beginning, the new recursive method should have better efficiency, in the sense that in every single step, the classic method calculate the sensitivity of all the parameters and update all of them, in contrast, the new recursive method only calculate parts of them. The following figure shows the number of calculation in every steps.

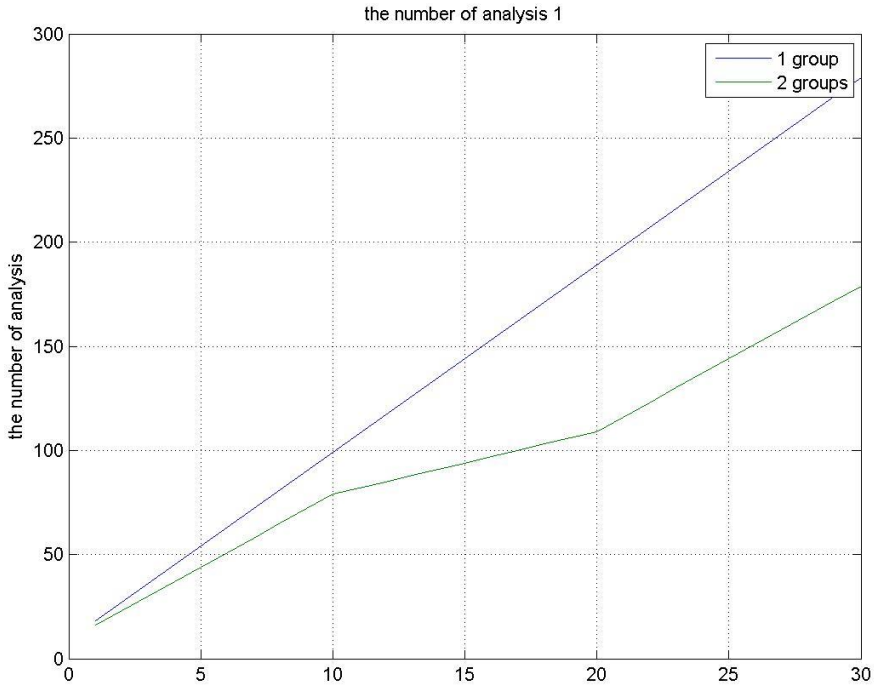

From the figure, we can see the new recursive method made less calculation to get the same results as the classic method. The more steps there are, the more significant difference there is. The difference is becoming more and more significant while the procedure processes. When there are more parameters in updating and the convergence takes more steps, the efficiency of the new recursive method will be more obvious.

2-5° Model

Other four models are selected for updating, and the following figures shows the results.

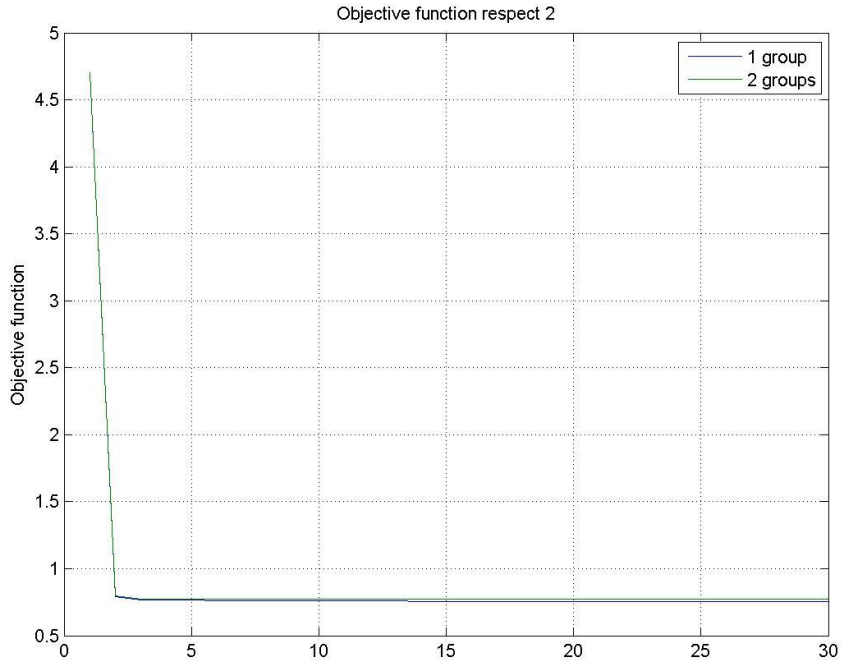

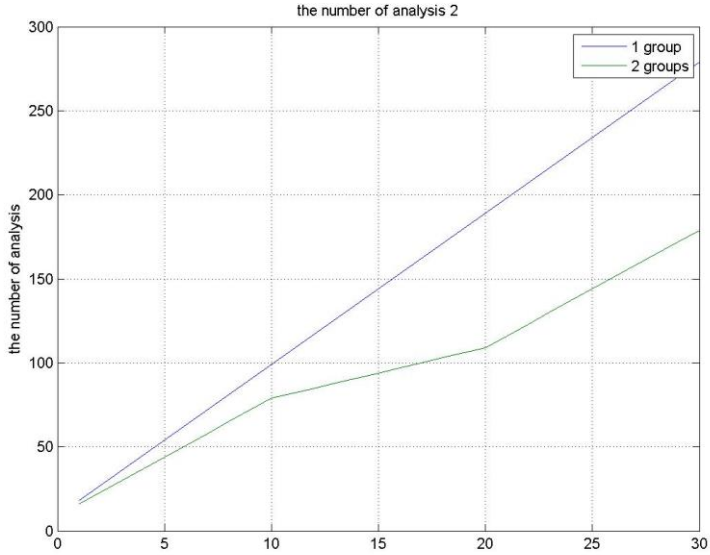
the number of analysis 2
1 group
2 groups
the number of analysis
0
50
100
150
200
250
300
0
5
10
15
20
25
30

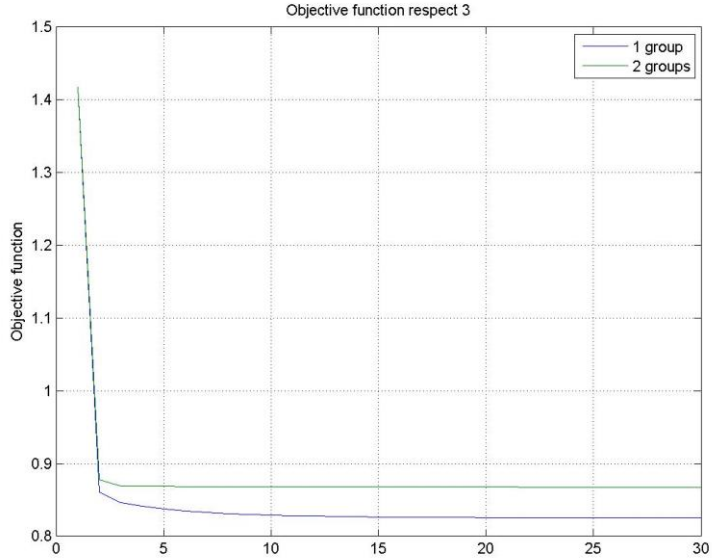
Objective function respect 3
1 group
2 groups
Objective function
0.8
0.9
1
1.1
1.2
1.3
1.4
1.5
0
5
10
15
20
25
30

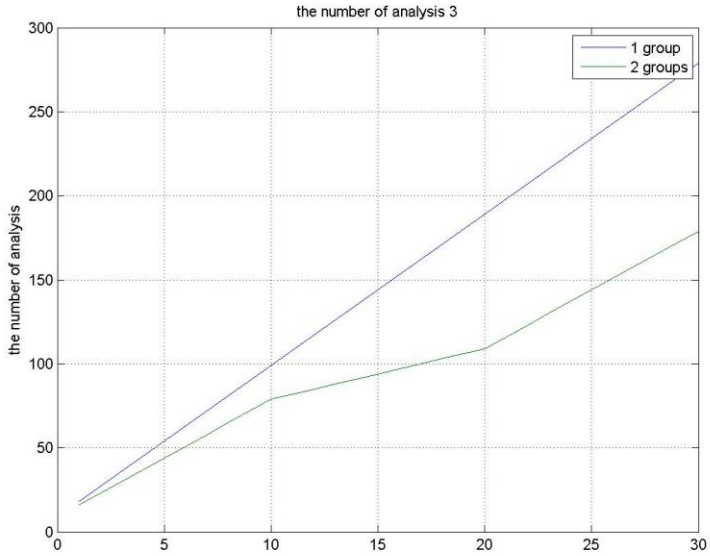
the number of analysis 3
1 group
2 groups
the number of analysis
300
250
200
150
100
50
0
0
5
10
15
20
25
30

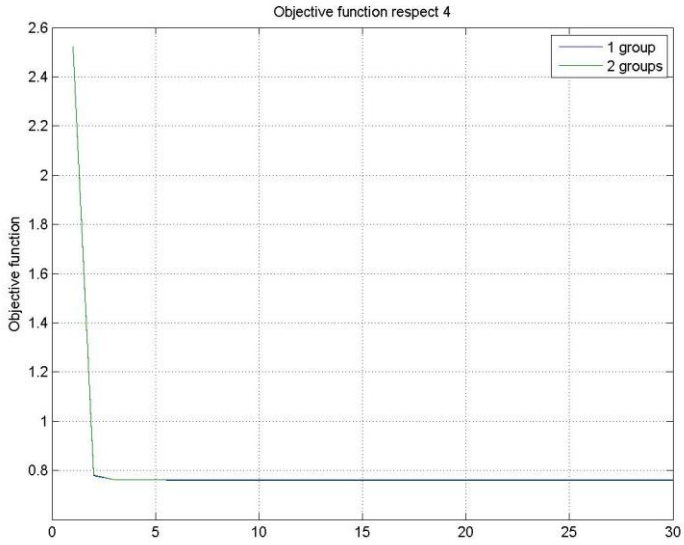
Objective function respect 4
1 group
2 groups
Objective function
2.6
2.4
2.2
2
1.8
1.6
1.4
1.2
1
0.8
0
5
10
15
20
25
30

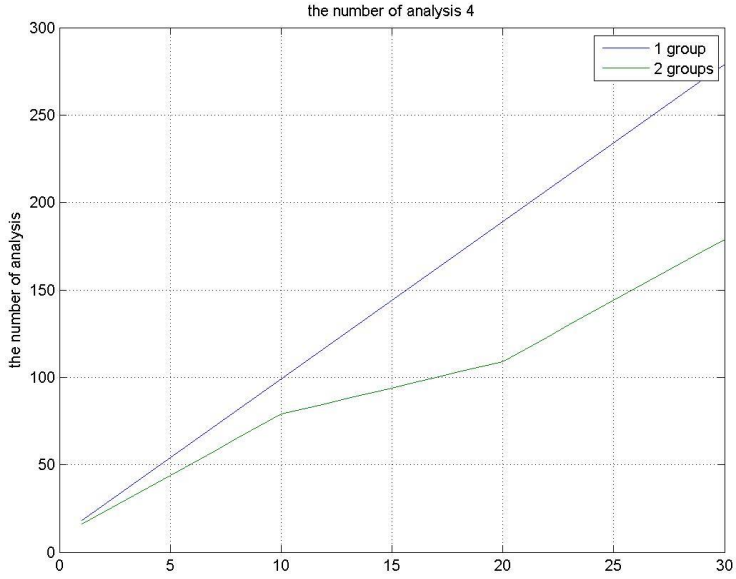
the number of analysis 4
1 group
2 groups
the number of analysis
0
50
100
150
200
250
300
0
5
10
15
20
25
30

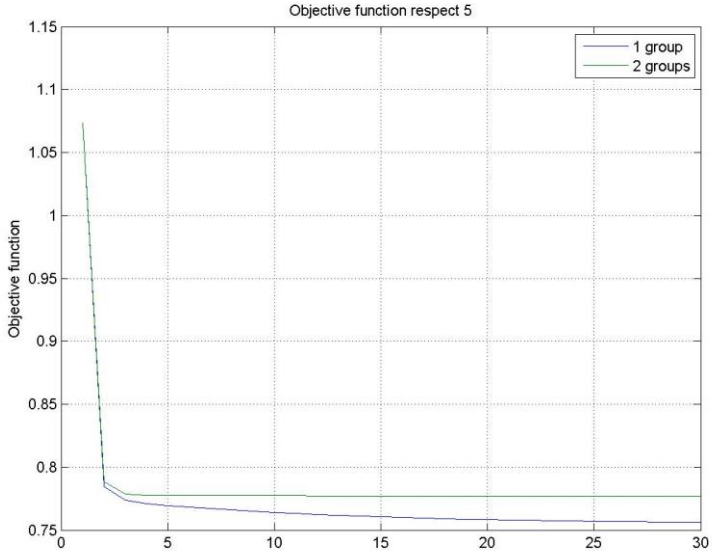
Objective function respect 5
1 group
2 groups
Objective function
0.75
0.8
0.85
0.9
0.95
1
1.05
1.1
1.15
0
5
10
15
20
25
30

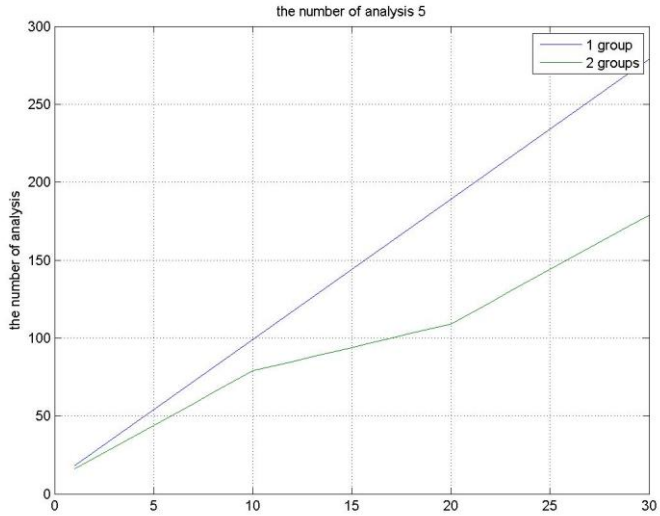

The results leads to the similar conclusion got from the first model, the new method has significant efficiency with respect to the classic method.

7.4.2.2 Comparison within the new recursive method

In this case, the model updating with 2 subsets is obviously better than the classic method. If we divide the parameters into more subsets the efficiency can be further improved? We will update the 6° mode with the classic method, new recursive method with 2 subsets and 3 subsets. The results are showed in the following figures:

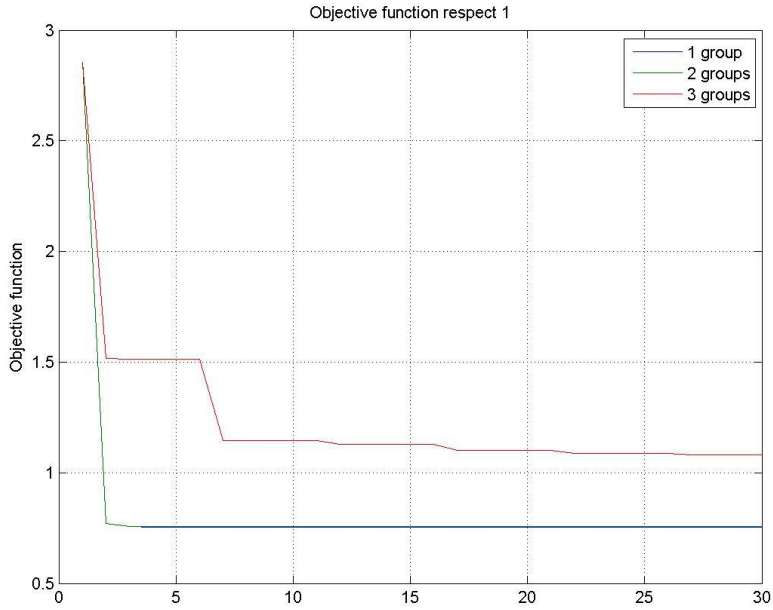

Obviously the results of the updating with 3 subsets are not good as classic method and recursive method with 2 subsets. Because there are only 8 parameters, 3 subsets are too much, which leads to the convergence into the local minimum.

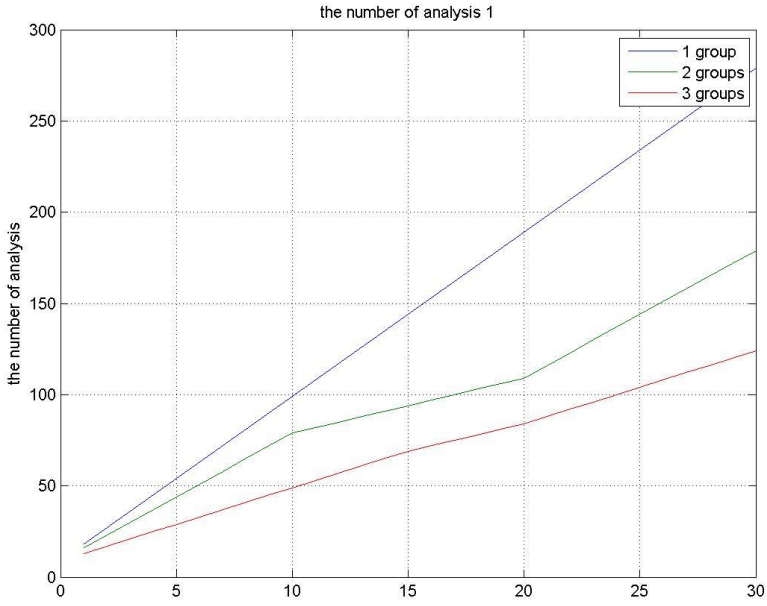

Of course the more subsets there are, the less the number of calculation there are. The efficiency is improved but the best results are missed. Let's try other beginning points to get more overall view.

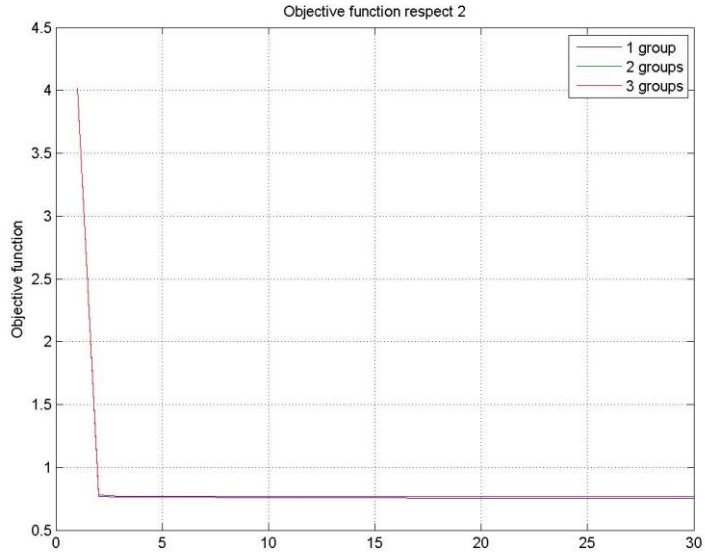
Objective function respect 2
Objective function
1 group
2 groups
3 groups
4.5
4
3.5
3
2.5
2
1.5
1
0.5
0
5
10
15
20
25
30

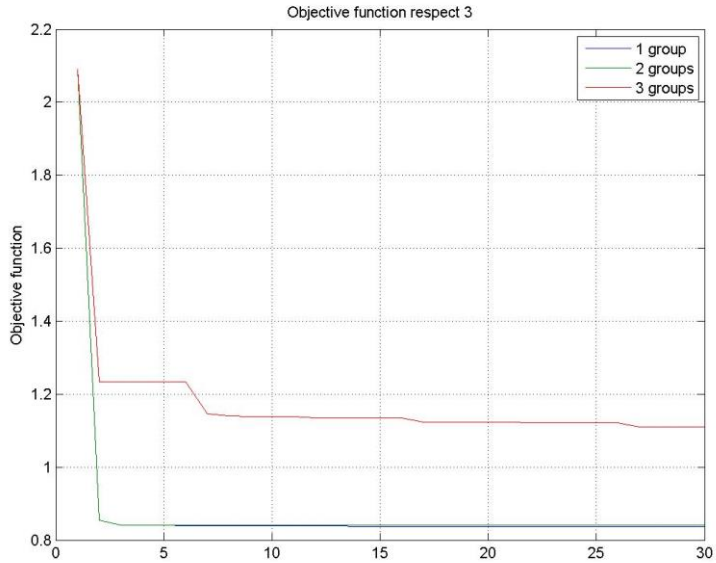
Objective function respect 3
Objective function
1 group
2 groups
3 groups
2.2
2
1.8
1.6
1.4
1.2
1
0.8
0
5
10
15
20
25
30

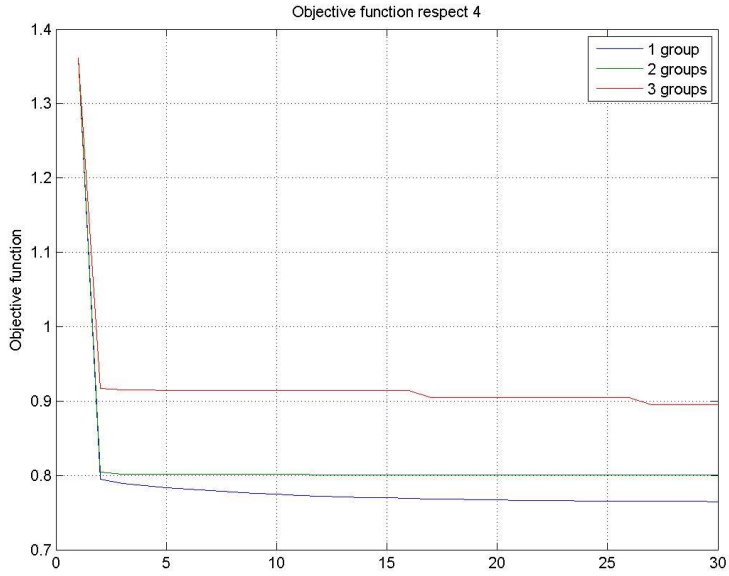
Objective function respect 4
Objective function
1 group
2 groups
3 groups
1.4
1.3
1.2
1.1
1
0.9
0.8
0.7
0
5
10
15
20
25
30

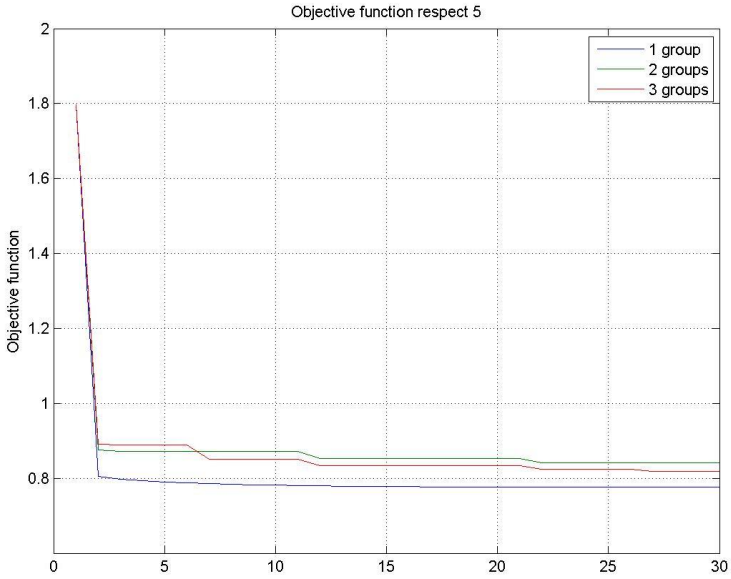
Objective function respect 5
Objective function
1 group
2 groups
3 groups
2
1.8
1.6
1.4
1.2
1
0.8
0
5
10
15
20
25
30

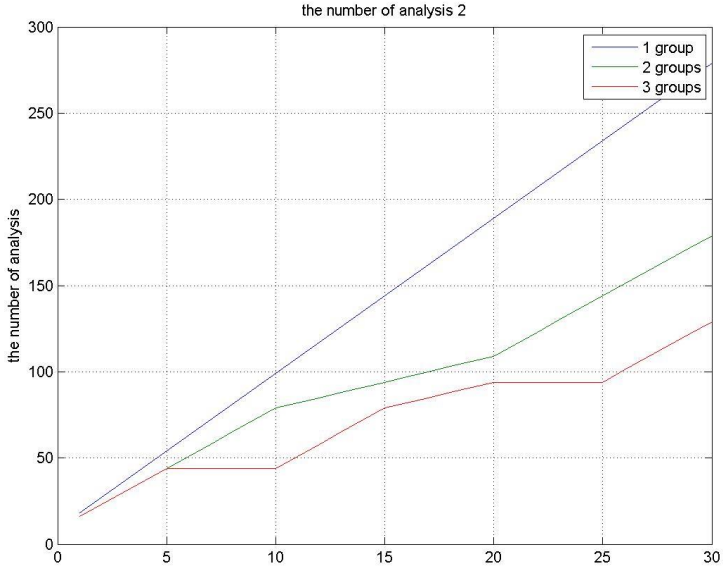
the number of analysis 2
the number of analysis
1 group
2 groups
3 groups
0
50
100
150
200
250
300
0
5
10
15
20
25
30

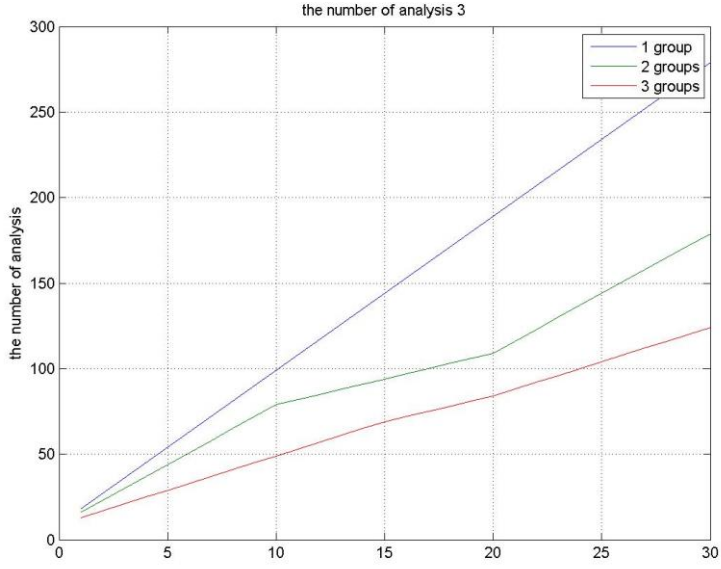
the number of analysis 3
the number of analysis
1 group
2 groups
3 groups
0
50
100
150
200
250
300
0
5
10
15
20
25
30

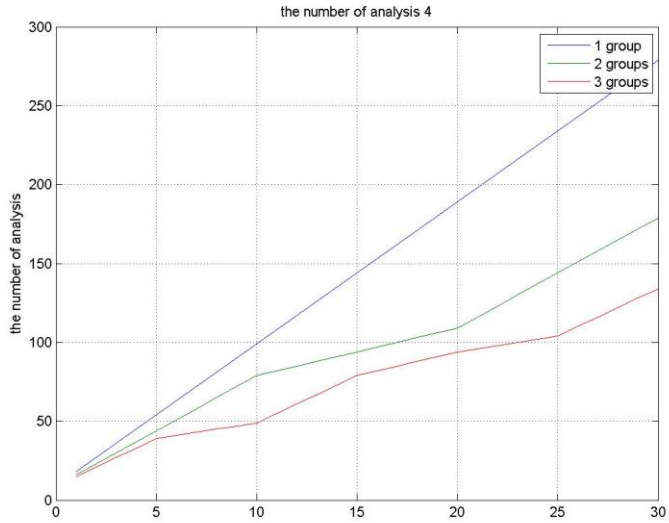
the number of analysis 4
1 group
2 groups
3 groups
the number of analysis
0
50
100
150
200
250
300
0
5
10
15
20
25
30

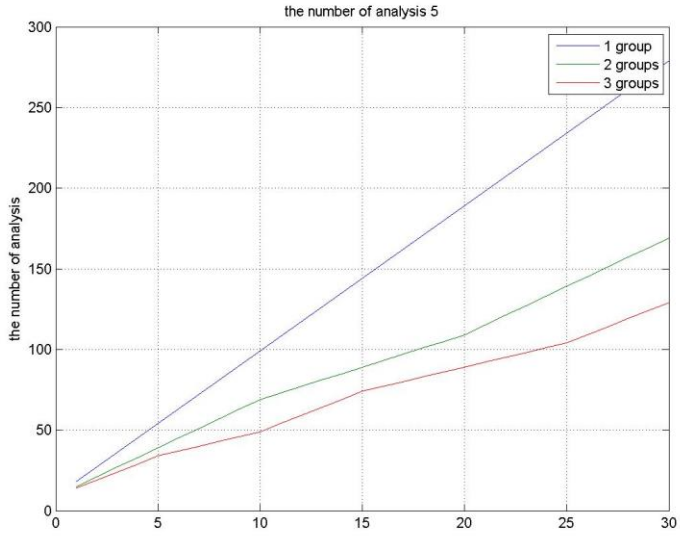
the number of analysis 5
1 group
2 groups
3 groups
the number of analysis
0
50
100
150
200
250
300
0
5
10
15
20
25
30

From the figures we can see that most of the cases, the model updating with 3 subsets leads to the local minimum, sometimes it can get the even good results as the classic method and the recursive method with 2 subsets.

The new method is a multiple method, we usually update many models, after the updating, the data mining and clustering technique are used. Obviously if there are too many local minimums, the results will mislead the engineers' insight of the real condition of the system.

So that, the number of subsets should be chosen carefully to get rid of this situation. The number of subsets should be chosen according to the number of parameters and the distribution of their sensitivity. A more rational technique should be developed to discover a complete and automatic way to choose the number of subsets.

Chapter 8

Conclusion

A new recursive, direct-search, hybrid model updating technique is presented to increase the efficiency and the robustness in the parametric system identification. The new methodology is applied to the finite element model updating of a benchmark structure, and proven more efficient with respect to the traditional sensitivity method and comparable robustness with the genetic algorithm. The new method is a robust tool to assist the engineers' physical insight in the structural system identification. Further development should be made to make the new method more comprehensive and systematic. During this work, the hybrid method is applied for the model updating, and the multiple model and data mining technique should be applied in the future.

References

Allemang RJ. A(2003). The modal assurance criterion- Twenty years of use and abuse. J Sound Vibration 2003;37:14

Antonacci, De Stefano Gattulli, Lepidi, Matta A(2011). ‘’comparative study on vibration-based parametric identification techniques for a three dimensional structure’’. Structural control and health monitoring. March 2011

Baruch, M. (1984). “Methods of Reference Basis for Identification of Linear Dynamic Structures,”

Bianco, A(2011). “Sviluppo di un algoritmo innovative per il model updating” (in italian). Thesis, Politecnico di Torino, October 2011.

C. Mares, J. E. Mottershead, M. I. Friswell, A(2006). “Stochastic model updating: Part 1—theory and simulated example”. Mechanical systems and signal processing. October 2006.

C. Minas, D. J. Inman, A(1991). “Identification of a Nonproportional Damping Matrix from Incomplete Modal Information”

Caicedo, Zàrate A(2008). ‘’finite element model updating: multiple alternatives’’. July 2008

Deraemaeker ,A(2007), Vibration based SHM : comparison of the performance of modal features vs features extracted from spatial filters under changing environmental conditions.

Fraraccio, Brugger, Betti A(2008). ‘’identification of damage detection structures subjected to base excitation’’. Experimental mechanics. February 2008

Friswell M.I. and Mottershead J.E. A. (1995). “Finite element model updating in structural dyn Model updating in structural dynamics: a survey

Gavin A(2013). ‘’the levemberg-Marquardt method for nonlinear least squares curve-fitting problems’’. September 2013

Ruocci G.; Quattrone A.; De Stefano A. (2011) Multi-domain feature selection aimed at the damage detection of historical bridges. In: JOURNAL OF PHYSICS. CONFERENCE SERIES, vol. 305, pp. 1-10. - ISSN 1742-6588

Goulet, Smith Kripakaran. A. (1995). ‘’Estimation Of Modelling In Structural System Identification’’. International Conference On Structural Health Monitoring Of Intelligent Infrastructure.

Hamerly, Elkan, A(2004). “Learning the k in k-means”

J.D. Collins, G.C. Hart, T.K. Hasselman, B. Kennedy.(1974). “Statistical identification of structures”, AIAA Journal, Vol. 12, No. 2, (1974), pp. 185-190.

J. L. Beck, L. S. Katafygiotis. (1998) “Updating models and their uncertainties” , Journal of engineering mechanics. April 1998

John E. Mottershead, Michael Link, Michael I. Friswell. A(2011). The sensitivity method in finite element model updating: A tutorial. Mechanical Systems and Signal processing 25(2011) 2275-2296.

Charles R Farrar , Keith Worden, A(2007). An introduction to structural health monitoring. DOI: 10.1098/rsta.2006.1928

Juang, Phan, Horta, Richard Longman Nasa Center A(2011). ‘’identification of observer/kalman filter markov parameters: theory and experiments’’. Virginia 23665

Mallano T., A.(2014) “FINITE ELEMENT MODEL UPDATING USING SENSITIVITY ANALYSIS”. Thesis, Politecnico di Torino, 2014

Matta, E, De Stefano, A, and Quattrone, A. (2009). Reliability issues in vibration-based system identification: lessons from the JETPACS case study, in: Proc. 4th Int. Conf. on SHM of Intelligent Infrastructure (SHMII-4), Zurich, Switzerland, July 22-24 2009, paper 325, CD-ROM.

Matta, E, De Stefano A(2011). ‘’Generating Alternatives From Multiple Models: How To Increase Robustness In Parametric System Identification’’. 5th international conference on structural helath monitoring of intelligent structure. December 2011

Matta, E, De Stefano, A., (2011). Generating alternatives from multiple models: how to increase robustness in parametric system identification, in: Proc. 5th Int. Conf. on SHM of Intelligent Infrastructure (SHMII-5), Cancun, Mexico, December 11-15, 2011

Mottershead, Friswell A(2013). ‘’model updating in structural dynamics: a survey’’. May 2013

Mukhaopadhyay, Betti A(2007). ‘’structural identification using response measurements under base excitation’’.

Mukhaopadhyay, Betti A(2007). ‘’4-dof system M-K identification and damage detection using shake table experimental data’’. (in processing)

Randall J. Allemang A(1982). “The Modal Assurance Criterion –Twenty Years of Use and Abuse”

Mukhaopadhyay, Lus, Betti A(2007). ‘’modal parameter based structural identification using input-output data: minima instrumentation and global identifiability issues’’.

Raphael Smith A(2003). ‘’a probabilistic search algorithm for finding optimally directed solutions’’ B. Raphael *, I.F.C. Smith

Raphael, Smith A(2003). ‘’a global stochastic algorithm for global search’’ applied mathematics and computation. 2003

Ravindran, kripakaran, Smith A(2007). ‘’evaluating reliability of multiple-model sstem identification’’. EG_ICE, Slovenia 2007

Robert_Nicloud, Raphael, Burdet Smith. A(2005). ‘’model identification of bridges using measurement data’’. Computer aided civil and infrastructure engineering 2005

Saitta, Raphael, Smith A(2005). ‘’data mining techniques for improving the reliability of system identification’’. Advanced engineering infomratics 19 . 2005.

Saitta, Raphael, Smith A(2006). ‘’combining two data mining methods for system identification’’. 2006

Smith, Saitta A(2007). ‘’improving knowledge of structural system behavior through multiple models’’, journal of structural engineering. 2007

Smith, Saitta A(2007). ‘’multiple-model updating to improve knowledge of structural system behavior’’. 17th Analysis and computational specialty conference.

Teughels, roeck A(2004). ‘’structural identification of the highway bridge z24 by fe model updating’’. Journal of sound and vibration 2004

Annex I

In this appendix I'm describing the principle structural theory and assumption and structure used in this thesis.

3D frame assumption

The 3D frame is a common problem in the civil engineering field and it is necessary to acquire as much as possible from the theory to not fall into errors that usually occurs during the building of the stiffness and mass matrix. We start from the evaluation of the Lagrangian degrees of freedom of the structure. In the space the degrees of freedom of each point are six: three translations along the axes and three rotations around the axes. If we want to model the structure as a shear-type system the structure, basically, can translate and rotate along the vertical axis; so the only degrees of freedom that is worth the consider are the rotation around the vertical axis and the translation along the horizontal axes. In a shear-type system structure the slab is considered to be a rigid body and the intern relative deformation of the slab are null. We can also say that the structure is shear-type if there are not much floors, otherwise the structure is too much slender and its behavior is similar to a bending type system. The reference system is right-handed and the vertical axis is z. We assume thus:

u_i the translation along the x axis;

v_i the translation along the y axis;

θ_i the rotation around the z axis.

The sub-stiffness matrices are built for every frame along x and y. So, we get $[K_x]_i$ and $[K_y]_i$, which dimensions are *nfxnf* and *nfxnf* where *nf* is the number of floors. The mass of each floor al lumped in the gravity center and the columns are not axially deformable, it means that they behaves like springs. If we assume that the structure has three stories we can write the differential equations of the motion for every frame as:

Assuming to consider only the frame in the x direction.

$$[M]\ddot{\mathbf{u}} + [C]\dot{\mathbf{u}} + [K]\mathbf{u} = \mathbf{F}(t) \qquad [I.1]$$

Where$\ddot{\mathbf{u}}$,$\dot{\mathbf{u}}$ and $\mathbf{u}$ are the accelerations, velocities and displacements for each floor.

$$\ddot{\mathbf{u}} = \{\ddot{u}_1\ \ddot{u}_2\ \ddot{u}_3\} \qquad [I.2]$$

$$\dot{\mathbf{u}} = \{\dot{u}_1\ \dot{u}_2\ \dot{u}_3\} \qquad [I.3]$$

$$\mathbf{u} = \{u_1\ u_2\ u_3\} \qquad [I.4]$$

The mass matrix, the damping matrix and the stiffness matrix are:

$$M = \begin{bmatrix} m_1 & 0 & 0 \\ 0 & m_2 & 0 \\ 0 & 0 & m_3 \end{bmatrix} \qquad [I.5]$$

$$K = \begin{bmatrix} k_1 + k_2 & -k_2 & 0 \\ -k_2 & k_2 + k_3 & -k_3 \\ 0 & -k_3 & k_3 \end{bmatrix} \qquad [I.6]$$

$$C = \begin{bmatrix} c_1 + c_2 & -c_2 & 0 \\ -c_2 & c_2 + c_3 & -c_3 \\ 0 & -c_3 & c_3 \end{bmatrix} \qquad [I.7]$$

If the frame wasn't shear-type, the [K] matrix would have been full and non-diagonal. The mass matrix, otherwise, would have been the same. Due to the

continuity within the slab and the frame, the displacements of the frame produce displacements of the slab:

$$S_{xi} = u_i - \theta_i y \quad [I.8]$$

$$S_{xi} = u_i - \theta_i y \quad [I.9]$$

If we assume for every plane that the damping is null and that there isn't any exciting force, it is possible to write a three dynamic equations, two of translations, one of rotation. The order:

$$\sum_m \{k_{xi}\}(x_{1i} - \theta_i y_m) + m_i(\ddot{x}_i - \ddot{\theta}_i \cdot y_{G_i}) = 0$$

$$\sum_{mn} \{k_{xi}\}(y - \theta_i y_m) + m_i(\ddot{y}_i - \ddot{\theta}_i \cdot y_{G_i}) = 0$$

$$-\sum_m \{k_{xi}\}(y - \theta_i y_m) \cdot y_m + \sum_n \{k_{xi}\}(y - \theta_i y_m) \cdot x_n + m_i(\ddot{u}_{2i} - \ddot{\theta}_i \cdot y_{G_i}) y_{G_i} + m_i(\ddot{y} + \ddot{\theta}_i \cdot x_{G_i}) x_{G_i} = 0$$

This equations are valid for every m-th frame and for every i-th floor. If we decide to write only one equation considering the all floors, the m_i, $\{k_{xi}\}$ and $m_i y_{G_i}$ are collapsed in only one matrix. Thus:

Principle of virtual work

This principle is used to get the stiffness coefficients inverting the analytical flexibility coefficients. We know from the Betti's Theorem that:

$$W_{ab} = W_{ba} \quad [I.10]$$

And it means that the Elastic Work produced by a system of forces called A applied to the displacements of a system called B, is equal to the Elastic Work of a

system of forces B applied on the displacements of the system called A.

$$\{F\}_a \cdot \{\delta\}_b = \{F\}_b \{\delta\}_a \qquad [I.11]$$

This theorem of elastic theory is very strong for the application. The best way to explain it is using it onto an examples.

There is also another theorem using in this approach called Maxwell's theorem that is a theorem that links the work of the external forces to the work of the internal strain and deformation.

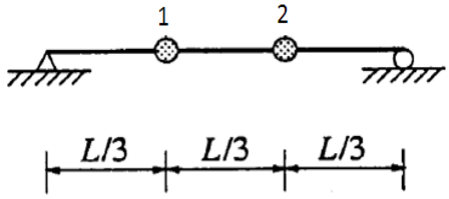

Image : representation of a beam with two point for investigation

We consider the same structure of the explanatory case. The flexibility matrix can be built evaluating the displacement due to an unitary force. So, using the Betti's theorem:

$$f_{11} \cdot 1 = \int M_1 \cdot \varepsilon_1 dV = \int \frac{M_1^2}{EI} dz$$

$$f_{22} \cdot 1 = \int M_2 \cdot \varepsilon_2 dV = \int \frac{M_2^2}{EI} dz$$

$$f_{12} \cdot 1 = f_{21} \cdot 1 = \int M_1 \cdot \varepsilon_2 dV = \int \frac{M_1 M_2}{EI} dz$$

The diagrams of the moments for a unit forces applied is:

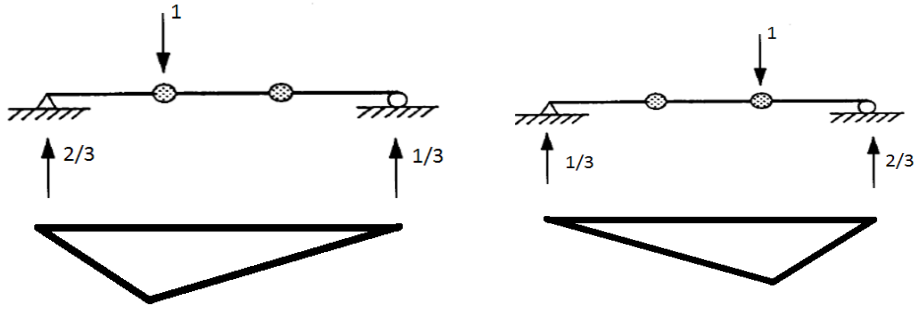

Image A.1: diagram of moment

Since the load is concentrated it is possible to apply the Simpson theorem for numerical evaluation of the integral.

So due to symmetry $f_{11} = f_{22}$ because they have the same diagram of moment. So:

$$\int \frac{M_2^2}{EI} dx = \frac{4}{243} \frac{l^3}{EI}$$

$$\int \frac{M_1 M_2}{EI} dx = \frac{7}{486} \frac{l^3}{EI}$$

So the flexibility matrix becomes:

$$F = \begin{bmatrix} \frac{4}{243} & \frac{7}{486} \\ \frac{7}{486} & \frac{4}{243} \end{bmatrix} \frac{l^3}{EI}$$

Since $K=F^{-1}$. It is easily notice that the stiffness matrix is equal to the one identified with previously.

Static condensation

In literature there exist a lot of methods to operate the reduction of the stiffness and mass matrices through the condensation of the less important degrees of freedom. One of those method is the static condensation. The first one who developed this method was Guyon. His approach can be explained with the following demonstration:

$$[\mathbf{K}] \cdot \mathbf{u} = \mathbf{F} \qquad \text{[I.12]}$$

Where F is a vector of the external applied forces and u is the vector of the degrees of freedom.

If we assume that it is possible to sort the stiffness matrix in a way in which the last coefficients are related to the secondary degrees of freedom can write that:

$$\begin{bmatrix} [K_{pp}] & [K_{ps}] \\ [K_{sp}] & [K_{ss}] \end{bmatrix} \begin{Bmatrix} [u_p] \\ [u_s] \end{Bmatrix} = \begin{Bmatrix} [F_p] \\ [F_s] \end{Bmatrix} \qquad \text{[I.13]}$$

With the subscripts p is indicated the stiffness sub-matrix of the principal Dofs; with s the secondary Dofs. If we want to reduce the degrees of freedom of the structure and delete the secondary ones, we can split the [7.8] into the two equations. From the second one:

$$\mathbf{K}_{sp} \cdot \mathbf{u}_p + \mathbf{K}_{ss} \cdot \mathbf{u}_s = \mathbf{F}_s \qquad \text{[7.9]}$$

$$\mathbf{u}_s = \mathbf{K}_{ss}^{-1} \cdot [\mathbf{F}_s - \mathbf{K}_{sp} \cdot \mathbf{u}_p] \qquad \text{[7.10]}$$

And from the first equation:

$$K_{pp} \cdot u_p + K_{ps} \cdot u_s = F_p \quad [7.11]$$

Replacing u_p of the [7.11] with the value obtained in the [7.10] we can write:

$$K_{pp} \cdot u_p + K_{ps} \cdot K_{ss}^{-1} \cdot [F_s - K_{sp} \cdot u_p] = F_p \quad [7.12]$$

And

$$[K_{pp} - K_{ps} \cdot K_{ss}^{-1} K_{sp}] \cdot u_p = F_p - K_{ss}^{-1} K_{sp} \cdot F_s \quad [7.13]$$

In which

$$K_{REDUCED} = [K_{pp} - K_{ps} \cdot K_{ss}^{-1} K_{sp}] \quad [7.14]$$

$$F_{REDUCED} = F_p - K_{ss}^{-1} K_{sp} \cdot F_s \quad [7.15]$$

When the reduction is applied onto the system also the mass matrix is reduced to respect the degrees of freedom of that system. So:

$$M = \begin{bmatrix} [M_{pp}] & [M_{ps}] \\ [M_{sp}] & [M_{ss}] \end{bmatrix} \quad [7.16]$$

$$M_{REDUCED} = [M_{pp} - M_{ps} M_{ss}^{-1} M_{sp} - (M_{ss} M_{sp})(M_{sp} - M_{ss} M_{ss}^{-1} M_{sp})] \quad [7.17]$$

The [7.15] is the stiffness matrix obtained taking into account the secondary degrees of freedom which equation is referred only to the primary one. And this methodology is used to describe the system of the steel frame.

Annex II

The algorithm developed is written in MATLAB®. the code mathematical step of the code are described very well in the capitol 4. In this appendix are explained the functions used in the code, how they work, how they should be run and how many times are recalled in the analysis.

Main

The main is the file that it is necessary to run to reach the updating of the model:

1. Generation of the models model. it is possible through an input by the user to generate the model using the permutation or not. If the use writes 'y'., it means that wants to generate the sets of parameters using the permutation
2. After the generation of the model a loop is run. The aim of this loop is try to optimize every model using the sensitivity analysis. If the number of parameter is Nm, this loop is run Nm times. At the end of this loop only the models associated to the objective function that reach the convergence are stored. For everyone of this model only the one associated with each minimum of the objective function is stored.
3. A loop inside the loop at the step 2 is built. This loop represents the core of the program. Its purpose is to calibrate natural frequencies and mode shape of a model with the experimental data. this loop is run until the objective function evaluate on every step converges or since the number

of iteration reaches Ni. If we have Nm models and we assume that is necessary to run the calibration Ni times, this loop is used $N_i X N_m$ times.

a. The first step in this loop is to build the sensitivity matrix, it basically corresponds to the Jacobean of the objective function so to run it is necessary to make the derivative for each parameters. In a numerical way it is done applying one per time a small perturbation to each parameters. The perturbed set of parameters is used to get the natural frequencies and mode shapes. The i-th column of the i-th parameter is built as the difference within the natural frequencies or mode shapes non perturbed respect to the perturbed one. The difference is divided by the infinitesimal perturbation. No measurements are used to build the sensitivity matrix [s]
b. The vector dz is built. It is the difference within the experimental measurement and the natural frequencies and mode shapes of the model.
c. The [S] and the dz are used to get the vector dθ to apply to the previous set of parameters. The method is rapidly convergent. It means that after few iteration the dθ converge to zeroes coefficients and it means that the calibration is reached. During the evaluation of the dθ, the value of J is evaluated as well.
d. J for every iteration, θ+dθ for every iteration are allocated.
e. A stopping criteria is applied if the convergence is reached prematurely. If $J_j - J_{j-1} < 10E\text{-}6$. The loop is stopped ant the

next model is analyzed. The user can change this value of the stopping criteria and decrease or increase it.

4. The model collected after the loop described at 3 are sorted from the one associated to the smallest value of the minima of the objective function to the one associated to the highest minima of the objective function. The threshold can have different values, decided by the user. It is possible that its value is percentage so, i.e. if its value is 90% we take only the first 90% of the sorted models. The model associated with high values of objective function it means that haven't reach a good calibration in dynamic behavior.
5. The G-means algorithm is run. It is based on the Anderson-Darling test, so it is very sensitive to the dispersion of the parameters in the domain space.
6. If the centroids after G-means are similar, they are collapsed into only one model. This mode is built using a weighted average. The weights belongs to the number of models belonging to each cluster. The bigger is the number of model into a cluster, the higher is the importance of this model.
7. If the model is unique the calibration show one model. if not, the solution is non-unique and more than one model is reached.

Permutation

It is the function used to generate the models. It the user selects this option the models are created dividing the domain of the parameters into bricks. The

bricks are combined to generate all the possible configuration. The bigger is the number of bricks, the exponentially bigger is the number of initial models. If the use doesn't want to generate these initial models with the permutation, he can do it deciding the number of combination and the interval of variation for each parameter. The generation occurs with the uniform probability density function.

Modal Analysis

This script runs the eigenvalue decomposition of the models. It is used to build the stiffness matrix, the mass matrix. These matrices are used to obtain the mode shapes and the natural frequencies for different purposes. One of the target of this script is evaluate the freq. and MS to build the sensitivity matrix, the other is to evaluate the freq. and MS of the model subjected to calibration to build the vector dz. It is used several times in the loop describe at number 3. If the number of parameter to be updated is Npar, this function is run (Npar+1)xNixNm. In this function the natural frequencies are sorted from the smaller to the higher, and of course the mode shapes as well. If the mode shapes obtained with the experimental are not mass normalized, in this loop the analytical one are transformed to be consistent.

Updating Lsqnonlin

It is the script that evaluates the incremental value $d\theta$ and the objective function J. Based on the choice of the user it is possible to obtain this increment and the value of J, through the expressions in the capitol 5, or using also the L.M.A.. The outputs of this script are $d\theta$, J and the updated parameters. J is stored in J_comb that is a matrix of dimension NixNm and the updated vector are stored

in the matrix c_comb, which dimension are NparxNixNm. The L.M.A. is applied using the matlab function Lsqnonlin which is a function that tries to minimize the least square objective function varying the vector dθ.

G-means

In this script only the model called c_good are clustered. These models are the one which objective function has reached the convergence and are the one selected with the threshold value. After this script a matrix containing the centroid is obtained. Its name is c_centroid, which dimension depends by the number of clusters.

Collapse

This script collapses all the model that after the G-means analysis have the value of the parameters very close one from each other.

Levemberg-Marquardt Algoritm

The method is shown in the following:

The Levenberg-Marquardt method is used to solve nonlinear least squares problems. In mathematics and computing, the LMA is also known as the damped least-squares (DLS) method. These minimization problems arise especially in least squares curve fitting. The LMA interpolates between the Gauss–Newton algorithm (GNA) and the method of gradient descent. The LMA is more robust than the GNA, so in many cases it finds a solution even if it starts very far off the final minimum. Like other numeric minimization

algorithms, the Levenberg–Marquardt algorithm is an iterative procedure. To start a minimization, the user has to provide an initial guess for the parameter vector that in this particular case is gotten by the [3.14] or [3.19]. In cases with multiple minima, the algorithm converges only if the initial guess is already somewhere close to the final solution.

In each iteration step, the parameter vector, dθ, is replaced by a new estimate, dθ + δ. If we assume a generic function *f* that has to be minimized, this method starts from a guess. Guess is a synonymous of model. A general least square expression could be:

$$J(d\theta) = \|z - f(d\theta)\| \qquad \text{[II.1]}$$

To determine δ, the functions $f(d\theta + \delta)$ are approximated by their linearization:

$$f(\theta, d\theta + \delta) \approx f(d\theta) + \nabla f \cdot \delta \qquad \text{[II.2]}$$

Where ∇ is the gradient of f when $d\theta$ is a vector. At the minimum of the sum of squares, J(dθ), the gradient of J with respect to δ will be zero. Taking the derivative with respect to δ and setting the result to zero gives:

$$\left(\nabla f^T \nabla f\right) \cdot \delta = \nabla f^T (z - f(d\theta)) \qquad \text{[II.3]}$$

Equation [3.23] looks like the one used to obtain the guess in [4.14] and conceptually it works in the same way, but it has been observed that the

application of this algorithm gives a perturbation of $d\theta$ that leads to a solution that is closer to the one related to the measurements. Levenberg's contribution is like the one applied by Thikonov and replaces this equation by a "damped version":

$$\left(\nabla f^T \nabla f + \lambda I\right) \cdot \delta = \nabla f^T (z - f(d\theta)) \qquad [II.4]$$

Where I is the identity matrix, giving as the increment, δ, to the estimated parameter vector, $d\theta$. The (non-negative) damping factor, λ, is adjusted at every iteration. If reduction of J is rapid, a smaller value can be used, bringing the algorithm closer to the Gauss–Newton algorithm, whereas, if an iteration gives insufficient reduction in the residual, λ can be increased, giving a step closer to the gradient descent direction. Therefore, for large values of λ, the step will be taken approximately in the direction of the gradient. If $d\theta + \delta$, falls below predefined limits, iteration stops and the last parameter vector, θ, is considered to be the solution. The combination of these two iterative procedures is effective to reach a good fitting and a minimum value of the objective function.